Volume 25, Number 4, 2025 ISSN 1562-8353

NONLINEAR DYNAMICS AND SYSTEMS THEORY
An International Journal of Research and Surveys

Volume 25 Number 4 2025

CONTENTS

NONLINEAR DYNAMICS & SYSTEMS THEORY
Volume 25, No. 4, 2025

Nonlinear Dynamics and Systems Theory

An International Journal of Research and Surveys

InforMath Publishing Group
http://www.e-ndst.kiev.ua

Nonlinear Dynamics and Systems Theory
An International Journal of Research and Surveys

INSTRUCTIONS FOR CONTRIBUTORS

(1) General. Nonlinear Dynamics and Systems Theory (ND&ST) is an international journal devoted to publishing peer-refereed, high quality, original papers, brief notes and review articles focusing on nonlinear dynamics and systems theory and their practical applications in engineering, physical and life sciences. Submission of a manuscript is a representation that the submission has been approved by all of the authors and by the institution where the work was carried out. It also represents that the manuscript has not been previously published, has not been copyrighted, is not being submitted for publication elsewhere, and that the authors have agreed that the copyright in the article shall be assigned exclusively to InforMath Publishing Group by signing a transfer of copyright form. Before submission, the authors should visit the website:

http://www.e-ndst.kiev.ua

for information on the preparation of accepted manuscripts. Please download the archive Sample_NDST.zip containing example of article file (you can edit only the file Samplefilename.tex).

(2) Manuscript and Correspondence. Manuscripts should be in English and must meet common standards of usage and grammar. To submit a paper, send by e-mail a file in PDF format directly to

Professor A.A. Martynyuk, Institute of Mechanics,
Nesterov str.3, 03057, Kiev-57, Ukraine
e-mail: journalndst@gmail.com

or to one of the Regional Editors or to a member of the Editorial Board. Final version of the manuscript must typeset using LaTex program which is prepared in accordance with the style file of the Journal. Manuscript texts should contain the title of the article, name(s) of the author(s) and complete affiliations. Each article requires an abstract not exceeding 150 words. Formulas and citations should not be included in the abstract. AMS subject classifications and key words must be included in all accepted papers. Each article requires a running head (abbreviated form of the title) of no more than 30 characters. The sizes for regular papers, survey articles, brief notes, letters to editors and book reviews are: (i) 10-14 pages for regular papers, (ii) up to 24 pages for survey articles, and (iii) 2-3 pages for brief notes, letters to the editor and book reviews.

(3) Tables, Graphs and Illustrations. Each figure must be of a quality suitable for direct reproduction and must include a caption. Drawings should include all relevant details and should be drawn professionally in black ink on plain white drawing paper. In addition to a hard copy of the artwork, it is necessary to attach the electronic file of the artwork (preferably in PCX format).

(4) References. Each entry must be cited in the text by author(s) and number or by number alone. All references should be listed in their alphabetic order. Use please the following style:

Journal: [1] H. Poincare, Title of the article. *Title of the Journal* **volume** (issue) (year) pages. [Language]

Book: [2] A.M. Lyapunov, *Title of the Book.* Name of the Publishers, Town, year.

Proceeding: [3] R. Bellman, Title of the article. In: *Title of the Book.* (Eds.). Name of the Publishers, Town, year, pages. [Language]

(5) Proofs and Sample Copy. Proofs sent to authors should be returned to the Editorial Office with corrections within three days after receipt. The corresponding author will receive a sample copy of the issue of the Journal for which his/her paper is published.

(6) Editorial Policy. Every submission will undergo a stringent peer review process. An editor will be assigned to handle the review process of the paper. He/she will secure at least two reviewers' reports. The decision on acceptance, rejection or acceptance subject to revision will be made based on these reviewers' reports and the editor's own reading of the paper.

NONLINEAR DYNAMICS AND SYSTEMS THEORY
An International Journal of Research and Surveys
Published by InforMath Publishing Group since 2001

Volume 25 Number 4 2025

CONTENTS

Founded by A.A. Martynyuk in 2001.
Registered in Ukraine Number: KB No 5267 / 04.07.2001.

NONLINEAR DYNAMICS AND SYSTEMS THEORY

An International Journal of Research and Surveys

Impact Factor from SCOPUS for 2024: SJR – 0.262, SNIP – 1.098 and CiteScore – 1.5

Nonlinear Dynamics and Systems Theory (ISSN 1562–8353 (Print), ISSN 1813–7385 (Online)) is an international journal published under the auspices of the S.P. Timoshenko Institute of Mechanics of National Academy of Sciences of Ukraine and Curtin University of Technology (Perth, Australia). It aims to publish high quality original scientific papers and surveys in areas of nonlinear dynamics and systems theory and their real world applications.

AIMS AND SCOPE

Nonlinear Dynamics and Systems Theory is a multidisciplinary journal. It publishes papers focusing on proofs of important theorems as well as papers presenting new ideas and new theory, conjectures, numerical algorithms and physical experiments in areas related to nonlinear dynamics and systems theory. Papers that deal with theoretical aspects of nonlinear dynamics and/or systems theory should contain significant mathematical results with an indication of their possible applications. Papers that emphasize applications should contain new mathematical models of real world phenomena and/or description of engineering problems. They should include rigorous analysis of data used and results obtained. Papers that integrate and interrelate ideas and methods of nonlinear dynamics and systems theory will be particularly welcomed.

PUBLICATION AND SUBSCRIPTION INFORMATION

Nonlinear Dynamics and Systems Theory will have 6 issues in 2025, printed in hard copy (ISSN 1562–8353) and available online (ISSN 1813–7385), by InforMath Publishing Group, Nesterov str., 3, Institute of Mechanics, Kiev, MSP 680, Ukraine, 03057. Subscription prices are available upon request from the Publisher, EBSCO Information Services (`mailto:journals@ebsco.com`), or website of the Journal: `http://e-ndst.kiev.ua`. Subscriptions are accepted on a calendar year basis. Issues are sent by airmail to all countries of the world. Claims for missing issues should be made within six months of the date of dispatch.

ABSTRACTING AND INDEXING SERVICES

Papers published in this journal are indexed or abstracted in: Mathematical Reviews / MathSciNet, Zentralblatt MATH / Mathematics Abstracts, PASCAL database (INIST–CNRS) and SCOPUS.

Nonlinear Dynamics and Systems Theory, **25** (4) (2025) 349–360

Blow up of Nonlinear Hyperbolic Equation with Variable Damping and Source Terms

S. Abdelhadi * and I. Hamchi

Laboratory of PDE and Applications, Department of Mathematics, University of Batna 2, Algeria.

Received: November 14, 2024; Revised: June 23, 2025

Abstract: In this work, we consider a nonlinear hyperbolic equation with variable damping and source terms. Our aim is to prove that the solution with negative initial energy blows up in finite time.

Keywords: *hyperbolic equation; damping term; source term; variable exponents; blow up.*

Mathematics Subject Classification (2020): 35B40, 37D30, 37K58, 46E35.

1 Introduction

In this work, we consider the following problem

$$\begin{cases} u_{tt} - div\,(A\nabla u) + u_t\,|u_t|^{m(.)-2} = u\,|u|^{p(.)-2} & \text{in } \Omega \times (0,T)\,, \\ u = 0 \quad \text{on } \partial\Omega \times (0,T)\,, \\ u(0) = u_0 \quad \text{and} \quad u_t(0) = u_1 \quad \text{in } \Omega, \end{cases} \tag{P}$$

where $T > 0$, Ω is a bounded domain of $\mathbb{R}^n$ $(n \in \mathbb{N}^*)$ with a smooth boundary $\partial\Omega$. $A = A(x,t)$ is an $n \times n$ symmetric matrix with real coefficients. The exponents $m(.)$ and $p(.)$ are given measurable functions on Ω.

When $A =$ Identity, the bibliography of works concerning problems of existence and nonexistence of global solution is truly long. **In the case of constant damping and source terms,** Ball [3] in 1977, considered the wave equation with source term and proved the blow up of solution when the energy of the initial data is negative. Haraux and Zuazua [8] in 1988, proved that the damping term of polynomial or arbitrary growth

* Corresponding author: mailto:s.abdelhadi@univ-batna2.dz

assured the global estimates of the wave equation for arbitrary initial data. The interaction between the damping and the source term was considered by Levine [9] in 1974, in the linear damping case $m = 2$. He showed that the solutions with negative initial energy blow up in finite time. Georgiev and Todorova [6] in 1994, extended Levine's result to the nonlinear damping case $m > 2$. They showed that solutions with any initial data are global if the damping term dominates the source term, then blow up in finite time if the source term dominates the damping term and the initial energy is sufficiently negative. Without imposing the condition that the initial energy is sufficiently negative, Messaoudi [10] in 2001, proved that any negative initial energy solution blow up in finite time. **In the case of variable damping and source term**, these problems have been considered by many authors using the Lebesgue spaces with variable exponent [5]. For instance, Antontsev [2] in 2011, considered the wave equation with $p(x,t)$-Laplacian and variable source term. In his work, he proved existence and blow up results under some assumptions on the initial energy data. In a recent study, Messaoudi and Talahmeh [11] in 2017, considered the quasilinear wave equation with variable exponent nonlinearities and proved that the solution with negative or positive initial energy blows up in finite time. In the same year, Messaoudi et al. [12] considered the nonlinear wave equation with variable source and damping terms and proved the blow up of solution with negative energy of initial data. In 2018, Ghegal et al. [7] considered the same system. They used the stable set method to prove the global existence result. Then, by some integral inequality, they showed the stability of this solution.

When $A(x,t) = a(x,t)$, where a is a given function, Sun et al. [13] in 2016, showed a result of blow up of solution when the energy of initial data is positive.

When $A = A(x,t)$, Boukhatem and Benyatou [4], in 2012, considered the hyperbolic equation with constant damping and source terms. They obtained a result of blow up of solution when the initial energy is positive.

In this work, we consider the case of variable coefficients ($A = A(x,t)$), variable damping and source terms and we show that the solution of (P) with negative initial energy blows up in finite time.

This paper consists of two sections in addition to Introduction. In Section 2, we give the assumptions and preliminary results needed to obtain our result. In Section 3, we prove the main result.

2 Assumptions and Preliminary Results

In this paper, we study the blow up behavior of the system (P) under the following assumptions:

- (H1) *For the matrix A:* Assume that

  1. A is of class $C^1\left(\bar{\Omega} \times [0, +\infty[\right)$.
  2. There exists a constant $a_0 > 0$ such that for all $\xi \in \mathbb{R}^n$, we have

$$A\xi\xi \geq a_0 \mid \xi \mid^2 \quad \text{and} \quad A'\xi\xi \leq 0.$$

- (H2) *For the exponents:* The exponents $m(.)$ and $p(.)$ are measurable functions on Ω such that

1. The following log-Holder continuity condition is satisfied:

$$|q(x)-q(y)| \leq -\frac{A}{\log|x-y|} \quad \text{for all } x,y \in \Omega, \quad \text{with} \quad |x-y|<\delta,$$

$$\text{where} \quad A>0 \quad \text{and} \quad 0<\delta<1.$$

2. We have

$$2 \leq m_1 \leq m(x) \leq m_2, \quad n=1,2.$$
$$2 \leq m_1 \leq m(x) \leq m_2 \leq \frac{2n}{n-2}, \quad n \geq 3,$$

with $m_1 := ess\inf_{x\in\Omega} m(x)$ and $m_2 := ess\sup_{x\in\Omega} m(x)$.

3. We assume that

$$2 \leq p_1 \leq p(x) \leq p_2, \quad n=1,2.$$
$$2 < p_1 \leq p(x) \leq p_2 \leq 2\frac{n-1}{n-2}, \quad n \geq 3,$$

with $p_1 := ess\inf_{x\in\Omega} p(x)$ and $p_2 := ess\sup_{x\in\Omega} p(x)$.

4. We assume that

$$m_2 < p_1 \leq p_2 \leq \frac{2n}{n-2}.$$

- (H3) *For the initial energy data:* we assume that

$$E(0)<0,$$

where

$$E(0) := \frac{1}{2}\parallel u_1 \parallel_2^2 + \frac{1}{2}\int_\Omega A(x,0)\nabla u_0 \nabla u_0 dx - \int_\Omega \frac{1}{p(x)} \mid u_0 \mid^{p(x)} dx.$$

Now, we introduce some preliminary results needed to prove our main result. The existence and uniqueness result for problem (P) is given in the following Theorem.

Theorem 2.1 *Let* $(u_0,u_1) \in H_0^1(\Omega)\times L^2(\Omega)$. *Then the problem* (P) *has a unique local solution*

$$u \in L^\infty((0,T);H_0^1(\Omega)),$$
$$u_t \in L^\infty((0,T);L^2(\Omega)) \cap L^{m(.)}(\Omega\times(0,T)),$$
$$u_{tt} \in L^2((0,T);H_0^1(\Omega)) \quad ,$$

for some $T>0$.

We define the energy functional for the local solution u of problem (P) by

$$E(t) = \frac{1}{2}\parallel u_t \parallel_2^2 + \frac{1}{2}\int_\Omega A\nabla u \nabla u dx - \int_\Omega \frac{1}{p(x)} |u|^{p(x)} dx, \qquad \forall t \in [0,T].$$

The following Lemma shows that E is a non-increasing function of t.

Lemma 2.1 *We have*

$$E'(t) = \frac{1}{2}\int_\Omega A'\nabla u\nabla u dx - \int_\Omega \mid u_t \mid^{m(x)} dx \leq 0, \qquad \forall\, t \in [0,T].$$

Proof. We multiply the first equation in (P) by u_t, integrate it over Ω, we obtain

$$\int_\Omega u_t u_{tt} dx - \int_\Omega u_t div\,(A\nabla u)\, dx - \int_\Omega u_t u\,|u|^{p(x)-2}\, dx = -\int_\Omega |u_t|^{m(x)}\, dx. \tag{1}$$

First, we have

$$\int_\Omega u_t u_{tt} dx = \frac{1}{2}\frac{d}{dt}\,\|u_t\|_2^2 \quad \text{and} \quad \int_\Omega u_t u\,|u|^{p(x)-2}\, dx = \frac{d}{dt}\int_\Omega \frac{1}{p(x)} \mid u \mid^{p(x)} dx. \tag{2}$$

On the other hand, by the generalized Green formula, we find

$$-\int_\Omega u_t div\,(A\nabla u)\, dx = \int_\Omega A\nabla u\nabla u_t dx. \tag{3}$$

But

$$\begin{aligned}\frac{d}{dt}\int_\Omega A\nabla u\nabla u dx &= \int_\Omega \frac{d(A\nabla u)}{dt}\nabla u dx + \int_\Omega A\nabla u\nabla u_t dx \\ &= \int_\Omega A'\nabla u\nabla u dx + \int_\Omega A\nabla u_t\nabla u dx + \int_\Omega A\nabla u\nabla u_t dx.\end{aligned}$$

Since A is symmetric

$$\int_\Omega A\nabla u\nabla u_t dx = \frac{1}{2}\frac{d}{dt}\int_\Omega A\nabla u\nabla u dx - \frac{1}{2}\int_\Omega A'\nabla u\nabla u dx$$

(3) becomes

$$-\int_\Omega u_t div\,(A\nabla u)\, dx = \frac{1}{2}\frac{d}{dt}\int_\Omega A\nabla u\nabla u dx - \frac{1}{2}\int_\Omega A'\nabla u\nabla u dx. \tag{4}$$

We replace (2) and (4) in (1) to obtain

$$\begin{aligned}&\frac{d}{dt}\left\{\frac{1}{2}\,\|u_t\|_2^2\, dx + \frac{1}{2}\int_\Omega A\nabla u\nabla u dx - \int_\Omega \frac{1}{p(x)} \mid u \mid^{p(x)} dx\right\} \\ = \;& \frac{1}{2}\int_\Omega A'\nabla u\nabla u dx - \int_\Omega \mid u_t \mid^{m(x)} dx.\end{aligned}$$

This implies the desired result. We set

$$H(t) = -E(t), \qquad \forall t \in [0,T].$$

Lemma 2.2 *We have*

$$0 < H(0) \leq H(t) \leq \frac{1}{p_1}\int_\Omega \mid u \mid^{p(x)} dx, \qquad \forall t \in [0,T]. \tag{5}$$

Proof.

- Since $E(0) < 0, \quad$ we find $\quad H(0) = -E(0) > 0.$

- From the definition of H and the monotonicity of E, we have

$$H(0) \leq H(t), \qquad \forall t \in [0, T].$$

- We have

$$H(t) = -\frac{1}{2} \|u_t\|_2^2 - \frac{1}{2} \int_\Omega A\nabla u \nabla u dx + \int_\Omega \frac{1}{p(x)} \mid u \mid^{p(x)} dx.$$

$(H1-2)$ implies that

$$H(t) \leq \int_\Omega \frac{1}{p(x)} \mid u \mid^{p(x)} dx.$$

By $(H2-3)$, we arrive at

$$H(t) \leq \frac{1}{p_1} \int_\Omega |u|^{p(x)} dx.$$

Let C be a generic positive constant and it may change from line to line. The following two Lemmas are also needed in our work.

Lemma 2.3 *There exists a constant $C > 0$ such that*

$$\int_\Omega \mid u \mid^{p(x)} dx \geq C \|u\|_{p_1}^{p_1} \tag{6}$$

and

$$\int_\Omega \mid u \mid^{m(x)} dx \leq C \left(\left(\int_\Omega \mid u \mid^{p(x)} dx \right)^{\frac{m_2}{p_1}} + \left(\int_\Omega \mid u \mid^{p(x)} dx \right)^{\frac{m_1}{p_1}} \right). \tag{7}$$

Proof. **Proof of** (6)**:** We have

$$\int_\Omega \mid u \mid^{p(x)} dx = \int_{\Omega_+} \mid u \mid^{p(x)} dx + \int_{\Omega_-} \mid u \mid^{p(x)} dx, \tag{8}$$

where

$$\Omega_+ = \{x \in \Omega / \mid u(x,t) \mid \geq 1\} \quad \text{and} \quad \Omega_- = \{x \in \Omega / \mid u(x,t) \mid < 1\}.$$

We have

$$\int_{\Omega_+} \mid u \mid^{p(x)} dx \geq \int_{\Omega_+} \mid u \mid^{p_1} dx \tag{9}$$

and

$$\int_{\Omega_-} \mid u \mid^{p(x)} dx \geq \int_{\Omega_-} \mid u \mid^{p_2} dx.$$

Since $p_1 \leq p_2$,

$$\int_{\Omega_-} |\, u \,|^{p(x)}\, dx \geq C \left(\int_{\Omega_-} |\, u \,|^{p_1}\, dx \right)^{\frac{p_2}{p_1}}. \tag{10}$$

We replace (9) and (10) in (8) to obtain

$$\int_{\Omega} |\, u \,|^{p(x)}\, dx \geq \int_{\Omega_+} |\, u \,|^{p_1}\, dx + C \left(\int_{\Omega_-} |\, u \,|^{p_1}\, dx \right)^{\frac{p_2}{p_1}}.$$

This implies that

$$\int_{\Omega} |\, u \,|^{p(x)}\, dx \geq \int_{\Omega_+} |\, u \,|^{p_1}\, dx \quad \text{and} \quad C \left(\int_{\Omega} |\, u \,|^{p(x)}\, dx \right)^{\frac{p_1}{p_2}} \geq \int_{\Omega_-} |\, u \,|^{p_1}\, dx.$$

By addition, we find

$$\int_{\Omega} |\, u \,|^{p(x)}\, dx + C \left(\int_{\Omega} |\, u \,|^{p(x)}\, dx \right)^{\frac{p_1}{p_2}} \geq \|u\|_{p_1}^{p_1}.$$

So

$$\left[1 + C \left(\int_{\Omega} |\, u \,|^{p(x)}\, dx \right)^{\frac{p_1}{p_2}-1} \right] \int_{\Omega} |\, u \,|^{p(x)}\, dx \geq \|u\|_{p_1}^{p_1}.$$

But, by (5) and $(H2-3)$, we find

$$(p_1 H(0))^{\frac{p_1}{p_2}-1} \geq \left(\int_{\Omega} |\, u \,|^{p(x)}\, dx \right)^{\frac{p_1}{p_2}-1}.$$

Then

$$\left[1 + C\, (p_1 H(0))^{\frac{p_1}{p_2}-1} \right] \int_{\Omega} |\, u \,|^{p(x)}\, dx \geq \|u\|_{p_1}^{p_1}.$$

Consequently, we obtain (6).

Proof of (7)**:** We have

$$\begin{aligned} \int_{\Omega} |\, u \,|^{m(x)}\, dx &= \int_{\Omega_+} |\, u \,|^{m(x)}\, dx + \int_{\Omega_-} |\, u \,|^{m(x)}\, dx \\ &\leq \int_{\Omega_+} |\, u \,|^{m_2}\, dx + \int_{\Omega_-} |\, u \,|^{m_1}\, dx. \end{aligned}$$

Since $m_1 \leq m_2 < p_1$,

$$\begin{aligned} \int_{\Omega} |\, u \,|^{m(x)}\, dx &\leq C \left[\left(\int_{\Omega_+} |\, u \,|^{p_1}\, dx \right)^{\frac{m_2}{p_1}} + \left(\int_{\Omega_-} |\, u \,|^{p_1}\, dx \right)^{\frac{m_1}{p_1}} \right] \\ &\leq C \left(\|u\|_{p_1}^{m_2} + \|u\|_{p_1}^{m_1} \right). \end{aligned}$$

By (6), we find the desired result.

Lemma 2.4 *For all*

$$0 < \alpha \leq \min\left\{\frac{p_1-2}{2p_1}, \frac{p_1-m_2}{p_1(m_2-1)}\right\} \quad \text{and} \quad k > 1,$$

we have

$$\int_\Omega H^{\alpha(m(x)-1)}(t) \mid u \mid^{m(x)} dx \leq C\left(\int_\Omega A\nabla u\nabla u dx + \int_\Omega \mid u \mid^{p(x)} dx\right) \tag{11}$$

and

$$\begin{aligned}\int_\Omega \mid u \mid\mid u_t \mid^{m(x)-1} dx &\leq C\frac{k^{1-m_1}}{m_1}\left(\int_\Omega A\nabla u\nabla u dx + \int_\Omega \mid u \mid^{p(x)} dx\right)\\ &+ \frac{(m_2-1)k}{m_2}H^{-\alpha}(t)H'(t).\end{aligned} \tag{12}$$

Proof. **Proof of** (11): We have

$$\int_\Omega H^{\alpha(m(x)-1)}(t) \mid u \mid^{m(x)} dx = \int_\Omega \left[\frac{H(t)}{H(0)}\right]^{\alpha(m(x)-1)} [H(0)]^{\alpha(m(x)-1)} \mid u \mid^{m(x)} dx.$$

Since $\dfrac{H(t)}{H(0)} \geq 1$, by $(H2-2)$, we find

$$\begin{aligned}&\int_\Omega H^{\alpha(m(x)-1)}(t) \mid u \mid^{m(x)} dx \leq \int_\Omega \left[\frac{H(t)}{H(0)}\right]^{\alpha(m_2-1)} [H(0)]^{\alpha(m(x)-1)} \mid u \mid^{m(x)} dx\\ \leq\ & [H(t)]^{\alpha(m_2-1)} \int_\Omega [H(0)]^{\alpha(m(x)-m_2)} \mid u \mid^{m(x)} dx.\end{aligned} \tag{13}$$

But

$$[H(0)]^{\alpha(m(x)-m_2)} \leq C \quad \text{for all} \quad x \in \Omega.$$

Indeed,

$$\text{if} \quad H(0) \leq 1, \text{ then} \quad [H(0)]^{\alpha(m(x)-m_2)} \leq [H(0)]^{\alpha(m_1-m_2)},$$

$$\text{if} \quad H(0) > 1, \text{ then} \quad [H(0)]^{\alpha(m(x)-m_2)} \leq [H(0)]^{\alpha(m_2-m_2)} = 1.$$

Then (13) becomes

$$\int_\Omega H^{\alpha(m(x)-1)}(t) \mid u \mid^{m(x)} dx \leq C\,[H(t)]^{\alpha(m_2-1)} \int_\Omega \mid u \mid^{m(x)} dx.$$

By (5) and (7), we find

$$\begin{aligned}&\int_\Omega H^{\alpha(m(x)-1)}(t) \mid u \mid^{m(x)} dx\\ \leq\ & C\left(\left(\int_\Omega \mid u \mid^{p(x)} dx\right)^{\frac{m_2}{p_1}+\alpha(m_2-1)} + \left(\int_\Omega \mid u \mid^{p(x)} dx\right)^{\frac{m_1}{p_1}+\alpha(m_2-1)}\right).\end{aligned}$$

We apply Lemma 4.1 from [12] to

$$2 \leq s = m_1 + \alpha p_1(m_2 - 1) \leq p_1,$$

and

$$2 \leq s = m_2 + \alpha p_1(m_2 - 1) \leq p_1,$$

and by $(H1-1)$, we obtain (11).
Proof of (12): By the Young inequality

$$XY \leq \frac{\delta^{\mu}}{\mu} X^{\mu} + \frac{\delta^{-\theta}}{\theta} Y^{\theta} \quad \text{for all} \quad X,\, Y \geq 0,\ \ \delta > 0 \quad \text{and} \ \ \frac{1}{\mu} + \frac{1}{\theta} = 1 \tag{14}$$

with

$$X = |u|\,, \quad Y = \mid u_t \mid^{m(x)-1}, \quad \mu = m(x) \quad \text{and} \quad \theta = \frac{m(x)}{m(x)-1},$$

we find

$$\begin{aligned} \int_{\Omega} \mid u \mid\mid u_t \mid^{m(x)-1} dx &\leq \int_{\Omega} \frac{\delta^{m(x)}}{m(x)} \mid u \mid^{m(x)} dx + \int_{\Omega} \frac{m(x)-1}{m(x)} \delta^{-\frac{m(x)}{m(x)-1}} \mid u_t \mid^{m(x)} dx \\ &\leq \frac{1}{m_1} \int_{\Omega} \delta^{m(x)} \mid u \mid^{m(x)} dx \\ &+ \frac{m_2 - 1}{m_1} \int_{\Omega} \delta^{-\frac{m(x)}{m(x)-1}} \mid u_t \mid^{m(x)} dx. \end{aligned}$$

Let $k > 0$. If we take

$$\delta = \left(kH^{-\alpha}(t)\right)^{-\frac{m(x)-1}{m(x)}} > 0,$$

then we find

$$\begin{aligned} \int_{\Omega} \mid u \mid\mid u_t \mid^{m(x)-1} dx &\leq \frac{1}{m_1} \int_{\Omega} k^{1-m(x)} H^{\alpha(m(x)-1)}(t) \mid u \mid^{m(x)} dx \\ &+ \frac{(m_2-1)k}{m_1} H^{-\alpha}(t) \int_{\Omega} \mid u_t \mid^{m(x)} dx. \end{aligned} \tag{15}$$

But, from the definition of H, Lemma 2.1 and $(H1-2)$, we have

$$\int_{\Omega} |u_t|^{m(x)} dx = \frac{1}{2} \int_{\Omega} A' \nabla u \nabla u dx + H'(t) \leq H'(t).$$

Then, for $k > 1$, (15) becomes

$$\int_{\Omega} \mid u \mid\mid u_t \mid^{m(x)-1} dx \leq \frac{k^{1-m_1}}{m_1} \int_{\Omega} H^{\alpha(m(x)-1)}(t) \mid u \mid^{m(x)} dx + \frac{(m_2-1)k}{m_2} H^{-\alpha}(t) H'(t).$$

By (11), we obtain the result.

3 Main Result

In this section, we state and prove our main result.

Theorem 3.1 *The solution of problem* (P) *blows up in finite time.*

Proof. We proceed in 4 steps.

Step 1. For $\epsilon > 0$, we consider the following functional:

$$L(t) = H^{1-\alpha}(t) + \epsilon \int_\Omega u u_t dx, \qquad \forall t \in [0,T].$$

If we derive the function L with respect to t, we obtain

$$L'(t) = (1-\alpha)\, H^{-\alpha}(t) H'(t) + \epsilon \left\| u_t \right\|_2^2 + \epsilon \int_\Omega u u_{tt} dx, \quad \forall t \in [0,T]. \tag{16}$$

But

$$\begin{aligned} \int_\Omega u u_{tt} dx &= \int_\Omega u div(A\nabla u) dx - \int_\Omega u u_t \mid u_t \mid^{m(x)-2} dx \\ &+ \int_\Omega \mid u \mid^{p(x)} dx. \end{aligned}$$

By the generalized Green formula, we obtain

$$\int_\Omega u u_{tt} dx = -\int_\Omega A\nabla u \nabla u dx - \int_\Omega u u_t \mid u_t \mid^{m(x)-2} dx + \int_\Omega \mid u \mid^{p(x)} dx. \tag{17}$$

Replacing (17) in (16), we find

$$\begin{aligned} L'(t) &\geq (1-\alpha)\, H^{-\alpha}(t) H'(t) + \epsilon \left\| u_t \right\|_2^2 - \epsilon \int_\Omega A\nabla u \nabla u dx \\ &- \epsilon \int_\Omega \mid u \mid\mid u_t \mid^{m(x)-1} dx + \epsilon \int_\Omega \mid u \mid^{p(x)} dx. \end{aligned}$$

By (12), we obtain

$$\begin{aligned} L'(t) &\geq \left[1 - \alpha - \epsilon \frac{(m_2-1)k}{m_2}\right] H^{-\alpha}(t) H'(t) + \epsilon \left\| u_t \right\|_2^2 \\ &- \epsilon \left(1 + C\frac{k^{1-m_1}}{m_1}\right) \int_\Omega A\nabla u \nabla u dx \\ &+ \epsilon \left(1 - C\frac{k^{1-m_1}}{m_1}\right) \int_\Omega \mid u \mid^{p(x)} dx. \end{aligned} \tag{18}$$

Add and subtract $\epsilon(1-\eta)p_1 H(t)$ for $0 < \eta < 1$ in the right-hand side of (18) and use the definition of H to obtain

$$\begin{aligned} L'(t) &\geq \left[1 - \alpha - \epsilon \frac{(m_2-1)k}{m_2}\right] H^{-\alpha}(t) H'(t) + \epsilon(1-\eta)p_1 H(t) + \epsilon \left\| u_t \right\|_2^2 \\ &- \epsilon \left(1 + C\frac{k^{1-m_1}}{m_1}\right) \int_\Omega A\nabla u \nabla u dx + \epsilon \left(1 - C\frac{k^{1-m_1}}{m_1}\right) \int_\Omega \mid u \mid^{p(x)} dx \\ &- \epsilon(1-\eta)p_1 \left(-\frac{1}{2} \left\| u_t \right\|_2^2 - \frac{1}{2} \int_\Omega A\nabla u \nabla u dx + \frac{1}{p_1} \int_\Omega \mid u \mid^{p(x)} dx\right). \end{aligned} \tag{19}$$

Then

$$\begin{aligned} L'(t) &\geq \left[1-\alpha-\epsilon\frac{(m_2-1)k}{m_2}\right]H^{-\alpha}(t)H'(t)+\epsilon(1-\eta)p_1H(t) \\ &+ \epsilon\left(\eta-C\frac{k^{1-m_1}}{m_1}\right)\int_\Omega \mid u \mid^{p(x)} dx+\epsilon\left(\frac{(1-\eta)p_1}{2}+1\right)\epsilon\left\|u_t\right\|_2^2 \\ &+ \epsilon\left(\frac{p_1-2}{2}-\frac{\eta p_1}{2}-C\frac{k^{1-m_1}}{m_1}\right)\int_\Omega A\nabla u\nabla u dx. \end{aligned}$$

For the fixed k sufficiently large, then for η sufficiently small, we arrive at

$$\begin{aligned} L'(t) &\geq \left[1-\alpha-\epsilon\frac{(m_2-1)k}{m_2}\right]H^{-\alpha}(t)H'(t)+\epsilon\gamma\left[H(t)+\int_\Omega \mid u \mid^{p(x)} dx+\epsilon\left\|u_t\right\|_2^2\right] \\ &+ \epsilon\beta\int_\Omega A\nabla u\nabla u dx, \end{aligned} \tag{20}$$

where

$$\gamma=\min\left\{(1-\eta)p_1,\eta-C\frac{k^{1-m_1}}{m_1},\frac{(1-\eta)p_1}{2}+1\right\}>0,$$

and

$$\beta=\frac{p_1-2}{2}-\frac{\eta p_1}{2}-C\frac{k^{1-m_1}}{m_1}=\frac{p_1-2}{2}-\eta\left(1+\frac{p_1}{2}\right)+\eta-C\frac{k^{1-m_1}}{m_1}>0.$$

If ϵ is chosen sufficiently small such that

$$1-\alpha-\epsilon\frac{m_2-1}{m_2}k\geq 0,$$

then, by (6), inequality (20) takes the form

$$L'(t)\geq \epsilon C\left[H(t)+\parallel u \parallel_{p_1}^{p_1}+\parallel u_t \parallel_2^2\right]. \tag{21}$$

Step 2. Since

$$L(0)=H^{1-\alpha}(0)+\epsilon\int_\Omega u_0(x)u_1(x)dx>0,$$

from the increase of L (see (21)), we find

$$L(t)\geq 0,\quad \forall t\in[0,T].$$

Step 3. By the definition of L, we find

$$L^{\frac{1}{1-\alpha}}(t) \leq \left[H^{1-\alpha}(t)+\epsilon\int_\Omega \mid u \mid\mid u_t \mid dx\right]^{\frac{1}{1-\alpha}}.$$

By the following inequality:

$$(a+b)^m\leq 2^m(a^m+b^m)\quad \text{for all } a,b\geq 0 \text{ and } m>0,$$

with

$$a = H^{1-\alpha}(t),\ b = \epsilon \int_\Omega \mid u \mid\mid u_t \mid dx \text{ and } m = \frac{1}{1-\alpha},$$

we obtain

$$L^{\frac{1}{1-\alpha}}(t) \quad \leq \quad 2^{\frac{1}{1-\alpha}} \left[H(t) + \left(\epsilon \int_\Omega \mid u \mid\mid u_t \mid dx \right)^{\frac{1}{1-\alpha}} \right].$$

But, by the Cauchy–Schwarz inequality, we have

$$\left(\int_\Omega \mid u \mid\mid u_t \mid dx \right)^{\frac{1}{1-\alpha}} \quad \leq \quad \parallel u \parallel_2^{\frac{1}{1-\alpha}} \parallel u_t \parallel_2^{\frac{1}{1-\alpha}} .$$

From the embedding $L^{p_1}(\Omega) \hookrightarrow L^2(\Omega)$, we find

$$\left(\int_\Omega \mid u \mid\mid u_t \mid dx \right)^{\frac{1}{1-\alpha}} \leq C \parallel u \parallel_{p_1}^{\frac{1}{1-\alpha}} \parallel u_t \parallel_2^{\frac{1}{1-\alpha}} .$$

Apply Young's inequality (14) with

$$X = \parallel u \parallel_{p_1}^{\frac{1}{1-\alpha}}, \quad Y = \parallel u_t \parallel_2^{\frac{1}{1-\alpha}}, \quad \mu = \frac{2(1-\alpha)}{1-2\alpha} \quad and \quad \theta = 2(1-\alpha),$$

we have

$$\left(\int_\Omega \mid u \mid\mid u_t \mid dx \right)^{\frac{1}{1-\alpha}} \leq C \left(\parallel u \parallel_{p_1}^{\frac{2}{1-2\alpha}} + \parallel u_t \parallel_2^2 \right).$$

We apply Corollary 4.4 from [12] with $2 \leq s = \frac{2}{1-2\alpha} \leq p_1$ to find

$$L^{\frac{1}{1-\alpha}}(t) \leq C \left[H(t) + \parallel u \parallel_{p_1}^{p_1} + \parallel u_t \parallel_2^2 \right], \quad \forall t \in [0, T]. \tag{22}$$

Step 4. We proceed by contradiction. By the continuation principal, we obtain that $T = +\infty$. By combining (21) and (22), we arrive at

$$L'(t) \quad \geq C L^{\frac{1}{1-\alpha}}(t), \quad \text{for all } t \geq 0.$$

A simple integration over $(0, t)$ gives

$$L(t) \geq \frac{1}{\left[L^{\frac{-\alpha}{1-\alpha}}(0) - \frac{\alpha C t}{(1-\alpha)} \right]^{\frac{1-\alpha}{\alpha}}}, \quad \text{for all } t \geq 0.$$

This leads to a contradiction.

4 Conclusion

In this work, we study the blow up of solutions of the nonlinear hyperbolic equation with variable damping and source terms. We present the assumptions and preliminary results required to obtain our main result. We also provide the energy identity associated with the solution. Finally, we state and prove the blow up result for the solution.

References

[1] S. Abdelhadi and I. Hamchi. Blow up of the wave equation with nonlinear first order perturbation term. *Advances in Mathematics: Scientific Journal* **11** (7) (2023) 565–575.

[2] S. Antontsev. Wave equation with $p(x,t)$-Laplacian and damping term: existence and blow up. *J. Difference Equ. Appl.* **3** (4) (2011) 503–525.

[3] J. Ball. Remarks on blow up and nonexistence theorems for nonlinear evolution equations. *Quart. J. Math. Oxford* (2) **28** (1977) 473–486.

[4] Y. Boukhatem and B. Benyatou. Blow up of solutions for semilinear hyperbolic equation. *Electron. J. Qual. Theory Differ. Equ.* **40** (2012) 1–12.

[5] L. Diening, P. Harjulehto, P. Hästö and M. Růžička. *Lebesgue and Sobolev Spaces with Variable Exponents*. Springer-Verlag, Heidelberg, 2011.

[6] V. Georgiev and G. Todorova. Existence of solutions of the wave equation with nonlinear damping and source terms. *J. Differ. Equ.* **109** (2) (1994) 295–308.

[7] S. Ghegal, I. Hamchi and S. Messaoudi. Global existence and stability of a nonlinear wave equation with variable-exponent nonlinearities. To appear in *Applicable Analysis*.

[8] A. Huraux and E. Zuazua. Decay estimates for some semilinear damped hyperbolic problems. *Arch. Ration. Mech. Anal.* **150** (1988) 191–206.

[9] H. Levine. Some additional remarks on the nonexistence of global solutions to nonlinear wave equations. *SIAM J. Math. Anal.* **5** (1) (1974) 138–146.

[10] S. Messaoudi. Blow up in a nonlinearly damped wave equation. *Math. Nachr.* **231** (1) (2001) 105–111.

[11] S. Messaoudi and A. Talahmeh. Blow up in solutions of a quasilinear wave equation with variable-exponent nonlinearities. *Math. Methods Appl. Sci.* (2017) 1099–1476.

[12] S. Messaoudi, A. Talahmeh and H. Al-Smail. Nonlinear damped wave equation: existence and blow up. *Comput. Math. Appl.* (2017) 0898–1221.

[13] L. Sun, Y. Ren and W. Gao. Lower and upper bounds for the blow up time for nonlinear wave equation with variable sources. *Comput. Math. Appl.* **71** (1) (2016) 267–277.

Nonlinear Dynamics and Systems Theory, **25** (4) (2025) 361–372

Dynamics of a Fractional Order Model for Mycobacterium Tuberculosis with Caputo-Fabrizio Derivatives

Y. A. Adi * and S. A. Septiani

Department of Mathematics, Faculty of Applied Science and Technology, Universitas Ahmad Dahlan, Yogyakarta, Indonesia

Received: November 25, 2024; Revised: June 21, 2025

Abstract: Tuberculosis is an infectious disease caused by the Mycobacterium tuberculosis (Mtb), bacteria that primarily attacks the lungs. Currently, tuberculosis remains a major public health challenge. This study develops a fractional-order mathematical model using the Caputo-Fabrizio derivatives to explore the growth dynamics of MTb in relation to vaccine administration. The methodology consists of the following steps: model formulation, equilibrium point determination, computation of the fundamental reproduction number R_0, equilibrium point stability analysis, and numerical simulation utilizing the Adam-Bashforth 3-step method. The main result reveals that the nonlinear dynamics of the model exhibits significant sensitivity to the fractional order. The model indicates that the infection-free equilibrium point is locally asymptotically stable if $R_0 < 1$, and the endemic equilibrium point is also locally asymptotically stable under specific circumstances. The fractional order can greatly influence the convergence rate towards equilibrium points, as numerical simulations further highlight that smaller fractional orders accelerate the convergence of immune response cells to stability, demonstrating the potential of fractional calculus to capture complex biological dynamics more effectively.

Keywords: *mycobacterium tuberculosis; fractional-order model; Caputo-Fabrizio derivatives; numerical simulation.*

Mathematics Subject Classification (2020): 34A08, 37N30, 70K75 92D30, 93-10.

* Corresponding author: mailto:yudi.adi@math.uad.ac.id

1 Introduction

Mycobacterium tuberculosis is the causative agent of tuberculosis (TB), a dangerous infectious disease that mostly affects the lungs. Despite treatment, tuberculosis is still one of the deadliest infectious diseases in the world, killing more people than HIV/AIDS combined [1]. One of the reasons why this disease still exists is the resistance of bacteria to the immune system, especially macrophages, which are essential for eliminating infections. Once TB germs enter the lungs, granulomas, a protective barrier that helps regulate bacterial development, are activated. The persistence of bacteria allows them to live inside these structures, postponing the immune response of the body and prolonging the illness. TB is difficult to control due to its rapid spread and drug resistance, even though it can be managed with the right antibiotics. Consequently, prevention, early detection, and effective management are essential in reducing the global burden of tuberculosis [2]. Governments, health organizations, and researchers around the world are working together to develop more comprehensive strategies to control the spread of tuberculosis and improve case management.

Various strategies and models have been explored in the investigation of TB. Recent research on TB prevention efforts at the cellular level can be found in several studies such as [3]. Another novel approach is to use fractional differential equations to model biological processes. Fractional models, as opposed to traditional models, take into account "memory" effects, which are situations in which previous occurrences impact future results. The fractional derivatives can be used to explain phenomena that show relaxation effects and memory retention since they incorporate memory and genetic characteristics [4]. This makes them especially helpful for tuberculosis, as the history of infection can affect the immune response and transmission rates. Fractional models provide a more accurate picture of TB dynamics by taking into consideration elements that are frequently missed in classical models. For example, Ibarguen-Mondragon et al. [5] formulate a model for the population dynamics of Mycobacterium tuberculosis (Mtb) to assess the impact of the competition among bacteria on the infection prevalence.

Recently, numerous fractional derivatives have also been investigated in recent works on tuberculosis epidemic modeling such as [6–8]. Zhang et al. [6] utilized the Caputo derivative to capture TB's transmission dynamics, incorporating the concept of memory behavior to illustrate how past infections affect disease progression and treatment. Meanwhile, Zafar et al. [7] explored machine learning approaches alongside fractional operators for various fractional orders. Recently, Olayiwola et al. [8] studied a mathematical model to investigate the impact of treatment on physical limitations in tuberculosis. Studies on TB control measures such as hospitalization, quarantine, and adherence to treatment, have used the Atangana-Baleanu-Caputo and Caputo-Fabrizio derivatives [9]. This broad variety of TB modeling is a result of continuous attempts to use fractional-order derivatives to better understand and treat TB. Based on the previous studies, in this study, we aim to develop a fractional-order-based mathematical model to analyze the interaction of MTb with host immune cells. This fractional-order approach was chosen to consider the memory effect on infection dynamics, which is not fully covered by models based on integer order [10].

The structure of this paper is as follows. Section 2 defines the methods; in particular, we describe the model formulation for the interaction between macrophages and Mycobacterium tuberculosis, the fractional model, and determine the existence and stability of the equilibrium point. Section 3 provides numerical results and discusses the

effect of a variation in order. Finally, Section 4 gives the conclusion.

2 Methods

2.1 Model description

In this section, we develop a mathematical model describing the interaction between macrophages and *Mycobacterium tuberculosis* (Mtb). The population is divided into four sub-populations: uninfected macrophages (M_U), infected macrophages (M_I), *Mycobacterium tuberculosis* bacteria (B), and T cells (T). The dynamics of *Mycobacterium tuberculosis* within granulomas are represented in the schematic diagram in Figure 1.

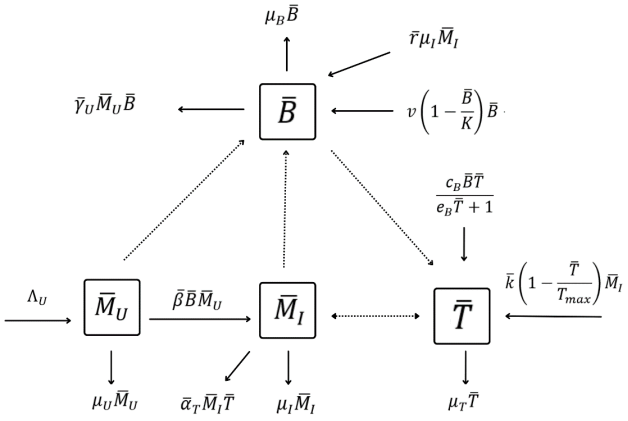

Figure 1: Schematic diagram of Mtb progression.

The population dynamics of uninfected macrophages ($M_U(t)$) are influenced by several factors, including the growth rate of uninfected macrophages per unit of time (Λ_U), the natural death rate of uninfected macrophages per unit of time ($\mu_U M_U(t)$), and the interaction between uninfected macrophages and bacteria per unit of time ($\beta B(t) M_U(t)$). This change in population is represented by the following equation:

$$\frac{dM_U(t)}{dt} = \Lambda_U - \beta B(t) M_U(t) - \mu_U M_U(t). \tag{1}$$

The population dynamics of infected macrophages ($M_I(t)$) are influenced by interactions between uninfected macrophages and bacteria per unit of time ($\beta B(t) M_U(t)$), interactions of T cells with infected macrophages per unit of time ($\alpha_T M_I(t) T(t)$), and the natural death rate of infected macrophages per unit of time ($\mu_I M_I(t)$):

$$\frac{dM_I(t)}{dt} = \beta B(t) M_U(t) - \alpha_T M_I(t) T(t) - \mu_I M_I(t). \tag{2}$$

The population of *Mycobacterium tuberculosis* bacteria ($B(t)$) is influenced by factors such as the bursting of infected macrophages when bacterial growth exceeds a threshold per unit of time ($r\mu_I M_I(t)$), the logistic growth of bacteria with the growth rate v

and maximum capacity K, phagocytosis by uninfected macrophages per unit of time ($\gamma_U M_U(t)B(t)$), and the natural death rate of bacteria per unit of time ($\mu_B B(t)$):

$$\frac{dB(t)}{dt} = r\mu_I M_I(t) + v\left(1 - \frac{B(t)}{K}\right)B(t) - \gamma_U M_U(t)B(t) - \mu_B B(t). \tag{3}$$

The T cell population ($T(t)$) is affected by T cell growth due to signals from infected macrophages per unit of time ($k(1 - T(t))M_I(t)$), immune memory from vaccination following a decay function per unit of time $\left(\frac{c_B BT}{e_B T+1}\right)$, and the natural death rate of T cells per unit of time ($\mu_T T(t)$):

$$\frac{dT(t)}{dt} = k\left(1 - \frac{T(t)}{T_{\max}}\right)M_I(t) + \frac{c_B BT}{e_B T + 1} - \mu_T T(t). \tag{4}$$

To simplify the model, we introduce the following non-dimensional variables:

$$M_U = \frac{M_U}{\Lambda_U/\mu_U}; \quad M_I = \frac{M_I}{\Lambda_U/\mu_U}; \quad B = \frac{B}{K}; \quad T = \frac{T}{T_{\max}}.$$

After substituting these variables into equations (1)–(4), the resulting system of differential equations becomes:

$$\begin{cases} \dot{M_U} &= \mu_U - \beta B M_U - \mu_U M_U, \\ \dot{M_I} &= \beta B M_U - \alpha_T M_I T) - \mu_I M_I, \\ \dot{B} &= r\mu_I M_I + v(1 - B)B - \gamma_U M_U B - \mu_B B, \\ \dot{T} &= k(1 - T)M_I + \frac{c_B BT}{e_B T+1} - \mu_T T, \end{cases} \tag{5}$$

where

$$\alpha_T = \alpha_T T_{\max}; \quad \beta = \beta K; \quad \gamma_U = \frac{\gamma_U \Lambda_U}{\mu_U}; \quad r = \frac{r\Lambda_U}{K\mu_U}; \quad k = \frac{k\Lambda_U}{\mu_U}.$$

2.2 Fractional model of Mycobacterium tuberculosis growth

Incorporating fractional calculus, we replace the integer-order derivatives $\frac{d}{dt}$ in equation (5) with the Caputo-Fabrizio fractional derivatives (${}_0^{CF}D_t^\alpha$) of order $\alpha \in (0, 1)$, we get:

$$\begin{cases} {}_0^{CF}D_t^\alpha M_U(t) &= \mu_U - \beta B M_U - \mu_U M_U, \\ {}_0^{CF}D_t^\alpha M_I(t) &= \beta B M_U - \alpha_T M_I T - \mu_I M_I, \\ {}_0^{CF}D_t^\alpha B(t) &= r\mu_I M_I + v(1 - B)B - \gamma_U M_U B - \mu_B B, \\ {}_0^{CF}D_t^\alpha T(t) &= k(1 - T)M_I + \frac{c_B BT}{e_B T+1} - \mu_T T, \end{cases} \tag{6}$$

with the initial conditions $M_U(0) \geq 0$, $M_I(0) \geq 0$, $B(0) \geq 0$, and $T(0) \geq 0$.

2.3 Equilibrium points

Equilibrium points can be found by setting each equation in system (6) to zero, so we have the infection-free equilibrium point

$$E_0 = (M_U, M_I, B, T) = (1, 0, 0, 0).$$

Next, the basic reproduction number, R_0, can be derived using the next-generation matrix method, where the classes responsible for infection are M_I and B. Thus, the differential equations used are

$$ {}_0^{CF}D_t^{\alpha} M_I = \beta B M_U - \alpha_T M_I T - \mu_I M_I, $$

$$ {}_0^{CF}D_t^{\alpha} B = r\mu_I M_I + v(1-B)B - \gamma_U M_U B - \mu_B B. $$

We can construct matrices $\mathcal{F}$ and $\mathcal{V}$, where $\mathcal{F}$ represents the rate of infection that increases the infected class, and $\mathcal{V}$ represents the rate of progression, recovery, and death that decreases the infected class. The matrices $\mathcal{F}$ and $\mathcal{V}$ are as follows:

$$ \mathcal{F} = \begin{pmatrix} \beta B M_U \\ v(1-B)B \end{pmatrix}, \quad \mathcal{V} = \begin{pmatrix} \alpha_T M_I T + \mu_I M_I \\ -r\mu_I M_I + \gamma_U M_U B + \mu_B B \end{pmatrix}. $$

The Jacobian matrices of $\mathcal{F}$ and $\mathcal{V}$ at E_0 are

$$ F = \begin{pmatrix} 0 & \beta \\ 0 & v \end{pmatrix}, \quad V = \begin{pmatrix} \mu_I & 0 \\ -r\mu_I & \gamma_U + \mu_B \end{pmatrix}. $$

Then the matrix G is given by

$$ G = FV^{-1} = \begin{pmatrix} \frac{\beta r}{\gamma_U + \mu_B} & \frac{\beta}{\gamma_U + \mu_B} \\ \frac{vr}{\gamma_U + \mu_B} & \frac{v}{\gamma_U + \mu_B} \end{pmatrix}. $$

The basic reproduction number R_0 is the spectral radius of the matrix G, it is

$$ R_0 = \frac{\beta r + v}{\gamma_U + \mu_B}. $$

Furthermore, the endemic equilibrium E_1 of system (6) is given by

$$ E_1 = (M_U^*, M_I^*, B^*, T^*), \tag{7} $$

where

$$ M_U^* = \frac{\mu_U}{\beta B^* + \mu_U}, \quad M_I^* = \frac{\beta B^* \mu_U}{(\beta B^* + \mu_U)(\alpha_T T + \mu_I)}, $$
$$ T^* = \frac{\mu_I}{\alpha_T A}\left(B^*\beta v - B^{*2}\beta v - B^*(v\mu_U + \beta\mu_B^*) + \mu_U(\gamma_U + \mu_B^*)(R_0 - 1)\right), $$

and B^* is the root of

$$ 0 = k(1 - T^*)M_I^* + \frac{c_B B T^*}{e_B T^* + 1} - \mu_T T^*. $$

After further substitutions and simplifications, we find that the resulting polynomial equation is of degree 7. Based on Abel-Ruffini's theorem, polynomial equations of degree higher than 5 generally cannot be solved algebraically [11], so we will solve them numerically in Section 3.1.

2.4 Stability of equilibrium points

The stability of the equilibrium points in the system of equations (6) is provided by the following theorem.

Theorem 2.1 *The infection-free equilibrium point* $E_0 = (M_U, M_I, B, T) = (1, 0, 0, 0)$ *is locally asymptotically stable if* $R_0 < 1$*, and unstable if* $R_0 > 1$*.*

Proof. The Jacobian matrix of the linearized system (6) at $E_0 = (M_U, M_I, B, T) = (1, 0, 0, 0)$ is

$$J(E_0) = \begin{pmatrix} -\mu_U & 0 & -\beta & 0 \\ 0 & -\mu_I & \beta & 0 \\ 0 & r\mu_I & v - \gamma_U - \mu_B & 0 \\ 0 & k & 0 & -\mu_T \end{pmatrix}.$$

The characteristic equation is

$$0 = (\lambda + \mu_U)(\lambda + \mu_T)\left[(\lambda + \mu_I)(\lambda - v + \gamma_U + \mu_B) - \beta r \mu_I\right].$$

The first two eigenvalues are

$$\lambda_1 = -\mu_U, \quad \lambda_2 = -\mu_T,$$

and the other two are the roots of the quadratic equation

$$\lambda^2 + \lambda W_1 + W_2 = 0, \tag{8}$$

where $W_1 = \gamma_U + \mu_B - v + \mu_I$ and $W_2 = \mu_I(\gamma_U + \mu_B - v - \beta r)$.

Thus, we have $|\arg(\lambda_1)| = |\arg(\lambda_2)| = \pi > \frac{\alpha\pi}{2}$. According to the Routh-Hurwitz criterion, the roots of equation (8) are negative if $W_1, W_2 > 0$. Following Ahmed [12], the roots of the quadratic equation (8) are negative if and only if $|\arg(\lambda_i)| > \frac{\alpha\pi}{2}$ or, equivalently, $R_0 < 1$. Thus, the infection-free equilibrium $E_0 = (M_U, M_I, B, T) = (1, 0, 0, 0)$ is locally asymptotically stable if $R_0 < 1$, and unstable if $R_0 > 1$.

Theorem 2.2 *Let* $D = \beta B^* + \mu_U$*,* $E = \beta B^*$*,* $F = \gamma_U B^*$*,* $G = \alpha_T T^* + \mu_I$*,* $H = r\mu_I$*,* $I = \beta M_U^*$*,* $K = \frac{c_B T^*}{e_B T^* + 1}$*,* $L = \alpha_T M_I^*$*,* $P = \frac{c_B e_B B^* T^*}{(e_B T^* + 1)^2} + k M_I^* + \mu_T$*,* $Q = \frac{c_B B^*}{e_B T^* + 1}$*, and* $R = \gamma_U M_U^* + 2vB^* + \mu_B$*. The endemic equilibrium point* E_1 *in* (7) *is locally asymptotically stable if* $s_1 > 0$*,* $s_4 > 0$*,* $s_1 s_2 - s_3 > 0$*,* $(s_1 s_2 - s_3)s_3 - s_1^2 s_4 > 0$*,* $A > 0$*, and* $B\beta v + \mu_U(\gamma_U + \mu_B)(R_0 - 1) > Y$*.*

Proof. Substituting the endemic equilibrium point E_1 into the Jacobian matrix of system (6), we get

$$J(E_1) = \begin{pmatrix} -D & 0 & -I & 0 \\ E & -G & I & -L \\ -F & H & -R + v & 0 \\ 0 & k - kT^* & K & Q - P \end{pmatrix}.$$

To ensure negative eigenvalues, we form the characteristic polynomial

$$p_1(\lambda) = \det(\lambda I - J(E_1)) = \lambda^4 + s_1\lambda^3 + s_2\lambda^2 + s_3\lambda + s_4,$$

where

$$
\begin{aligned}
s_1 &= D + G + P - Q + R - v,\\
s_2 &= (R - v + G + P - Q)D + (R - v + P - Q)G + (R - v)P + (v - R)Q - k(T^* - 1)L\\
&\quad - FI - HI,\\
s_3 &= ((R - v + P - Q)G + (R - v)P + (v - R)Q - k(T - 1)L - HI)\, D\\
&\quad + ((R - v)P + (v - R)Q - FI)\, G + (-FI - HI)P + (FI + HI)Q\\
&\quad + (-k(T - 1)R + k(T - 1)v + HK)\, L + EHI,\\
s_4 &= ((P - Q)(R - v)G - HPI + HQI - L(k(T - 1)R - k(T - 1)v - HK))\, D\\
&\quad - FGI(P - Q) + EHIP - EHIQ + kFIL(T - 1).
\end{aligned}
$$

By the Routh-Hurwitz criterion, the polynomial $p_1(\lambda)$ of order 4 will have all negative roots if and only if $s_1 > 0$, $s_4 > 0$, $s_1 s_2 - s_3 > 0$, $(s_1 s_2 - s_3)s_3 - s_1^2 s_4 > 0$,$A > 0$, and $B\beta v + \mu_U(\gamma_U + \mu_B)(R_0 - 1) > Y$. Thus, the endemic equilibrium $E_1 = (M_u^*, M_I^*, B^*, T^*)$ is locally asymptotically stable if these conditions are met.

3 Results and Discussion

3.1 Numerical simulation

In this section, we provided numerical simulations for the system of equations (6) using the Adams-Bashforth 3-step method.

We perform simulations for a first-order system using the possible parameter values from [3, 5]. We take the set of parameter values

$$
\begin{aligned}
\beta = 2.5 \times 10^{-5}, \alpha_T = 2.5 \times 10^{-5}, r = 0.1, v = 0.4, \gamma_U = 1.25 \times 10^{-8}, k = 0.4848, \quad (9)\\
c_B = 5 \times 10^{-3}, e_B = 10^{-4}, \mu_U = 0.02, \mu_I = 0.1, \mu_B = 0.42, \mu_T = 0.02.
\end{aligned}
$$

With this set of parameter values, we have $R_0 = 0.8571$ and the resulting interaction graph of M_U, M_I, B, T over time t is shown in Figure 2a. It can be seen that eventually the populations M_U, M_I, B, and T will move towards E_0.

Furthermore, we performed simulations using the parameter $\mu_B = 0.12$ and kept the values of the other parameters as before. With these parameter values, we have $R_0 = 3.0 > 1$ and the infective equilibrium points $E_1 = (0.9991673, 1.66529 \times 10^{-4}, 0.6666602, 4.82067 \times 10^{-3})$. The interaction graph of M_U, M_I, B, T over t is shown in Figure 2b. It is observed that the population of uninfected macrophages increases steadily towards the equilibrium point. Infected macrophages decrease as a result of interactions with T cells. Bacterial levels initially increase but eventually decrease due to interactions with uninfected macrophages. T cells increase in response to the presence of infected cells but decrease as infected macrophages decline.

Next, as for the stability of the equilibrium point E_0, Figure 3 shows that with varying initial conditions, the population will converge to E_0. In Figure 3, the simulation with various initial values shows that all growth graphs of uninfected macrophages, bacteria, and T cells converge towards the equilibrium point E_0, where the population of M_U approaches one, B approaches zero, and T approaches zero. This suggests that the equilibrium point E_0 is asymptotically stable and satisfies the condition $R_0 < 1$, which confirms Theorem 2.1. In this case, the bacteria cannot infect a sufficient number of

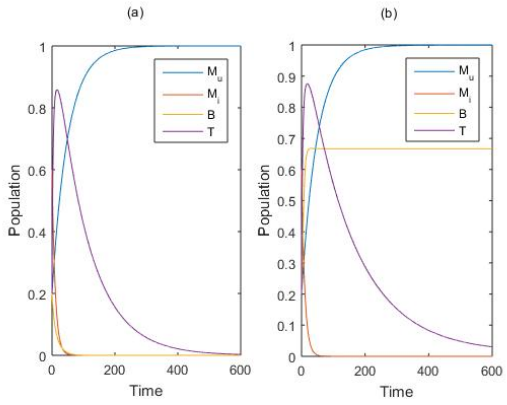

Figure 2: The dynamics interaction of M_U, M_I, B, T with respect to the set of parameter values in (9), (a) $R_0 = 0.8571$, (b)$R_0 = 3.00$.

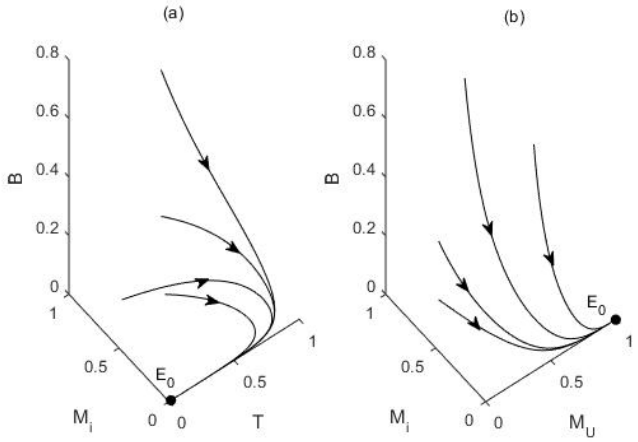

Figure 3: Phase portrait with different initial values confirms converge to E_0. (a) the phase portrait of M_I, B, T; (b) the phase portrait of M_U, M_I, B.

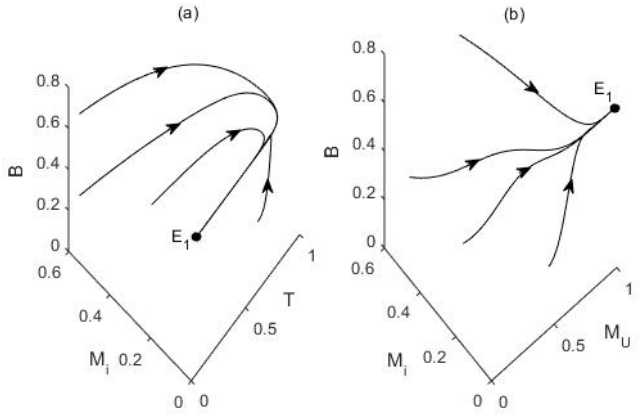

Figure 4: Phase portrait with different initial values confirm converge to E_1. (a) the phase portrait of M_I, B, T; (b) the phase portrait of M_U, M_I, B.

macrophages, the bacterial growth rate is low, or the immune response is capable of controlling the infection.

The graphical illustration related to the stability of the endemic equilibrium point is presented in Figure 4. In Figure 4a, the simulation with various initial values shows that the infected macrophages, bacteria, and T cells converge towards the endemic equilibrium point E_1. In Figure 4b, the simulation using various initial values shows that all growth graphs of uninfected macrophages, bacteria, and T cells converge towards the endemic equilibrium point E_1. The movement graphs of uninfected macrophages, infected macrophages, bacteria, and T cells show variables moving towards the equilibrium point $E_1 = (M_U^*, M_I^*, B^*, T^*)$ with $R_0 = 3.0$, indicating an average of 3 new infected macrophages per day. This suggests that the equilibrium point E_1 is asymptotically stable and satisfies the conditions $A > 0, B\beta v + (\gamma_U \Lambda_U + \mu_U \mu_B)(R_0 - 1) > Y, s_1 > 0, s_4 > 0, s_1 s_2 - s_3 > 0$, and $(s_1 s_2 - s_3)s_3 - s_1^2 s_4 > 0$, thus confirming Theorem 2.2.

The locally asymptotically stable equilibrium point E_1 implies that the number of uninfected macrophages remains significantly higher than the number of infected macrophages and bacteria, representing a latent state. This state suggests that bacterial growth exists but is still controllable by the immune system. If the immune system weakens, inactive bacteria may become active again, leading to active tuberculosis. This is consistent with [13], which states that the BCG tuberculosis vaccine has an efficacy of 60—80% against severe tuberculosis. According to [14], no tuberculosis vaccine has been shown to fully prevent and eliminate Mycobacterium tuberculosis infection, indicating that the bacteria remain in the human body.

Following [15], we calculate the sensitivity indices of each parameter with respect to the basic reproduction number R_0 presented in Table 1.

From Table 1, the most influential parameters on R_0 are the bacterial growth rate v and the bacterial death rate μ_B. The parameter v has a positive relationship with R_0,

Parameter	Sensitivity Index
β	$+6.25 \times 10^{-9}$
r	$+6.25 \times 10^{-9}$
v	$+1.000000000$
γ_U	-2.5×10^{-16}
μ_B	-1.00000000

Table 1: Sensitivity indices of R_0.

while μ_B has a negative relationship with R_0. If the parameter v is increased by 10% from 0.4 to 0.44, then R_0 increases from 0.8 to 0.88. Conversely, if v is decreased by 10% from 0.4 to 0.36, then R_0 decreases from 0.8 to 0.72. This result confirms that the sensitivity analysis aligns with the tested results on R_0.

3.2 Effect of variational order

In this section, we present numerical simulation results with fractional orders $\alpha = 0.6, 0.75, 0.85$, and 1 using the parameters in (9). The simulation results for uninfected macrophages, infected macrophages, bacteria, and T cells are illustrated in Figure 5.

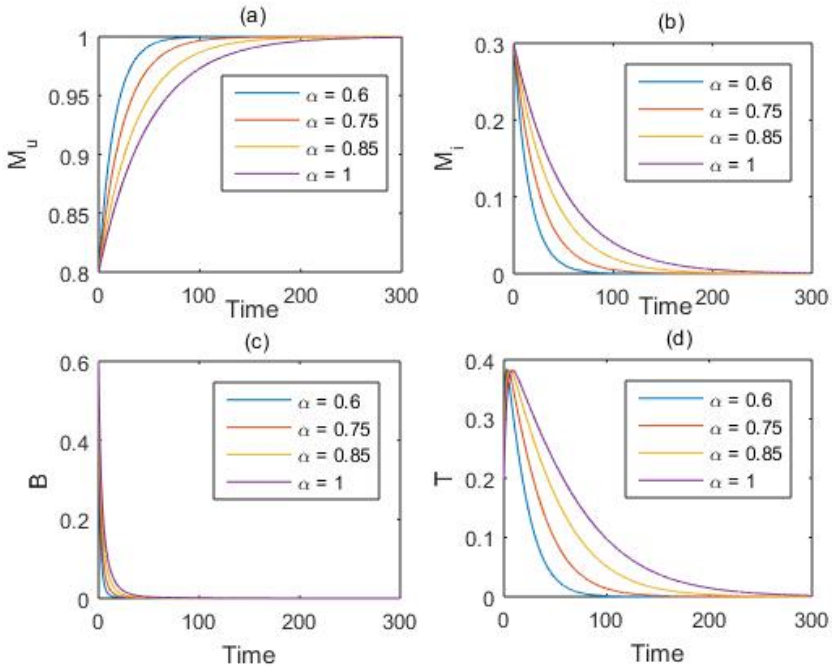

Figure 5: Graphs of uninfected macrophages, uninfected macrophages, bacteria Mtb, and T cells with different orders.

Figure 5a shows the population of uninfected macrophages with orders $\alpha = 0.6, 0.75, 0.85, 1$, all moving towards the equilibrium point with the same trend, regardless of the different orders used. The graph with order 0.6 reaches equilibrium faster

than with order 0.75, the graph with order 0.8 reaches equilibrium faster than with order 0.85, and so on. From the results of the numerical simulation, the graphs of uninfected macrophages, infected macrophages, bacteria and T cells converge to the equilibrium point, even when different orders are used, but follow the same trend as shown in Figure 5b-d. These figures indicate that the smaller the order used, the faster the immune response cells grow toward the equilibrium point.

4 Conclusion

This study presents a fractional-order mathematical model with the Caputo-Fabrizio derivative to understand the dynamics of Mycobacterium tuberculosis (Mtb) infection. The model offers a novel approach that incorporates memory effects, an aspect often overlooked in classical models. Key findings show that the fractional order value strongly influences the stability of the system and the rate of convergence of the immune response to a steady state. This provides new insights into how infections can persist or be controlled over time. Furthermore, the sensitivity of the model to certain parameters such as bacterial growth and death rates, demonstrates the importance of these elements in determining the overall behavior of the system. These results open up opportunities for broader applications in nonlinear dynamics, especially in studying other biological systems with similar characteristics, for example, chronic infections or complex ecological interactions. By integrating stability analysis, numerical simulations, and a memory effect-based approach, this study makes novel contributions to understanding complex biological interactions. This model is not only relevant for understanding TB dynamics, but also has the potential to develop more effective control strategies in the future.

Acknowledgment

We thank Universitas Ahmad Dahlan for supporting and funding this work under the supported research grant for professorship candidates.

References

[1] World Health Organization. Global Tuberculosis Report, 2022.

[2] T. Parbhoo, H. Schurz, J. M. Mouton and S. L. Sampson. Persistence of Mycobacterium tuberculosis in response to infection burden and host-induced stressors. *Frontiers in Cellular and Infection Microbiology* **12** (2022) 981827.

[3] M. Yao, Y. Zhang and W. Wang. Bifurcation analysis for an in-host mycobacterium tuberculosis model. *Discret. Contin. Dyn. Syst. - Ser. B* **26** (4) (2021) 2299–2322.

[4] I. M. Batiha, I. H. Jebril, S. Alshorm, M. Aljazzazi and S. Alkhazaleh. Numerical Approach for Solving Incommensurate Higher-Order Fractional Differential Equations. *Nonlinear Dyn. Syst. Theory* **24** (2) (2024) 123–134.

[5] E. Ibargüen-Mondragón, L. Esteva, and E. M. Burbano-Rosero. Mathematical model for the growth of Mycobacterium tuberculosis in the granuloma. *Math. Biosci. Eng.* **15** (2) (2018) 407–428.

[6] X. H. Zhang, A. Ali, M. .A Khan, M. Y. Alshahrani, T. Muhammad, S. Islam. Mathematical analysis of the TB model with treatment via a Caputo-type fractional derivative. *Discrete Dyn. Nat. Soc.* **2021** (2021) 1–15.

[7] Z. U. A. Zafar, S. Zaib, M. T. Hussain, C. Tunc and S. Javeed. Analysis and numerical simulation of the tuberculosis model using different fractional derivatives. *Chaos Solitons Fractals* **160** (2022) 11202.

[8] M. O. Olayiwola and K. A. Adedokun. A novel tuberculosis model incorporating a Caputo fractional derivative and treatment effect via the homotopy perturbation method. *Bull Natl Res Cent* **47** (121) (2023).

[9] X. Liu X, M. Arfan, M. Ur. Rahman and B. Fatima. Analysis of a SIQR-type mathematical model under the Atangana-Baleanu fractional diferential operator. *Comput Methods Biomech Biomed Engin* **26** (1) (2023) 98–112.

[10] M. Amira and F. Hannachi. A Novel Fractional-Order Chaotic System and Its Synchronization via Adaptive Control Method. *Nonlinear Dyn. Syst. Theory* **23** (4) (2023) 359–366.

[11] V. B. Alekseev. Abel's Theorem in Problems and Solutions. In: *Abel's Theorem Probl. Solut.* (2004) p. 103.

[12] E. Ahmed, A. M. A. El-Sayed and H. A. A. El-Saka, On some Routh-Hurwitz conditions for fractional order differential equations and their applications in Lorenz, Rossler, Chua and Chen systems. *Physics Letters A* **358** (1) (2006) 1-4.

[13] A. Roy, M. Eisenhut, R. J. Harris. et al. Effect of BCG vaccination against Mycobacterium tuberculosis infection in children: Systematic review and meta-analysis. *BMJ (Clinical research ed.)* **349** (2014) 1–11.

[14] J. Tang, W. C. Yam and Z. Chen. Mycobacterium tuberculosis infection and vaccine development. *Tuberculosis* **98** (2016) 30–41.

[15] Y. A. Adi and Suparman. An investigation of Susceptible-–Exposed—Infectious—Recovered (SEIR) tuberculosis model dynamics with pseudo-recovery and psychological effect. *Healthcare Analytics* **6** (2024) 100361.

Nonlinear Dynamics and Systems Theory, **25** (4) (2025) 373–385

Comparison of K-Nearest Neighbor and Neural Network for Forecasting Occupancy Rate at Hotel XYZ

M. Y. Anshori [1*], P. Katias [1], T. Herlambang [2], M. S. Azmi [3], Z. B. Othman [4] and K. Oktafianto [5]

[1] *Department of Management, Universitas Nahdlatul Ulama Surabaya, Indonesia.*
[2] *Department of Information Systems, Universitas Nahdlatul Ulama Surabaya, Indonesia.*
[3] *Department of Software Engineering, Fakulti Teknologi Maklumat dan Komunikasi, Universiti Teknikal Malaysia Melaka (UTeM), Malaysia.*
[4] *Department of Diploma Studies, Fakulti Teknologi Maklumat dan Komunikasi, Universiti Teknikal Malaysia Melaka (UTeM), Malaysia.*
[5] *Department of Mathematics, University of PGRI Ronggolawe, Indonesia.*

Received: July 12, 2024; Revised: July 4, 2025

Abstract: The occupancy rate of a hotel is an important factor to see the development of providers business performance. By forecasting occupancy rate, the hotel can identify business opportunities or adjust room prices, determine hotel operations, and take this into consideration for strategic decision making. In this study, occupancy rate forecasting for Hotel XYZ was carried out by comparing the k-nearest neighbor (k-NN) and neural network methods. The dataset used in this study included rooms available, rooms sold out, and available occupancy percentage data in Hotel XYZ from April 2018 to June 2023. The simulation was carried out by dividing the data into training data and testing data with a ratio of 70:30 and 80:20. Model creation was carried out by applying the k-NN and neural network methods to the Hotel XYZ data set. Forecasting results that were obtained using k-NN showed an optimal RMSE at 70%:30% split of data with an RMSE of 0.080 at k-value 3, while forecasting results obtained using the neural network showed an optimal RMSE at 70%:30% data split with an RMSE of 0.007 for two hidden layers. The comparison of results of forecasting by k-NN and neural network showed an optimal RMSE when using neural network method with an RMSE of 0.004, a GAP of 0.076 compared to using k-NN. The results of this study can be used by Hotel XYZ to make better decisions in determining hotel policies in the future and goals set by the hotel.

Keywords: *hotel; occupancy rate; forecasting; k-nearest neoghbor; neural network.*

Mathematics Subject Classification (2020): 68T45, 68T10.

* Corresponding author: mailto:yusak.anshori@unusa.ac.id

1 Introduction

Business development in the hotel sector in Indonesia has shown a positive trend, as can be seen from the increasing occupancy rate. The occupancy rate of star classified hotels in September 2023 reached an average of 53.02%, an increase of 3.00 points compared to the occupancy rate in September 2022 of 50.02% and YTD 2023 reached an average of 49.43%, an increase of 4.04 compared to the YTD 2022 occupancy rate of 45.40% [1]. The occupancy rate of non-star classified hotels in September 2023 reached an average of 24.82%, an increase of 1.43 points compared to the occupancy rate in September 2022 of 23.39% and YTD 2023 reached an average of 23.72%, an increase of 1.52 points compared to the YTD 2022 occupancy rate of 22.21% [2]. Along with this growth, competition among hoteliers is also increasing. In-depth knowledge of the level of competition is crucial to identify opportunities, face challenges, and develop effective strategies to compete competitively.

Occupancy rate is the percentage of sold room occupancy rate [3] and is one of the indicators that can be used to see the development of business efficiency of hotel service providers in a certain period [4]. This occupancy can be calculated before the current date, which is commonly called a forecast, or after the date passed [5]. By forecasting occupancy rate, the hotel can identify business opportunities or adjust room prices, determine hotel operations, and take this into consideration for strategic decision making.

In 1951, Evelyn Fix and Joseph Hodges created the k-nearest neighbor algorithm (k-NN) in statistics as a non-parametric supervised learning technique. Regression and classification are two uses for it. The input in both situations consists of a data set's k closest training samples [6]. K-NN is referred to as case-based reasoning, which is a methodology based on reasoning of cases in terms of training data of a case stored, trained, and accessed to solve new problems [7]. K-NN makes firm predictions on test data based on k-nearest neighbor comparisons. The near or far of neighbors is usually calculated based on Euclidian distance. The best k value for this algorithm depends on the data, usually a high k value will reduce the effect of noise on the application [8].

Neural networks have been around since 1943, when Warren McCulloch and Walter Pitts introduced the first neural network model calculations. This model describes the way artificial neurons can be used to process information binary. In 1950, Frank Ronseblatt continued his research by discovering a two-layer network called a perceptron. A neural network is a model with a flexible function structure, so the neural network model is rapidly developing and has been widely applied in various fields. Neural networks can be used to find solutions to problems when classical methods prove difficult or fail frequently [9].

In the previous studies, several forecasting methods were applied for the estimation of closed hotels and restaurants in Jakarta because of corona virus disease spread using an adaptive neuro fuzzy inference system [10], forecasting the number of Demam Berdarah Dengue (DBD) patients using the fuzzy method [11], predicting the number of visitors per period to beach attractions using triple exponential smoothing [12], classifying the price range of smartphones in the market using backpropagation and Learning Vector Quantification (LVQ) [13], for stock price estimation using Unscented Kalman Filter (UKF) [14], forecasting of occupied rooms in the hotel using linear support vector machine [15], profitability estimation using H-Infinity and Ensemble Kalman Filter (EnKF) [16], the analysis of demand and supply of blood in hospital in Surabaya city using panel

data regression [17], prediction of sunlight intensity using neural network and Adaptive Neuro Fuzzy Inference System (ANFIS) [18], estimation of closed hotels and restaurants because of Covid-19 spread using backpropagation neural network [19]. See also the neural network algorithm for breast cancer diagnosis [20], electronic nose for classifying civet coffee using Support Vector Machine (SVM), k-nearest neighbors (k-NN), and decision tree [21], forecasting agricultural products in Malang Regency using k-NN [22], forecasting average room rate using k-NN [23], forecasting occupancy rate using neural network [24]. In this study, the k-NN and neural network methods with data ratios of 70%: 30% and 80%: 20% are applied for forecasting occupancy rate at Hotel XYZ so that the results can be used in identifying opportunities, operational implementation, and strategic decision making for management.

2 Research Method

2.1 Occupancy rate

Occupancy rate is the level of occupancy of hotel rooms calculated based on the number of rooms rented by guests and compared to the number of rooms available in a certain period [5]. The calculation of occupancy rate is shown in (1) with the result of the calculation being a percentage index measured from 0% to 100%.

$$Occupancy\ Rate\ \% = \frac{RoomSold}{RoomAvailable} \times 100\%. \tag{1}$$

The occupancy shows the number of rooms sold out of the number of available rooms. This ratio can fluctuate every day, the ratio in one month or one year is the average percentage of rooms sold. The highest occupancy rate is the best indicator for the hotel and a measure of the success of hotel operations.

2.2 K-Nearest neighbor

K-nearest neighbor (k-NN) is a classification technique that makes firm predictions on test data based on the comparison of K nearest neighbors [8]. The nearest neighbor is the trained object that has the greatest similarity value or the smallest dissimilarity with the previous data. The number of nearest neighbors is expressed by the value of k. The best k value depends on the data. In general, a high k value will reduce the effect of noise on classifications but make the boundaries between each classification even more blurred [25].

The purpose of the k-NN algorithm is to classify new objects based on attributes and training samples. The results of the new test sample are classified based on the majority of categories in k-NN using the neighborhood classification as the predictive value of the new test data sample. The distance used is Euclidean Distance with the following formula:

$$d_i = \sqrt{\Sigma_{i=1}^{n}(p_i - q_i)^2}, \tag{2}$$

$$d_i = \sqrt{(p_1 - q_1)^2 + (p_2 - q_2)^2 + \ldots + (p_n - q_n)^2}, \tag{3}$$

where p_i is the sample data; q_i is the test data; i is the data variable; d is the distance; n is the data dimension.

The working principle of k-NN is to find the closest distance between the data to be evaluated and the nearest k (neighbor) in the training data. The sequence of k-NN

work processes [25], [26] is as follows. Specify the parameter k (the number of the closest neighbors). Calculate the square of each object's Euclid jar (query instance) against the given sample data using an equation. Then sort the objects into groups that have the smallest Euclidean distance. Collect the nearest neighbor classification category.

By using the nearest neighbor category, that is, the most majority, one can predict the value of the query instance that has been calculated.

2.3 Neural network

The basis of neural networks consists of inputs, weights, processing units, and outputs. Neural networks can be applied to classifying patterns, mapping patterns obtained from inputs into new patterns in outputs, storing patterns to be recalled, mapping similar patterns, optimizing problems, and predicting. Neural networks start from preparing data for training and learning, finding neural network architecture, training and learning processes, and testing processes [27]. Neural networks can be divided into three parts called layers. Input layer, responsible for receiving information, signals, features, or measurements from the external environment. Hidden layers, responsible for extracting patterns related to the process or system being analyzed. The output layer, responsible for producing and presenting the final tissue, results from processing by neurons in the previous layer.

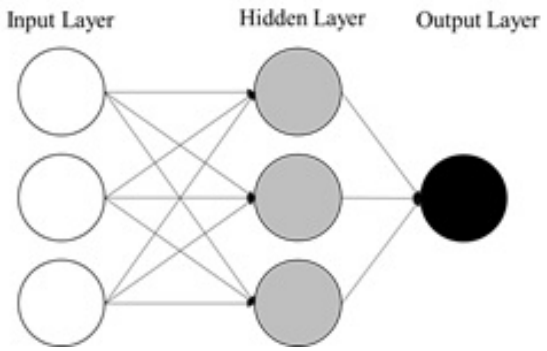

Figure 1: Arrangement of neural networks in layers.

Neural networks can change structures to solve problems based on internal and external information flowing through the network. Neural networks can be used to model the relationship between input and output to find patterns of data. Neurons are a basic part of the processing of a neural network. The basic shape of a neuron can be seen in Figure 2 below.

The weight vector (w) contains weights that connect the various parts of the network. The term "w" is used in the terminology of neural networks and is a suggestion of the expression of connections between two neurons, that is, the weight of information flowing from neuron to other neurons in the neural network. The first stage is the process of summing inputs $x_1, x_2, \ldots, x_n$, which is multiplied by its weight $w_1, w_2, \ldots, w_n$ and is expressed as

$$Net = (w_1x_1 + w_2x_2 + w_3x_3 + \ldots + w_nx_n)\,. \tag{4}$$

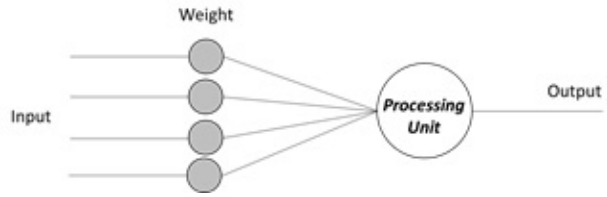

Figure 2: Basic form of neurons.

This concept can be written in vector notation as follows:

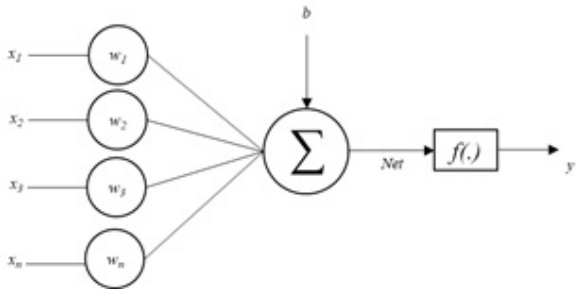

Figure 3: Perceptron model.

A threshold value of b is called a bias, which plays an important role for some neuron models and is referred to as a separate neuron model parameter. Various input conditions and influences on output are required to include a nonlinear activation function $f(\cdot)$ in the arrangement of neurons [28]. This aims to achieve an adequate level if the input signal is small and avoid the risk of output going to inappropriate limits. Like the perceptron model in Figure 2, the output of the neuron can be expressed in terms of $y = f(net)$.

3 Result and Discussion

The dataset used in this study includes rooms available, rooms sold out, and available occupancy percentage data in Hotel XYZ. The dataset used is from April 2018 to June 2023 (63 months). Furthermore, the data is split into training data and testing data. Then a test analysis is carried out with k-nearest neighbor and neural network. After that, a comparison of RMSE results from several tests of the algorithm is carried out.

3.1 Making a comparison model of K-Nearest neighbor and neural network

At this stage, the Hotel XYZ dataset testing process is carried out using k-NN and neural network. The Hotel XYZ dataset that has been entered is then selected for the rooms available, rooms sold out, and available occupancy percentage attributes. The Hotel XYZ dataset is further divided into training data and testing data using a ratio of 70 : 30 and 80 : 20. The model is designed using k-NN with k-values 3 to 7 and using the neural network with one hidden layer and two hidden layers.

3.2 K-Nearest neighbor algorithm test analysis

At this stage, a comparison of the results of the test was carried out using the k-NN algorithm with k-values 3 to 7 at the split of data with a percentage ratio of 70 : 30 and 80 : 20. The results of the k-NN algorithm testing can be seen in Table 1.

k-Values	Training Data	Testing Data	RMSE	k-Values	Training Data	Testing	RMSE
3	70%	30%	0.080	3	80%	20%	0.102
4	70%	30%	0.079	4	80%	20%	0.101
5	70%	30%	0.082	5	80%	20%	0.098
6	70%	30%	0.086	6	80%	20%	0.106
7	70%	30%	0.090	7	80%	20%	0.120

Table 1: Test Results Using k-NN.

From forecasting carried out using k-NN at 70% : 30% split of data, it is clear that the best RSME is for k-value 3 with an RMSE of 0.080. The comparison of the simulation with k-values 3 to 7 at 70% : 30% data split can be seen in Figure 4.

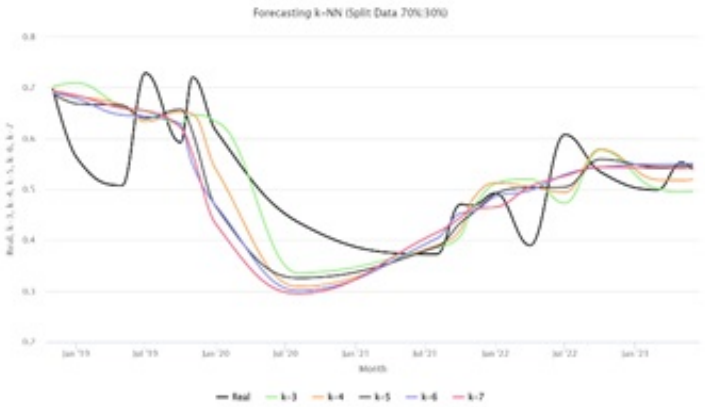

Figure 4: Occupancy rate prediction using k-NN (split of data 70% : 30%).

Figure 5 shows the comparison of real occupancy rate data and occupancy rate prediction at 70% : 30% data split using the k-NN algorithm with k-value 3. In the graph, the black line shows real occupancy data, and the green line shows occupancy forecasting data with k-value 3. There was a significant decrease in August 2021 with an occupancy rate of 0.37 in real data and an occupancy rate of 0.39 in forecasting data. The highest ARR was in July 2019 with an occupancy rate of 0.73 in real data and an occupancy rate of 0.65 in forecasting data.

From forecasting carried out using k-NN at 80% : 20% split of data, it is clear that the best RSME is for k-value 5 with an RMSE of 0.098. The comparison of the simulation with k-values 3 to 7 at 80% : 20% data split can be seen in Figure 6.

Figure 7 shows the comparison of real occupancy rate data and occupancy rate prediction at 80% : 20% data split using the k-NN algorithm with k-value 5. In the graph,

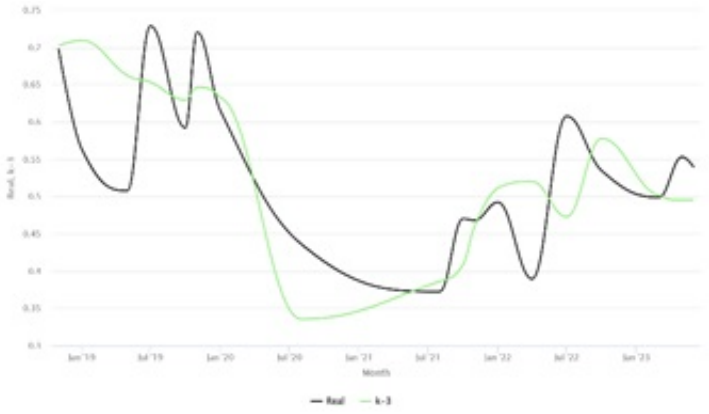

Figure 5: Occupancy rate prediction using k-NN with k-value 3 (split of data 70% : 30%).

Figure 6: Occupancy rate prediction using k-NN (split of data 80% : 20%).

the black line shows real occupancy data, and the green line shows occupancy forecasting data using k-NN with k-value 5. There was a significant decrease in April 2020 with an occupancy rate of 0.19 in real data and an occupancy rate of 0.35 in forecasting data. The highest ARR was December 2019 with an occupancy rate of 0.73 in real data and an occupancy rate of 0.57 in forecasting data.

3.3 Neural network algorithm test analysis

At this stage, a comparison of the results of the test was carried out using a neural network algorithm at the split of data with a percentage ratio of 70:30 and 80:20. In testing, the neural network algorithms for one hidden layer and two hidden layers were used. The results of the neural network algorithm testing can be seen in Table 2.

From forecasting carried out using neural network at 70% : 30% split of data, it is clear that the best RSME is found for one hidden layer with an RMSE of 0.004. The

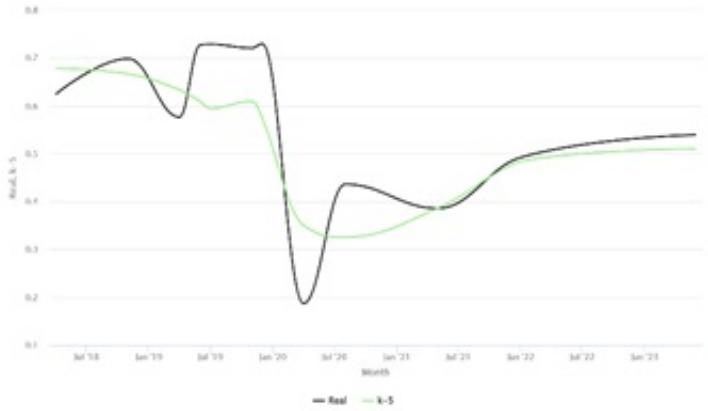

Figure 7: Occupancy rate prediction using k-NN with k-value 5 (split of data 80% : 20%).

Hidden Layer	Training Data	Testing Data	RMSE	Hidden Layer	Training Data	Testing Data	RMSE
1	70%	30%	0.004	1	80%	20%	0.005
2	70%	30%	0.007	2	80%	20%	0.015

Table 2: Test Results Using Neural Network.

comparison of the simulation with one hidden layer and two hidden layers at 70% : 30% data split can be seen in Figure 8.

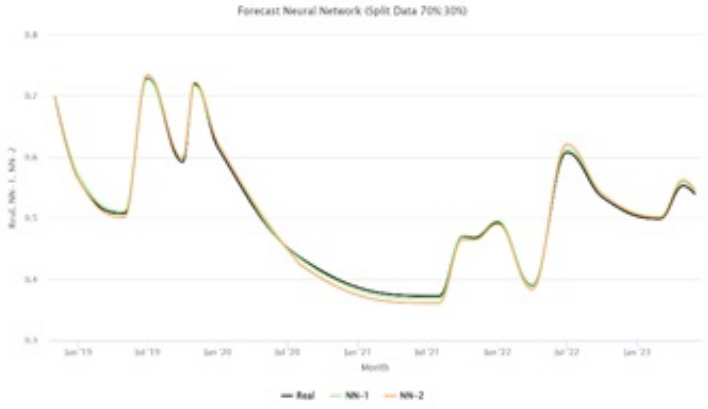

Figure 8: Occupancy rate prediction using neural network (split of data 70% : 30%).

Figure 9 shows the comparison of real occupancy rate data and occupancy rate prediction at 70% : 30% data split using the neural network algorithm with one hidden layer. In the graph, the black line shows real occupancy data, and the green line shows occupancy forecasting data using the neural network with one hidden layer. There was a

significant decrease in August 2021 with an occupancy rate of 0.367 in real data and an occupancy rate of 0.372 in forecasting data. The highest ARR was in July 2020 with an occupancy rate of 0.729 in real data and an occupancy rate of 0.27 in forecasting data.

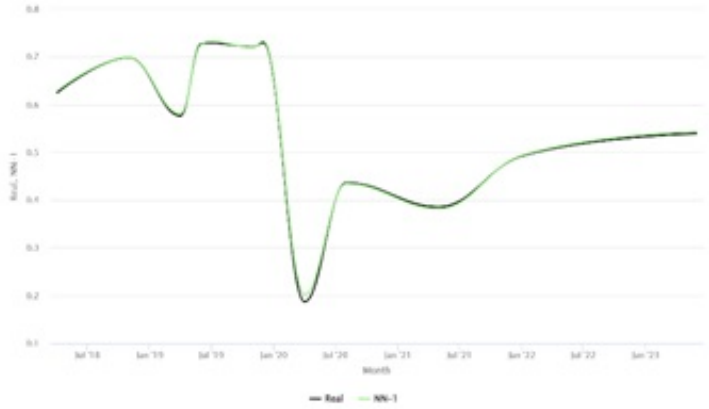

Figure 9: Occupancy rate prediction using neural network with one hidden layer (split of data 70% : 30%).

From forecasting carried out using neural network at 80% : 20% split of data, it is clear that the best RSME is found for one hidden layer with an RMSE of 0.005. The comparison of the simulation with one hidden layer and two hidden layers at 80% : 20% data split can be seen in Figure 10.

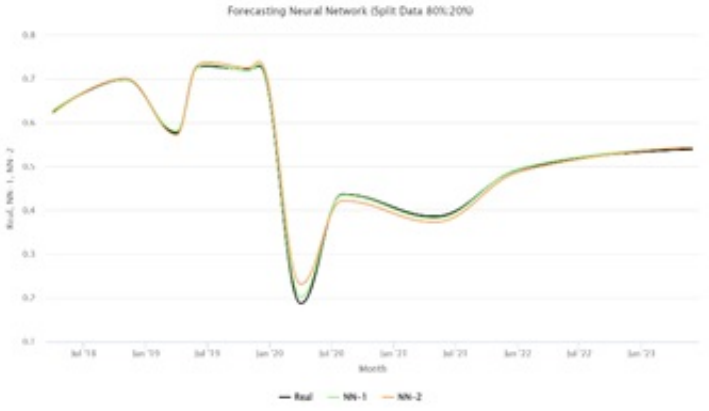

Figure 10: Occupancy rate prediction using neural network (split of data 80% : 20%).

Figure 11 shows the comparison of real occupancy rate data and occupancy rate prediction at 80% : 20% data split using the neural network algorithm with one hidden layer. In the graph, the black line shows real occupancy data, and the green line shows occupancy forecasting data using the neural network with one hidden layer. There was a significant decrease in August 2021 with an occupancy rate of 0.367 in real data and

an occupancy rate of 0.372 in forecasting data. The highest ARR was July 2020 with an occupancy rate of 0.729 in real data and an occupancy rate of 0.27 in forecasting data.

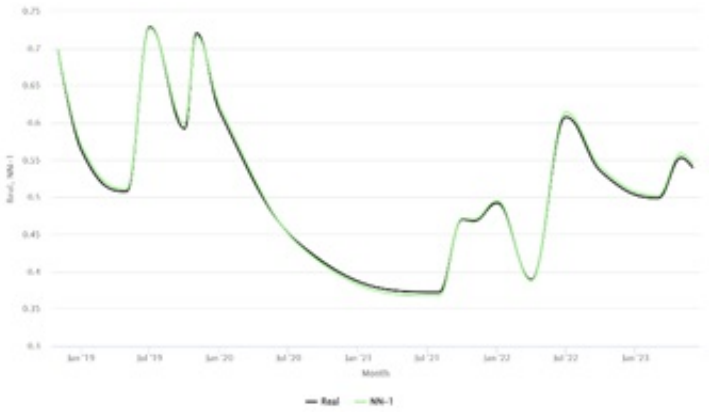

Figure 11: Occupancy rate prediction using neural network with one hidden layer (split of data 80% : 20%).

3.4 Algorithm testing comparison

At this stage, the most optimal RMSE results from each test with k-NN and neural network are compared. The results of the comparison of these algorithm tests are shown in Table 3.

Algorithm	Split data (%)	RSME	Remarks
k-NN	70:30	0.080	k-value = 3
	80:20	0.098	k-value = 5
Neural network	70:30	0.004	one hidden layer
	80:20	0.005	one hidden layer

Table 3: Comparison of Algorithm Testing.

From the comparison results, the most optimal RMSE result for k-NN at 70% : 30% data split with k-value 3 is an RMSE of 0.080, while for neural networks also at 70% : 30% data split with one hidden layer, an RMSE is 0.004. The results of comparison of occupancy rate forecasting using k-NN and neural network at 70% : 30% split of data can be seen in Figure 12. In the graph, the black line shows real occupancy rate data, the green line shows occupancy rate prediction data using the k-NN algorithm with k-value 3, and the orange line shows occupancy rate prediction data using the neural network algorithm with one hidden layer.

The comparison results for occupancy rate forecasting using k-NN and neural network resulted in the most optimal RMSE for the neural network algorithm with one hidden layer resulting in an RMSE of 0.004, a difference of 0.076 compared to using the k-NN algorithm. The evaluation of RMSE results for the k-NN and neural network algorithms reveals that the neural network, specifically with one hidden layer at 70% : 30% data

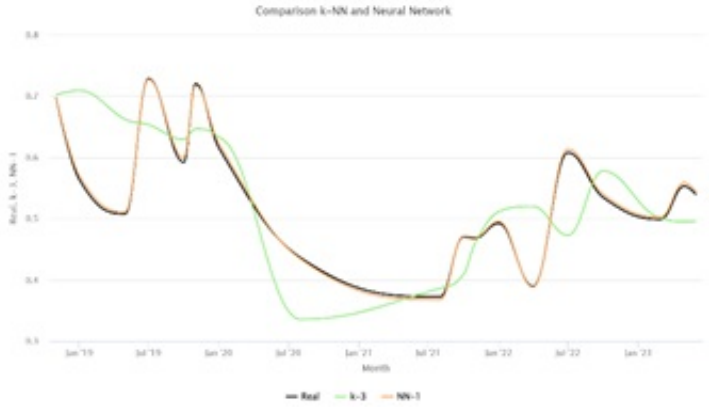

Figure 12: Comparison of occupancy rate predictions using k-NN and neural network (split of data 70% : 30%).

split, outperforms k-NN with a noticeable margin. The optimal RMSE of 0.004 for the neural network demonstrates its effectiveness in occupancy rate forecasting compared to the best-performing k-NN configuration, which achieved an RMSE of 0.080 at 70% : 30% data split and k-value of 3. These findings underscore the superiority of the neural network approach in this specific context.

4 Conclusion

Based on a comparison of tests using k-nearest neighbor and neural network to determine occupancy rate forecasting at Hotel XYZ with split of data 70% : 30% and 80% : 20%, the most optimal RMSE results were obtained using the neural network with one hidden layer at 70% : 30% split of data with an RMSE of 0.004. So, it is recommended for Hotel XYZ to use a neural network with one hidden layers for occupancy rate forecasting, which can later support better decisions in determining hotel policies in the future and goals set by the hotel. For other research, this study can be a reference to increase knowledge and conduct further investigations and develop other methods.

Acknowledgment

High appreciation to the Kemdikbudristek for the very fund support for the completion of the research conducted in the year of 2024 with contract number 109/E5/PG.02.00.PL/2024, 054/SP2H/PT/LL7/2024, and 1104/UNUSA-LPPM/Adm.I/VI/2024.

References

[1] Anonim. *Star Hotel Room Occupancy Rate 2023*. November 2023.

[2] Anonim. *Non-Star Hotel Room Occupancy Rate in 2023*. Sep. 03, 2023. [Online]. Available: https://kemenparekraf.go.id/direktori-statistik/tingkat-penghunian-kamar-hotel-non-bintang-tahun-2023.

[3] B. Hermawan. *Hotel Operational Analysis*. NEM, Pekalongan, Indonesia, 2022.

[4] BPS-Statistics Indonesia. *Occupancy Rate of Hotel Room 2022*. Jakarta, May 2023.

[5] S. Sofiani and I. S. Djunaid. *Hotel Front Office Management*. Yogyakarta: Star Universe Media, 2023.

[6] F. Sabry. *K Nearest Neighbor Algorithm: Fundamentals and Applications*. One Billion Knowledgeable, 2022.

[7] M. Arhami and M. Nasir. *Data Mining – Algorithms and Implementation*. Penerbit Andi, 2020.

[8] J. Indriyanto. *K-Nearest Neighbor Algorithm for Insurance Customer Prediction*. NEM, 2021.

[9] S. Chakraverty and S. K. Jeswal. *Applied Artificial Neural Network Methods for Engineers and Scientists*. World Scientific, 2021.

[10] D. Novita et al. Comparison of K-Nearest Neighbor and Neural Network for Prediction International Visitor in East Java. *BAREKENG: Journal of Mathematics and Its Applications* **18** (3) (2024) 2057–2070.

[11] F. S. Rini, T. D. Wulan and T. Herlambang. Forecasting the Number of Demam Berdarah Dengue (DBD) Patients Using the Fuzzy Method at the Siwalankerto Public Health Center. In: *AIP Conference Proceedings*, American Institute of Physics Inc., Jan. 2023.

[12] A. Rahim, A. D. Rahajoe and M. Mahaputra. Prediction of the Number of Visitors Per Period to Beach Tourism Sites Using Triple Exponential Smoothing (Case Study of Gili Labak Beach, Sumenep). *JIFTI-Scientific Journal of Information Technology and Robotics* **3** (2) (2021) 39–43.

[13] T. Herlambang, V. Asy'ari, R. P. Rahayu, A. A. Firdaus and N. Juniarta. Comparison of Naïve Bayes and K-Nearest Neighbor Models For Identifying The Highest Prevalence Of Stunting Cases In East Java. *BAREKENG: Journal of Mathematics and Its Applications* **18** (4) (2024) 2153–2164.

[14] D. F. Karya, P. Katias, T. Herlambang and D. Rahmalia. Development of Unscented Kalman Filter Algorithm for stock price estimation. *J. Phys. Conf. Ser.* **1211** (1) (2019) 012031.

[15] I. Indasah, A. Y. P. Asih, T. Herlambang, P. Triwinanto and K. Oktafianto. Forecasting Air Pollution Levels Using Support Vector Regression and K-Nearest Neighbor Algorithm. *Nonlinear Dynamics and System Theory* **25** (2) (2025) 153–160.

[16] A. Muhith. The Analysis of Demand and Supply of Blood in Hospital in Surabaya City Using Panel Data Regression. *Nonlinear Dynamics and System Theory* **22** (5) (2022) 550–560.

[17] A. Muhith, I. H. Susanto, D. Rahmalia, D. Adzkiya and T. Herlambang. Profitability estimation of XYZ company using H-infinity and Ensemble Kalman Filter. In: *The Analysis of Demand and Supply of Blood in Hospital in Surabaya City Using Panel Data Regression*, 2022.

[18] D. Rahmalia et al. Comparison between Neural Network (NN) and Adaptive Neuro Fuzzy Inference System (ANFIS) on sunlight intensity prediction based on air temperature and humidity. *J. Phys. Conf. Ser.* **1538** (1) (2020) 012044.

[19] F. A. Susanto, et al. Estimation of Closed Hotels and Restaurants in Jakarta as Impact of Corona Virus Disease (Covid-19) Spread Using Backpropagation Neural Network. *Nonlinear Dynamics and System Theory* **22** (4) (2022) 457–467.

[20] F. S. Nugraha, M. J. Shidiq, and S. Rahayu. Analysis of Neural Network Classification Algorithm for Breast Cancer Disease Diagnosis). *Nusa Mandiri Pillar Journal* **15** (2) (2019) 149–156.

[21] D. B. Maghfira et al. Electronic Nose for Classifying Civet Coffee and Non-Civet Coffee. *Nonlinear Dynamics and System Theory* **23** (3) (2023) 323–337.

[22] P. Andrean. Application of K-NN Method to Predict Agricultural Results in Malang Regency. *Journal of Informatics Engineering Students* **3** (1) (2019) 235–242.

[23] V. Asy'ari, M. Y. Anshori, T. Herlambang, I. W. Farid, D. Fidita Karya, and M. Adinugroho. Forecasting average room rate using k-nearest neighbor at Hotel S. In: *International Conference on Advanced Mechatronics, Intelligent Manufacture and Industrial Automation (ICAMIMIA)*), IEEE, Nov. 2023, 496–500.

[24] V. Asy'Ari, et al. Forecasting average room rate using k-nearest neighbor at Hotel S. In: *International Conference on Advanced Mechatronics, Intelligent Manufacture and Industrial Automation (ICAMIMIA)*), 2023.

[25] U. Hidayah and A. Sifaunajah. *Easy Way to Understand K-Nearest Neighbor Algorithm Visual Basic 6.0 Case Study*. Jombang: LPPM KH. A. Wahab Hasbullah University, 2019.

[26] F. Gorunescu. *Data Mining: Concepts, Models and Techniques*. Berlin, Heidelberg: Springer Berlin Heidelberg, 2011.

Nonlinear Dynamics and Systems Theory, **25** (4) (2025) 386–398

Stability Analysis of a COVID-19 SIR Model with Direct and Indirect Transmission

Akram Boukabache *

Department of Sciences, Teacher Education College of Setif - Messaoud Zeghar, P.O. Box 556, El-Eulma 19600, Sétif, Algeria

Received: July 17, 2024; Revised: July 14, 2025

Abstract: This paper develops a SIR model for COVID-19 that incorporates both direct and indirect transmission dynamics through two distinct incidence rates. To capture the infection rate, we employ a nonlinear Beddington-DeAngelis function and a bilinear incidence function. The model's solutions are shown to be positive and bounded, with two equilibrium points identified: the disease-free equilibrium E_0 and the endemic equilibrium E^*. We establish that E_0 is locally and globally asymptotically stable when the basic reproduction number $R_0 < 1$. Conversely, under specific parameter conditions, E^* is uniformly asymptotically stable for $R_0 > 1$. Numerical simulations are provided to validate the theoretical results.

Keywords: *epidemic model; direct-indirect transmission; incidence function; stability analysis.*

Mathematics Subject Classification (2020): 92B05, 65L10, 93D05, 34D20.

1 Introduction

The COVID-19 pandemic has spurred research across many fields, including the development of mathematical models to assess the impact of interventions on disease control. Kermack and McKendrick [10] pioneered the use of compartmental models for disease dynamics research, leading to the development of various models such as SIR, SIRS, and SEIRS [1, 2, 7, 9, 11, 12].

Incidence functions are crucial in epidemic models as they determine how susceptible individuals transition to infected, significantly influencing model predictions. Epidemiological models often assume well-mixed populations in uniform environments. These models typically use the bilinear incidence rate βSI [10,17] or the standard incidence rate

* Corresponding author: mailto:akramboukabache@gmail.com

$\frac{\beta SI}{N}$ [11,13], where β represents the transmission coefficient and N is the total population. However, when a model incorporates a more realistic population structure with varied mixing patterns and potentially nonlinear transmission dynamics, these standard rates might need adjustments. The probability of infection per contact might be influenced by the number of infected individuals. As the infected population grows, the infection rate may not increase proportionally due to saturation effects, leading to a nonlinear relationship. To address this, nonlinear incidence rates such as the Beddington-DeAngelis rate, $\frac{\beta SI}{1+\alpha_1 S+\alpha_2 I}$, [3, 5] have been incorporated into epidemiological models to better capture the complexities of disease transmission.

Recently, Ahmed et al. [1] conducted a bifurcation analysis of an SIR epidemic model that incorporates both direct and indirect transmission rates. They employed a standard incidence rate, $\frac{\beta SI}{S+I}$, for direct transmission and a bilinear incidence term, βSI, for indirect transmission. This approach takes into account the various ways in which diseases spread through different types of contact. However, their study focused on bifurcation analysis. In this paper, we investigate the stability of an SIR model that incorporates the Beddington-DeAngelis term for direct transmission and the bilinear term for indirect transmission. This combination offers a more realistic representation of transmission dynamics. A constant recruitment rate Λ ensures a steady flow of susceptible individuals due to births. Direct transmission is influenced by the average number of meetings m_i between susceptible and infected individuals within a time interval Δt and the probability of infection success s_c. The Beddington-DeAngelis term $\frac{\beta_d SI}{1+\alpha_1 S+\alpha_2 I}$ captures this, here, $\beta_d = m_i s_c > 0$ and $\frac{S}{1+\alpha_1 S+\alpha_2 I}$ is the proportion of the susceptible population in time t. In contrast, indirect transmission occurs when susceptible individuals come into contact with the virus on surfaces, without directly interacting with infected individuals. This is modeled as a mass contact process with an indirect infection rate $\beta_i > 0$. The bilinear incidence term $\beta_i SI$ represents the rate of indirect COVID-19 transmission through contaminated surfaces. To the best of our knowledge, there is no SIR model that combines direct (Beddington-DeAngelis) and indirect (bilinear) transmissions.

The manuscript is organized as follows. Section 2 establishes the well-posedness of the model by demonstrating the existence, positivity, and boundedness of its solutions. In Section 3, we analyze the model, compute the basic reproduction number, and prove the existence of equilibria. Section 4 delves into the analytical properties of the model, including the stability analysis of the equilibria. Numerical simulations are given in Section 5, and concluding remarks are offered in the closing section.

2 Model Formulation and Analysis

We consider the total population at time t, it is denoted by $N(t)$ and divided into three compartments: susceptible individuals $S(t)$, infected individuals $I(t)$ and recovered individuals $R(t)$, where $N(t) = S(t)+I(t)+R(t)$. Susceptible individuals are healthy but vulnerable to infection, while infected individuals can transmit the disease and eventually transit to the recovered state, either through immunity or treatment.

Based on the previous assumptions, the SIR model with direct and indirect transmis-

sions is described by the following system of differential equations:

$$\begin{aligned}
\frac{dS}{dt} &= \Lambda - \frac{\beta_d SI}{1+\alpha_1 S+\alpha_2 I} - \beta_i SI - \mu S,\\
\frac{dI}{dt} &= \frac{\beta_d SI}{1+\alpha_1 S+\alpha_2 I} + \beta_i SI - (d+\gamma+\mu)\, I,\\
\frac{dR}{dt} &= \gamma I - \mu R
\end{aligned} \tag{1}$$

with the given initial conditions $S(0) \geq 0, I(0) \geq 0$ and $R(0) \geq 0$.

The parameters involved in this model and their corresponding interpretations are given in Table 2. The flowchart of the SIR model is illustrated in Figure 1.

Parameter	Description
Λ	Recruitment rate
β_d	Direct transmission rate
β_i	Indirect transmission rate
α_1	Measure of inhibition (taken by susceptibles)
α_2	Measure of inhibition (taken by infectives)
μ	Natural death rate
d	Infection death rate
γ	Natural recovery rate

Table 1: Description of biological parameters.

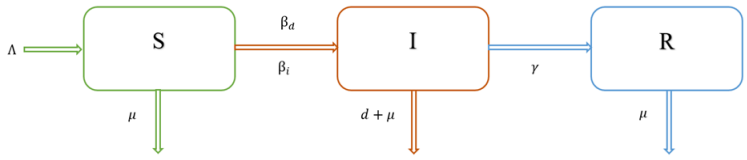

Figure 1: Flowchart of the proposed model.

For problems concerning population dynamics, it is crucial to ensure that solutions remain non-negative and bounded for all time. To achieve this, we define the region $\Omega = \{(S,I,R) \in \mathbb{R}^3_+ : S \geq 0, I \geq 0, R \geq 0\}$.

Theorem 2.1 *For any non-negative initial data, the solutions of* (1) *exist, remain bounded and non-negative in* Ω. *Moreover, we have*

$$N(t) \leq \frac{\Lambda}{\mu}.$$

Proof. Based on the well-established theory of differential equations in a functional framework (see, e.g., [8]), we can ensure a unique local solution for problem (1). To establish solution positivity, we prove invariance of the positive set Ω. We have

$$\left.\frac{dS}{dt}\right|_{S=0} = \Lambda > 0, \qquad \left.\frac{dI}{dt}\right|_{I=0} = 0 \geq 0, \qquad \left.\frac{dR}{dt}\right|_{R=0} = \gamma I \geq 0.$$

Hence, for all $t \geq 0$, the positivity of all solutions initiating in Ω is guaranteed.

For the boundedness, we utilize the fact that $N = S + I + R$. By summing the equations of the model (1), we have

$$\frac{dN}{dt} = \Lambda - \mu N - dI.$$

As $I \geq 0$, we get

$$\frac{dN}{dt} \leq \Lambda - \mu N,$$

and therefore,

$$N(t) \leq \frac{\Lambda}{\mu} + \left(N(0) - \frac{\Lambda}{\mu}\right) e^{-\mu t}.$$

Thus, $\lim_{t\to\infty} \sup N(t) \leq \frac{\Lambda}{\mu}$ and $\frac{dN}{dt} < 0$ if $N > \frac{\Lambda}{\mu}$. This reveals that the total population size $N(t)$ is bounded, and so is each compartment $S(t)$, $I(t)$ and $R(t)$.

3 The Steady States

The existence of a disease-free equilibrium (DFE) and that of an endemic equilibrium for our model are established in this subsection. Due to the fact that the first two equations of the system (1) are not affected by $R(t)$, and considering that the total population number is $N(t) = S(t) + I(t) + R(t)$, we may omit the last equation of the system (1). As a result, the problem can be reduced to

$$\begin{aligned} \frac{dS}{dt} &= \Lambda - \frac{\beta_d SI}{1 + \alpha_1 S + \alpha_2 I} - \beta_i SI - \mu S, \\ \frac{dI}{dt} &= \frac{\beta_d SI}{1 + \alpha_1 S + \alpha_2 I} + \beta_i SI - \delta I, \end{aligned} \tag{2}$$

where $\delta = d + \gamma + \mu$ and $S, I \geq 0$.

In order to find the equilibria of the system (2), we solve the following system:

$$\Lambda - \frac{\beta_d SI}{1 + \alpha_1 S + \alpha_2 I} - \beta_i SI - \mu S = 0,$$

$$\frac{\beta_d SI}{1 + \alpha_1 S + \alpha_2 I} + \beta_i SI - \delta I = 0.$$

Obviously, $E_0 = \left(\frac{\Lambda}{\mu}, 0\right)$ is the DFE of (2).

When the system reaches the DFE point E_0, the disease vanishes completely. At this point, the infected population becomes zero, and the remaining population consists only of susceptible individuals.

3.1 Basic reproduction number

The basic reproduction number R_0 is crucial in epidemiology as it predicts disease spread and informs control strategies. It estimates the average number of new infections caused by one infected individual. By using the next-generation matrix method [15], we can easily find R_0. Let $X(t) = (S(t), I(t))$, then it follows from model (2) that

$$\frac{dX}{dt} = \mathcal{F} - \mathcal{V},$$

where

$$\mathcal{F} = \begin{pmatrix} \Lambda - \frac{\beta_d SI}{1+\alpha_1 S+\alpha_2 I} - \beta_i SI \\ \frac{\beta_d SI}{1+\alpha_1 S+\alpha_2 I} + \beta_i SI \end{pmatrix} \qquad \text{and} \qquad \mathcal{V} = \begin{pmatrix} \mu S \\ \delta I \end{pmatrix}.$$

So, the Jacobian matrices of new infected terms $\mathcal{F}$ and other transfer terms $\mathcal{V}$ at E_0 are

$$F = \begin{pmatrix} 0 & -\frac{\beta_d \Lambda}{\mu+\alpha_1 \Lambda} - \frac{\beta_i \Lambda}{\mu} \\ 0 & \frac{\beta_d \Lambda}{\mu+\alpha_1 \Lambda} + \frac{\beta_i \Lambda}{\mu} \end{pmatrix} \qquad \text{and} \qquad V = \begin{pmatrix} \mu & 0 \\ 0 & \delta \end{pmatrix}.$$

So

$$FV^{-1} = \begin{pmatrix} 0 & -\frac{\beta_d \Lambda}{(\mu+\alpha_1 \Lambda)\delta} - \frac{\beta_i \Lambda}{\mu\delta} \\ 0 & \frac{\beta_d \Lambda}{(\mu+\alpha_1 \Lambda)\delta} + \frac{\beta_i \Lambda}{\mu\delta} \end{pmatrix}.$$

As R_0 is the spectral radius of FV^{-1}, we get

$$R_0 = \frac{\beta_d \Lambda}{(\mu + \alpha_1 \Lambda)\,\delta} + \frac{\beta_i \Lambda}{\mu\delta} = R_0^d + R_0^i.$$

Note that R_0^d represents the basic reproduction number for only direct transmission, where a susceptible individual becomes infected through contact with an infected individual R_0^i, on the other hand, it captures the contribution of indirect transmission, where an infected individual contaminates the environment, leading to subsequent infections. Public health interventions can target these specific pathways. Quarantine measures reduce direct transmission, lowering R_0^d. Improved hygiene practices reduce indirect transmission, lowering R_0^i. Consequently, the overall ability of the disease to spread (reflected by R_0) will also go down. This makes sense because there are fewer ways for people to catch it.

3.2 Existence of endemic equilibrium

In the presence of infection, we show, in the following result, that the system (2) has a unique endemic equilibrium.

Theorem 3.1 *If $R_0 > 1$, the model (2) has a unique endemic equilibrium point $E^* = (S^*, I^*)$.*

Proof. Consider the system (2), where $E^* = (S^*, I^*)$,

$$\begin{aligned} \frac{\beta_d S^* I^*}{1 + \alpha_1 S^* + \alpha_2 I^*} + \beta_i S^* I^* &= \Lambda - \mu S^*, \\ \frac{\beta_d S^* I^*}{1 + \alpha_1 S^* + \alpha_2 I^*} + \beta_i S^* I^* &= \delta I^*, \end{aligned} \tag{3}$$

which implies that

$$\Lambda - \mu S^* = \delta I^*.$$

We get S^* as a function of I^* as follows:

$$S^* = \frac{\Lambda - \delta I^*}{\mu}. \tag{4}$$

Now, we take the S^* quadratic equation out from the first equation of (3) as

$$\alpha_1 (\beta_i I^* + \mu) S^{*^2} + (\beta_d I^* - \alpha_1 \Lambda + (\beta_i I^* + \mu)(1 + \alpha_2 I^*)) S^* - \Lambda (1 + \alpha_2 I^*) = 0. \quad (5)$$

Substituting (4) into (5) gives the cubic equation in I^*:

$$a_1 (I^*)^3 + a_2 (I^*)^2 + a_3 I^* = 0,$$

where

$$\begin{aligned} a_1 &= \delta\beta_i (\delta\alpha_1 - \mu\alpha_2), \\ a_2 &= \delta\mu (\delta\alpha_1 - \mu\alpha_2) + \beta_i\Lambda (2\delta\alpha_1 - \mu\alpha_2) - \delta\mu (\beta_i + \beta_d), \\ a_3 &= \mu\Lambda\beta_d + \Lambda\beta_i (\mu + \Lambda\alpha_1) - \delta\mu (\mu + \alpha_1\Lambda). \end{aligned}$$

The constant term a_3 can be rewritten as

$$\begin{aligned} a_3 &= \delta\mu (\mu + \alpha_1\Lambda) \left(\frac{\Lambda\beta_d}{\delta (\mu + \alpha_1\Lambda)} + \frac{\Lambda\beta_i}{\delta\mu} - 1 \right) \\ &= \delta\mu (\mu + \alpha_1\Lambda)(R_0 - 1). \end{aligned}$$

It is easily seen that $a_3 > 0$ if $R_0 > 1$. Additionally, we note that $a_1, a_2 < 0$ if $2\delta\alpha_1 < \mu\alpha_2$. According to the Descartes rule of signs, see Wang [16], the equation (2) possesses a unique non-negative I^*.

The value of S^* is then calculated using equation (4). As a result, the model (2) has a unique endemic equilibrium point $E^* = (S^*, I^*)$ if $R_0 > 1$.

4 Stability Analysis

4.1 Local stability

The local stability results for the model (2) are ensured by the following results.

Theorem 4.1 *If $R_0 < 1$, the model (2) at E_0 is locally asymptotically stable and unstable for $R_0 > 1$.*

Proof. The Jacobian matrix of the system (2) at E_0 is given by

$$J = \begin{pmatrix} -\mu & -\frac{\beta_d\Lambda}{\mu+\alpha_1\Lambda} - \frac{\beta_i\Lambda}{\mu} \\ 0 & \frac{\beta_d\Lambda}{\mu+\alpha_1\Lambda} + \frac{\beta_i\Lambda}{\mu} - \delta \end{pmatrix}.$$

The eigenvalues of J are $\lambda_1 = -\mu$ and $\lambda_2 = \delta (R_0 - 1)$. The matrix J has negative eigenvalues when $R_0 < 1$. Thus, E_0 of the model (2) is locally asymptotically stable. If $R_0 > 1$, the eigenvalue $\lambda_2 > 0$, so E_0 is unstable.

Theorem 4.2 *If $R_0 > 1$, the model (2) at the disease endemic equilibrium point E^* is locally asymptotically stable under the following conditions:*

$$\frac{\beta_d S^* (1 + \alpha_1 S^*)}{(1 + \alpha_1 S^* + \alpha_2 I^*)^2} < l, \quad (6)$$

where

$$l = \min \left(\mu + \delta + \frac{\beta_d I^* (1 + \alpha_2 I^*)}{(1 + \alpha_1 S^* + \alpha_2 I^*)^2} + \beta_i I^*, \delta + \frac{\beta_d I^* (1 + \alpha_2 I^*)\delta}{\mu (1 + \alpha_1 S^* + \alpha_2 I^*)^2} + \frac{\beta_i I^* \delta}{\mu} \right).$$

Proof. The Jacobian matrix of the system (2) at E^* is given by

$$J(E^*) = \begin{pmatrix} -\mu - \frac{\beta_d I^*(1+\alpha_2 I^*)}{(1+\alpha_1 S^*+\alpha_2 I^*)^2} - \beta_i I^* & -\frac{\beta_d S^*(1+\alpha_1 S^*)}{(1+\alpha_1 S^*+\alpha_2 I^*)^2} - \beta_i S^* \\ \frac{\beta_d I^*(1+\alpha_2 I^*)}{(1+\alpha_1 S^*+\alpha_2 I^*)^2} + \beta_i I^* & \frac{\beta_d S^*(1+\alpha_1 S^*)}{(1+\alpha_1 S^*+\alpha_2 I^*)^2} + \beta_i S^* - \delta \end{pmatrix}.$$

The characteristics equation $\det(J - \lambda I)$ associated to $J(E^*)$ is derived and given as

$$\lambda^2 + a_1\lambda + a_2 = 0, \tag{7}$$

where

$$a_1 = \mu + \delta + \frac{\beta_d I^*(1+\alpha_2 I^*)}{(1+\alpha_1 S^*+\alpha_2 I^*)^2} + \beta_i I^* - \frac{\beta_d S^*(1+\alpha_1 S^*)}{(1+\alpha_1 S^*+\alpha_2 I^*)^2} - \beta_i S^*,$$

$$a_2 = \mu\delta + \frac{\beta_d I^*(1+\alpha_2 I^*)\delta}{(1+\alpha_1 S^*+\alpha_2 I^*)^2} + \beta_i I^*\delta - \frac{\mu\beta_d S^*(1+\alpha_1 S^*)}{(1+\alpha_1 S^*+\alpha_2 I^*)^2} - \mu\beta_i S^*.$$

Thanks to the assumption (6), we know that $a_i > 0, i = 1, 2$. Therefore, by the Routh–Hurwitz criterion [4], all roots of (7) have negative real parts. Thus, E^* is locally asymptotically stable.

Remark 4.1 Taking into account the sign of real parts of λ in (7), we can establish the following:

- if
$$\mu\delta + \frac{\beta_d I^*(1+\alpha_2 I^*)\delta}{(1+\alpha_1 S^*+\alpha_2 I^*)^2} + \beta_i I^*\delta < \frac{\mu\beta_d S^*(1+\alpha_1 S^*)}{(1+\alpha_1 S^*+\alpha_2 I^*)^2} + \mu\beta_i S^*, \tag{8}$$
the endemic equilibrium E^* is a saddle point.
- if
$$\mu + \delta + \frac{\beta_d I^*(1+\alpha_2 I^*)}{(1+\alpha_1 S^*+\alpha_2 I^*)^2} + \beta_i I^* < \frac{\beta_d S^*(1+\alpha_1 S^*)}{(1+\alpha_1 S^*+\alpha_2 I^*)^2} + \beta_i S^*, \tag{9}$$
the endemic equilibrium E^* is unstable.

4.2 Global stability

We employed a Lyapunov function to analyze the global stability of both the DFE and endemic equilibrium of the system. The stability of the DFE is established by the following theorem.

Theorem 4.3 *If $R_0 \leq 1$, the model (2) at the DFE E_0 is globally asymptotically stable.*

Proof. We consider the following Lyapunov function:

$$L(S, I) = \frac{1}{1+\alpha_1 S^0}\left(S - S^0 - S^0 \ln\frac{S}{S^0}\right) + I. \tag{10}$$

Taking derivative of (10) with respect to time t, one has

$$\begin{aligned}\frac{dL}{dt}(S, I) &= \frac{1}{1+\alpha_1 S^0}\left(1 - \frac{S^0}{S}\right)\frac{dS}{dt} + \frac{dI}{dt} \\ &= \frac{1}{1+\alpha_1 S^0}\left(1 - \frac{S^0}{S}\right)\left(\Lambda - \frac{\beta_d SI}{1+\alpha_1 S+\alpha_2 I} - \beta_i SI - \mu S\right) \\ &\quad + \frac{\beta_d SI}{1+\alpha_1 S+\alpha_2 I} + \beta_i SI - \delta I.\end{aligned}$$

Given that $S^0 = \frac{\Lambda}{\mu}$ and after simplification, we have

$$\begin{aligned}
\frac{dL}{dt} &= \frac{-\mu\left(S^0 - S\right)^2}{\left(1+\alpha_1 S^0\right)S} + \frac{\delta I}{\left(1+\alpha_1 S+\alpha_2 I\right)}R_0^d + \frac{\delta\alpha_1 SI}{\left(1+\alpha_1 S+\alpha_2 I\right)}R_0^d \\
&\quad - \delta I + \frac{\delta I\left(1+\alpha_1 S\right)}{\left(1+\alpha_1 S^0\right)}R_0^i \\
&= \frac{-\mu\left(S^0 - S\right)^2}{\left(1+\alpha_1 S^0\right)S} + \frac{\delta I}{\left(1+\alpha_1 S+\alpha_2 I\right)}\left(R_0^d - 1\right) \\
&\quad + \frac{\delta\alpha_1 SI}{\left(1+\alpha_1 S+\alpha_2 I\right)}\left(R_0^d - 1\right) - \frac{\delta\alpha_2 I^2}{1+\alpha_1 S+\alpha_2 I} + \frac{\delta I\left(1+\alpha_1 S\right)}{\left(1+\alpha_1 S^0\right)}R_0^i \\
&= \frac{-\mu\left(S^0 - S\right)^2}{\left(1+\alpha_1 S^0\right)S} + \frac{P}{1+\alpha_1 S+\alpha_2 I}\left(R_0^d - 1\right) - \frac{\delta\alpha_2 I^2}{1+\alpha_1 S+\alpha_2 I} \\
&\quad + \frac{P}{\left(1+\alpha_1 S^0\right)}R_0^i,
\end{aligned}$$

where $P = \delta\left(\alpha_1 S + 1\right)I$. We end the proof by noting that

$$\begin{aligned}
&\frac{P}{1+\alpha_1 S+\alpha_2 I}\left(R_0^d - 1\right) + \frac{P}{\left(1+\alpha_1 S^0\right)}R_0^i \\
&\leq \frac{P}{\left(1+\alpha_1 S+\alpha_2 I\right)}\left(R_0 - 1\right) + \frac{P}{\left(1+\alpha_1 S^0\right)}\left(R_0 - 1\right).
\end{aligned}$$

Thus

$$\begin{aligned}
\frac{dL}{dt} &\leq \frac{-\mu\left(S^0 - S\right)^2}{\left(1+\alpha_1 S^0\right)S} + \frac{P\left(\left(1+\alpha_1 S^0\right) + \left(1+\alpha_1 S+\alpha_2 I\right)\right)}{\left(1+\alpha_1 S+\alpha_2 I\right)\left(1+\alpha_1 S^0\right)}\left(R_0 - 1\right) \\
&\quad - \frac{\delta\alpha_2 I^2}{1+\alpha_1 S+\alpha_2 I}.
\end{aligned}$$

It is obvious that $\frac{dL}{dt} < 0$ if $R_0 \leq 1$ for all $(S, I) \neq \left(S^0, 0\right)$. Also, $\frac{dL}{dt} = 0$ if and only if (S, I) is at E_0. Hence, the La Salle invariance principle states that the DFE point of system (2) is globally asymptotically stable.

Theorem 4.4 *If $R_0 > 1$, the model (2) at the endemic equilibrium E^* is globally asymptotically stable under the following conditions:*

$$\left(\frac{1+\alpha_1 S^* + \alpha_2 I^*}{1+\alpha_1 S+\alpha_2 I} - 1\right)\left(\frac{I^*}{I} - \frac{S^*}{S}\right) \leq 0. \tag{11}$$

Proof. We consider the following Lyapunov function:

$$L\left(t\right) = S - S^* - S^* \ln\frac{S}{S^*} + \left(I - I^* - I^* \ln\frac{I}{I^*}\right). \tag{12}$$

Taking the time derivative of (12), we have

$$\frac{dL\left(t\right)}{dt} = \left(1 - \frac{S^*}{S}\right)\frac{dS\left(t\right)}{dt} + \left(1 - \frac{I^*}{I}\right)\frac{dI\left(t\right)}{dt}.$$

Substituting the values of $\frac{dS(t)}{dt}$ and $\frac{dI(t)}{dt}$ into the above equation, and using the equalities

$$\Lambda = \frac{\beta_d S^* I^*}{1+\alpha_1 S^* + \alpha_2 I^*} + \beta_i S^* I^* + \mu S^*,$$
$$\delta I^* = \frac{\beta_d S^* I^*}{1+\alpha_1 S^* + \alpha_2 I^*} + \beta_i S^* I^*$$

give

$$\begin{aligned}
\frac{dL(t)}{dt} &= \left(1-\frac{S^*}{S}\right) \\
&\left(\frac{\beta_d S^* I^*}{1+\alpha_1 S^* + \alpha_2 I^*} + \beta_i S^* I^* + \mu S^* - \frac{\beta_d SI}{1+\alpha_1 S + \alpha_2 I} - \beta_i SI - \mu S\right) \\
&+ \left(1-\frac{I^*}{I}\right)\left(\frac{\beta_d SI}{1+\alpha_1 S+\alpha_2 I} + \beta_i SI - \delta I\right) \\
&= -\mu\frac{(S-S^*)^2}{S} + \frac{\beta_d S^* I^*}{1+\alpha_1 S^* + \alpha_2 I^*} + \beta_i S^* I^* - \frac{\beta_d SI}{1+\alpha_1 S+\alpha_2 I} \\
&- \beta_i SI - \frac{\beta_d (S^*)^2 I^*}{S(1+\alpha_1 S^* + \alpha_2 I^*)} - \frac{\beta_i (S^*)^2 I^*}{S} + \frac{\beta_d S^* I}{1+\alpha_1 S+\alpha_2 I} \\
&+ \beta_i S^* I + \frac{\beta_d SI}{1+\alpha_1 S+\alpha_2 I} + \beta_i SI - \frac{\beta_d S^* I}{1+\alpha_1 S^* + \alpha_2 I^*} \\
&- \beta_i S^* I - \frac{\beta_d SI^*}{1+\alpha_1 S+\alpha_2 I} - \beta_i SI^* + \frac{\beta_d S^* I^*}{1+\alpha_1 S^* + \alpha_2 I^*} + \beta_i S^* I^*.
\end{aligned}$$

It follows that

$$\begin{aligned}
\frac{dL(t)}{dt} &= \mu\left(2-\frac{S^*}{S}-\frac{S}{S^*}\right) + \beta_i S^* I^*\left(2-\frac{S^*}{S}-\frac{S}{S^*}\right) \\
&+ \frac{\beta_d S^* I^*}{1+\alpha_1 S^* + \alpha_2 I^*}\left(2-\frac{S^*}{S}-\frac{S}{S^*}\right) + \frac{\beta_d S^* I^*}{1+\alpha_1 S^* + \alpha_2 I^*} \\
&\left(\frac{I(1+\alpha_1 S^* + \alpha_2 I^*)}{I^*(1+\alpha_1 S+\alpha_2 I)} - \frac{I}{I^*} - \frac{S(1+\alpha_1 S^* + \alpha_2 I^*)}{S^*(1+\alpha_1 S+\alpha_2 I)} + \frac{S}{S^*}\right) \\
&= \left(\mu + \frac{\beta_d S^* I^*}{1+\alpha_1 S^* + \alpha_2 I^*} + \beta_i S^* I^*\right)\left(1-\frac{S^*}{S}\right)\left(1-\frac{S}{S^*}\right) \\
&+ \frac{\beta_d S^* I^*}{1+\alpha_1 S^* + \alpha_2 I^*}\left(\frac{1+\alpha_1 S^* + \alpha_2 I^*}{1+\alpha_1 S+\alpha_2 I} - 1\right)\left(\frac{I^*}{I} - \frac{S^*}{S}\right).
\end{aligned}$$

Clearly,

$$\left(1-\frac{S^*}{S}\right)\left(1-\frac{S}{S^*}\right) \le 0,$$

and by (11),

$$\left(\frac{1+\alpha_1 S^* + \alpha_2 I^*}{1+\alpha_1 S+\alpha_2 I} - 1\right)\left(\frac{I^*}{I} - \frac{S^*}{S}\right) \le 0,$$

where strict equality holds when $S = S^*$ and $I = I^*$. Thus, E^* is globally asymptotically stable.

5 Numerical Simulations

In this section, we assess the computational performance of the SIR model (2). We employed the Non-standard Finite Difference scheme for the numerical simulations. All numerical simulations and figure generations were performed in Matlab

5.1 Stability of disease-free equilibrium

In a disease-free equilibrium, the infection is completely absent among the population. The specific values used for the biological parameters are presented in Table 2 [14].

Parameter	Value
Λ	5
β_d	0.003
β_i	0.00006 (Assumed)
α_1	0.002
α_2	0.001
μ	0.05
d	0.06
γ	0.002

Table 2: Parameter values.

For these values of parameters, $R_0 < 1$ and E_0 exists at $(250, 0)$. This implies that the disease eventually disappear from the population. As shown in Figure 2, the solutions of the system (2) with the initial values $S(0) = 85$ and $I(0) = 12$ converge towards E_0, which confirms that that E_0 is globally asymptotically stable.

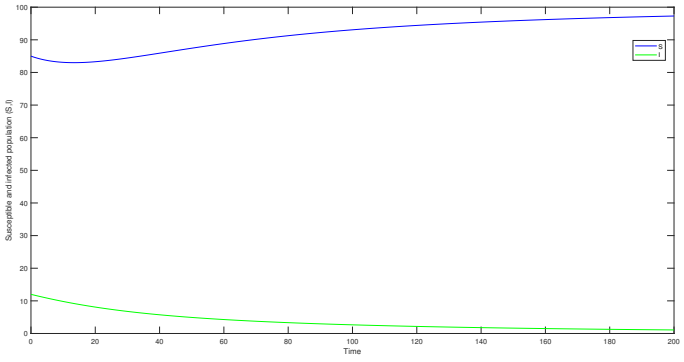

Figure 2: Dynamical behavior of the susceptible and infected populations.

5.2 Stability of endemic equilibrium

We choose the set of parameters given in Table 3 [6].

We find that $R_0 > 1$ and the condition $2\delta\alpha_1 < \mu\alpha_2$ holds. The numerical solutions, depicted in Figure 3, show that the susceptible and infected populations, with the initial

Parameter	Value
Λ	7
β_d	0.003
β_i	0.0000001 (Assumed)
α_1	0.002
α_2	0.5
μ	0.02
d	0.05
γ	0.002

Table 3: Parameter values.

values $S(0) = 250$ and $I(0) = 45$, converge towards an endemic equilibrium point $E^* = (277.8749, 20.0348)$. This indicates that E^* is globally asymptotically stable.

Furthermore, in Figure 4, we utilize the parameters from Table 4 to demonstrate that $E^* = (5.2041, 3.5738)$ is globally asymptotically stable. This implies that, for the given parameter set, the trajectories of both S and I will converge towards the same steady-state value of E^* regardless of the initial values assigned to S and I.

Parameter	Value
Λ	1.97
β_d	0.05
β_i	0.01 (Assumed)
α_1	0.001
α_2	0.1
μ	0.2
d	0.03
γ	0.03

Table 4: Parameter values.

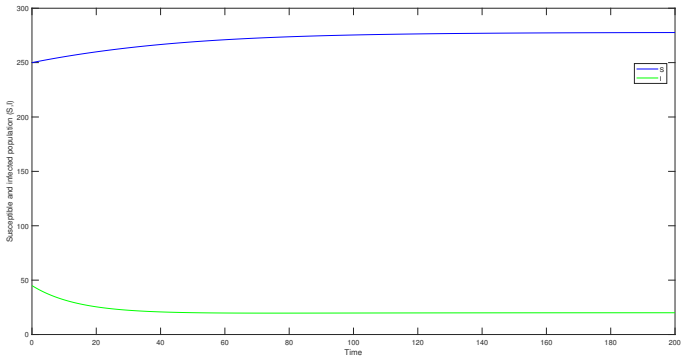

Figure 3: Dynamical behavior of the susceptible and infected populations.

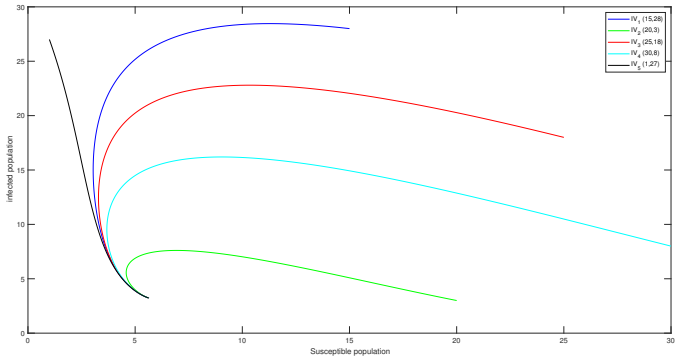

Figure 4: Global stability of the endemic equilibrium point.

6 Conclusion

This study developed a SIR model incorporating both direct and indirect transmission pathways to investigate the dynamics of COVID-19. By utilizing a Beddington-DeAngelis infection rate and a bilinear incidence term, the model captured the intricate complexities of disease spread. The model's well-posedness was confirmed through the identification of a positively invariant region. A rigorous analysis of the DFE E_0 and endemic equilibrium E^* is conducted. The basic reproduction number R_0 is decomposed into its direct R_0^d and indirect R_0^i components, reflecting the dual transmission mechanisms. Our findings demonstrate that E_0 is both locally and globally asymptotically stable when $R_0 < 1$, indicating disease eradication. Conversely, for $R_0 > 1$, E_0 becomes unstable, giving rise to E^*. The local and global stability of E^* is investigated under specific conditions.

The findings underscore that to effectively eradicate the disease ($R_0 < 1$), a comprehensive approach is needed targeting both R_0^d and R_0^i. Reducing R_0^d through measures such as mask-wearing, social distancing, and improved ventilation, in conjunction with decreasing R_0^i via hand hygiene and surface disinfection, is crucial. By quantifying the relative contributions of these transmission modes to the overall R_0, policymakers can optimize resource allocation and implement targeted control strategies. For instance, environments with high levels of indirect transmission (e.g., hospitals, nursing homes) necessitate enhanced cleaning protocols and personal protective equipment to reduce disease spread.

This study provides a basic framework for understanding COVID-19 transmission dynamics. Future investigations should incorporate additional factors such as age structure and vaccination to refine the model's predictive accuracy. By combining these insights with real-world data, we can develop more effective public health measures to protect communities from subsequent outbreaks.

References

[1] M. Ahmed, M.H.O.R. Khan and M.M. Alam Sarker. COVID-19 SIR model: Bifurcation analysis and optimal control. *Results in Control and Optimization* **12** (2023) 100246.

[2] A.Y.P. Asih, B. Gunawan, N. Hidayati, T. Herlambang, D. Rahmalia and K. Oktafianto. Weights optimization using firefly algorithm for dengue fever optimal control model by

vaccination, treatment and abateseae. *Nonlinear Dynamics and Systems Theory* **23** (3) (2023) 237–248.

[3] J.R. Beddington. Mutual interference between parasites or predators and its effect on searching efficiency. *The Journal of Animal Ecology* (1975) 331–340.

[4] N.P. Bhatia and G.P. Szegő. *Stability Theory of Dynamical Systems*. Springer-Verlag, Berlin, 1970.

[5] D.L. DeAngelis, R.A. Goldstein, and R.V. O'Neill. A model for tropic interaction. *Ecology* **56** (4) (1975) 881–892.

[6] B. Dubey, P. Dubey, and U.S. Dubey. Dynamics of an SIR model with nonlinear incidence and treatment rate. *Applications and Applied Mathematics: An International Journal (AAM)* **10** (2) (2015) 5.

[7] M. El Hassnaoui, S. Melliani, and M. Oukessou. Application of accretive operators theory to linear SIR model. *Nonlinear Dynamics and Systems Theory* (2022) 379.

[8] J.K. Hale and S.M.V. Lunel. *Introduction to Functional Differential Equations*. Springer Science & Business Media, Berlin, 2013.

[9] Y. Jin, W. Wang, and S. Xiao. An SIRS model with a nonlinear incidence rate. *Chaos, Solitons & Fractals* **34** (5) (2007) 1482–1497.

[10] W.O. Kermack and A.G. McKendrick. A contribution to the mathematical theory of epidemics. *Proceedings of the Royal Society of London. Series A, Containing papers of a mathematical and physical character* **115** (772) (1927) 700–721.

[11] A. Korobeinikov and G.C. Wake. Lyapunov functions and global stability for SIR, SIRS, and SIS epidemiological models. *Applied Mathematics Letters* **15** (8) (2002) 955–960.

[12] H. Ouedraogo and A. Guiro. Analysis of dengue disease transmission model with general incidence functions. *Nonlinear Dynamics and Systems Theory* (2023).

[13] M. Parsamanesh and M. Erfanian. Global dynamics of an epidemic model with standard incidence rate and vaccination strategy. *Chaos, Solitons & Fractals* **117** (2018) 192–199.

[14] Swati and Nilam. Fractional order SIR epidemic model with Beddington–De Angelis incidence and Holling type II treatment rate for COVID-19. *Journal of Applied Mathematics and Computing* **68** (6) (2022) 3835–3859.

[15] P. van den Driessche and J. Watmough. Reproduction numbers and sub-threshold endemic equilibria for compartmental models of disease transmission. *Mathematical Biosciences* **180** (1–2) (2002) 29–48.

[16] X. Wang. A simple proof of Descartes's rule of signs. *The American Mathematical Monthly* **111** (6) (2004) 525–526.

[17] F. Zhang, Z.-z. Li and F. Zhang. Global stability of an SIR epidemic model with constant infectious period. *Applied Mathematics and Computation* **199** (1) (2008) 285–291.

Nonlinear Dynamics and Systems Theory, **25** (4) (2025) 399–409

The Limit-Point/Limit-Circle Problem for Fractional Differential Equations

J. R. Graef *

Department of Mathematics, University of Tennessee at Chattanooga, Chattanooga, TN 37403, USA

Received: October, 5, 2024; Revised: July 15, 2025

Abstract: In this paper, the author examines the famous limit-point/limit-circle problem introduced by Hermann Weyl more than one-hundred years ago (1910) and popularized in Volume 2 of the well known treatise by Dunford and Schwartz. They visit this problem in the case where it involves fractional derivatives; this has not been studied before.

Keywords: *fractional equation; limit-point problem; limit-circle problem; square integrability.*

Mathematics Subject Classification (2020): 34B20, 34C10.

Dedication: This paper is dedicated to the memory of T. A. (Ted) Burton on the occasion of the ninetieth anniversary of his birth.

1 Introduction

A problem with more than a one-hundred year history going back to the seminal work of Hermann Weyl in [27] is the limit-point/limit-circle problem. It began with his work on eigenvalue problems for the second order linear differential equation

$$(a(t)y')' + r(t)y = \lambda y, \quad t \in [0, \infty), \quad \lambda \in \mathbb{C}, \tag{C}$$

which he classified as being of the *limit-circle* type if every solution is square integrable (belongs to L^2), and to be of *limit-point* type if at least one solution does not belong to L^2. This problem has important connections to the solution of certain boundary value problems as can be seen in the works of Titchmarsh [25, 26].

* Corresponding author: mailto:John-Graef@utc.edu

Weyl showed that if $\Im(\lambda) \neq 0$, then (C) always has a solution $y \in L^2(\mathbb{R}_+)$ (the terminology "limit-point or limit-circle" arises somewhat naturally from the proof of this fact); and if equation (C) is of the limit-circle type for some $\lambda_0 \in \mathbb{C}$, then (C) is limit-circle for all $\lambda \in \mathbb{C}$. In particular, if equation (C) is limit-circle for $\lambda = 0$, then it is limit–circle for all values of λ, and if (C) is not limit–circle for $\lambda = 0$, then it is not limit–circle for any value of λ.

The problem then reduces to whether equation (C) with $\Im(\lambda) \neq 0$ has one (limit-point case) or two linearly independent solutions (limit-circle case) in L^2. This is known as the *Weyl Alternative*. The limit-point/limit-circle problem then becomes that of determining conditions under which each of these two cases holds.

For additional discussion on the background and history of the limit-point/limit-circle problem, we refer the reader to the classic work of Dunford and Schwartz [9], the work of Coddington and Levinson [6], and the monographs [2] and [3].

Probably the best known limit-circle result for the equation

$$(a(t)y'(t))' + r(t)y(t) = 0, \quad t \geq t_0, \tag{L}$$

is that of Dunford and Schwartz [9, Sect. XIII.6.20, p. 1410].

Theorem 1.1 *Assume that*

$$\int_0^\infty \left| \left[\frac{(a(u)r(u))'}{a^{\frac{1}{2}}(u)r^{\frac{3}{2}}(u)} \right]' + \frac{\{[a(u)r(u)]'\}^2}{4a^{\frac{3}{2}}(u)r^{\frac{5}{2}}(u)} \right| du < \infty. \tag{1}$$

If

$$\int_0^\infty [1/(a(u)r(u))^{\frac{1}{2}}]du < \infty, \tag{2}$$

then equation (L) *is of the limit–circle type, i.e., every solution* $y(t)$ *of* (L) *satisfies*

$$\int_{t_0}^\infty y^2(u)du < \infty.$$

Their corresponding limit–point result is the following.

Theorem 1.2 *Assume that* (1) *holds. If*

$$\int_0^\infty [1/(a(u)r(u))^{\frac{1}{2}}]du = \infty, \tag{3}$$

then equation (L) *is of the limit–point type, i.e., there is a solution* $y(t)$ *of* (L) *such that*

$$\int_{t_0}^\infty y^2(u)du = \infty.$$

Interest in extending these results to nonlinear equations began in the mid-twentieth century with the papers of Atkinson [1], Burlak [4], Detki [7], Elias [10], Hallam [18], Suyemoto and Waltman [24], and Wong [28], and continued with the work of Graef and Spikes [13–15, 23].

Here we wish to ask whether results in the spirit of Theorems 1.1 and 1.2 can be found for equations with fractional derivatives. In particular, we will study the nonlinear fractional differential equation

$$(N^\alpha(a(t)(N^\alpha y)(t)))(t) + r(t)y^{2k-1}(t) = 0, \tag{NF}$$

where $\mathbb{R} = (-\infty, \infty)$, $\mathbb{R}_+ = [0, \infty)$, $\alpha \in (0, 1]$, a, $r : \mathbb{R}_+ \to \mathbb{R}_+$ are continuous, a', $r' \in AC_{loc}(\mathbb{R}_+)$, a'', $r'' \in L^2_{loc}(\mathbb{R}_+)$, $a(t) > 0$, $r(t) > 0$, and k is a positive integer. Here, N^α is the nonconformable fractional derivative developed by Nápoles Valdes *et al.* [17, 19–21], which is defined as follows.

Definition 1.1 ([17, Definition 2.1], [21, Definition 1]) Let $f : [0, \infty) \to \mathbb{R}$. The nonconformable fractional derivative of f of order $\alpha \in (0, 1)$ is defined by

$$(N^\alpha f)(t) = \lim_{\epsilon \to 0} \frac{f(t + \epsilon e^{t^{-\alpha}}) - f(t)}{\epsilon}$$

for all $t > 0$.

Corresponding to the nonconformable fractional derivative, we have the nonconformable fractional integral.

Definition 1.2 ([21, Definition 2]) Let $f : [0, \infty) \to \mathbb{R}$. The nonconformable fractional integral of f of order $\alpha \in (0, 1)$ is defined by

$$({}_N J^\alpha_{t_0} f)(t) = \int_{t_0}^{t} \frac{f(s)}{e^{s^{-\alpha}}} ds.$$

In light of Definitions 1.1 and 1.2, we see that the following lemma is needed.

Lemma 1.1 ([21, Theorem 3]) *If f is N^α–differentiable on (t_0, ∞) with $\alpha \in (0, 1]$, then for $t > t_0$:*

(a) If f is differentiable, then $({}_N J^\alpha_{t_0}(N^\alpha f))(t) = f(t) - f(t_0)$;

(b) $(N^\alpha({}_N J^\alpha_{t_0} f))(t) = f(t)$.

As a convenience to the reader, we next list some properties of the nonconformable fractional derivative.

Lemma 1.2 ([17, Theorem 2.3]) *Let f and g be N^α differentiable at a point $t > 0$, with $\alpha \in (0, 1]$. Then:*

(1) $N^\alpha(c) = 0$ for any constant $c \in \mathbb{R}$;

(2) $N^\alpha(fg)(t) = f(t)(N^\alpha g)(t) + g(t)(N^\alpha f)(t)$;

(3) $N^\alpha\left(\frac{f}{g}\right) = \dfrac{g(t)(N^\alpha f)(t) - f(t)(N^\alpha g)(t)}{g^2(t)}$;

(4) If f is differentiable (in the ordinary sense), then $(N^\alpha f)(t) = e^{t^{-\alpha}} f'(t)$.

One very important advantage of using the nonconformable fractional derivative is the existence of a chain rule, which we state here.

Lemma 1.3 ([17, Theorem 3.1]) *Let $\alpha \in (0, 1]$, g be N^α differentiable at $t > 0$, and f be differentiable at $g(t)$. Then*

$$N^\alpha(f \circ g)(t) = f'(g(t))(N^\alpha g)(t).$$

The following Gronwall type inequality for nonconformable fractional derivatives was obtained in [16].

Lemma 1.4 ([16, Lemma 2.7]) *Let $c \in \mathbb{R}_+$ and a, $u : \mathbb{R} \to \mathbb{R}_+$. If*

$$u(t) \le c + ({}_N J^{\alpha}_{t_0} au)(t), \tag{4}$$

then

$$u(t) \le c \exp\{({}_N J^{\alpha}_{t_0} a)(t)\}. \tag{5}$$

At this point, it seems that some discussion of notation is needed. If f is a function of u, then $(N^{\alpha} f)(u)$ denotes the nonconformable fractional derivative of f with respect to u. However, if f is a function of u, and u in turn is a function of z, then we denote the derivative of f with respect to z by $(N^{\alpha} f(u))(z)$, or $(N^{\alpha} f)(z)$ if no ambiguity exists. With respect to integration, in the notation $({}_N J^{\alpha}_{t_0} f)(t)$, t_0 denotes the initial point for the integration and t is the terminal point, which may be ∞.

2 Nonlinear Limit-Point and Limit-Circle Results

We first have to define what we mean by nonlinear limit-point and limit-circle solutions of equation (NF).

Definition 2.1 A solution $y(t)$ of equation (NF) is said to be of the nonlinear limit-circle type if

$$({}_N J^{\alpha}_{t_0} y^{2k})(\infty) < \infty,$$

and to be of the nonlinear limit-point type if

$$({}_N J^{\alpha}_{t_0} y^{2k})(\infty) = \infty.$$

To simplify the notation in what follows, we let

$$\gamma = 1/2(k+1) \quad \text{and} \quad \omega = (2k+1)/2(k+1).$$

We begin our analysis of equation (NF) by transforming it as follows. Let

$$s = \left({}_N J^{\alpha}_{t_0} \frac{r^{\gamma}}{a^{\omega}} \right)(t), \quad y(t) = x(s(t)), \tag{T}$$

and notice that

$$\gamma + \omega = 1 \quad \text{and} \quad \omega - \gamma = 2\omega - 1 = k/(k+1).$$

Then, by Lemma 1.3,

$$(N^{\alpha} y)(t) = (N^{\alpha} x)(s) \frac{ds(t)}{dt} = (N^{\alpha} x)(s) \left[r^{\gamma}(t)/a^{\omega}(t) \right]$$

and

$$a(t)(N^{\alpha} y)(t) = (N^{\alpha} x)(s) \left[r^{\gamma}(t) a^{1-\omega}(t) \right],$$

so that

$$\begin{aligned} N^\alpha(a(t)(N^\alpha y))(t) &= (N^{2\alpha}x)(s)[r^\gamma(t)a^{1-\omega}(t)]\,[r^\gamma(t)/a^\omega(t)] + (N^\alpha x)(s)[r^\gamma(t)a^{1-\omega}(t)]' \\ &= (N^{2\alpha}x)(s)[r^{2\gamma}(t)a^{1-2\omega}(t)] + (N^\alpha x)(s)[r^\gamma(t)a^{1-\omega}(t)]' \\ &= (N^{2\alpha}x)(s)[r^{2\gamma}(t)a^{1-2\omega}(t)] + (N^\alpha x)(s)[r^\gamma(t)a^\gamma(t)]' \\ &= (N^{2\alpha}x)(s)[r^{2\gamma}(t)a^{1-2\omega}(t)] + \gamma(N^\alpha x)(s)(r(t)a(t))^{\gamma-1}(r(t)a(t))'. \end{aligned}$$

Equation (NF) then becomes

$$(N^{2\alpha}x)(s)[r^{2\gamma}(t)a^{1-2\omega}(t)] + \alpha(N^\alpha x)(s)(r(t)a(t))^{\gamma-1}(r(t)a(t))' + r(t)x^{2k-1}(s) = 0,$$

or

$$(N^{2\alpha}x)(s) + \gamma(N^\alpha x)(s)\frac{(a(t)r(t))'}{a^\gamma(t)r^{\gamma+1}(t)} + (a(t)r(t))^{\omega-\gamma}x^{2k-1}(s) = 0,$$

which we will write as

$$(N^{2\alpha}x)(s) + \gamma P(t)(N^\alpha x)(s) + R(t)x^{2k-1}(s) = 0, \tag{E_s}$$

where

$$P(t) = \frac{[a(t)r(t)]'}{a^\gamma(t)r^{\gamma+1}(t)} \quad \text{and} \quad R(t) = (a(t)r(t))^{\omega-\gamma}.$$

Remark 2.1 If $k = 1$, the transformation (T) does not reduce to the transformation used, for example, in [9].

3 Limit-Point and Limit-Circle Results

We first have to define what we mean by nonlinear limit-point and limit-circle solutions of equation (NF).

Definition 3.1 A solution $y(t)$ of equation (NF) is said to be of the nonlinear limit-circle type if

$$({}_N J^\alpha_{t_0} y^{2k})(\infty) < \infty,$$

and to be of the nonlinear limit-point type if

$$({}_N J^\alpha_{t_0} y^{2k})(\infty) = \infty.$$

Equation (E_s) can then be written as the system

$$\begin{cases} (N^\alpha x)(s) = z(s) - \gamma P(t)x(s), \\ (N^\alpha z)(s) = \gamma(N^\alpha P)(t)x(s) - R(t)x^{2k-1}(s). \end{cases} \tag{S}$$

The motivation for the form of this system is due to Burton and Patula [5].

We define a Liapunov (energy) function V for this system by

$$V(s) = V(x, z, s) = \frac{z^2}{2} + R(t)\frac{x^{2k}}{2k}.$$

Then, along solutions of system (S),

$$(N^\alpha V)(s) = \gamma(N^\alpha P(t))(s)xz + x^{2k}\left[\frac{(N^\alpha R(t))(s)}{2k} - \gamma R(t)P(t)\right]. \tag{6}$$

Now by Lemma 1.3,

$$\frac{(N^\alpha R(t))(s)}{2k} = \frac{R'(t)(N^\alpha t)(s)}{2k} = \frac{R'(t)}{2k}\frac{a^\omega(t)}{r^\gamma(t)}$$
$$= \frac{\omega-\gamma}{2k}(a(t)r(t))^{\omega-\gamma-1}(a(t)r(t))'\frac{a^\omega}{r^\gamma} = \gamma(a(t)r(t))'\frac{a^{2\omega-\gamma-1}}{r^{2\gamma-\omega+1}} \quad (7)$$

and

$$\gamma R(t)P(t) = \gamma(a(t)r(t))'\frac{a^{\omega-2\gamma}(t)}{r^{2\gamma-\omega+1}(t)} = \gamma(a(t)r(t))'\frac{a^{2\omega-\gamma-1}(t)}{r^{2\gamma-\omega+1}(t)}. \quad (8)$$

In view of (7) and (8), we see from (6) that

$$(N^\alpha V)(s) = \gamma(N^\alpha P(t))(s)x(s)z(s) = \gamma P'(t)\frac{a^\omega(t)}{r^\gamma(t)}x(s)z(s) \quad (9)$$

since $(N^\alpha P(t))(s) = P'(t)\frac{a^\omega(t)}{r^\gamma(t)}$. Notice that

$$|xz| = \frac{|R^{1/2}(t)xz|}{R^{1/2}(t)} \le \left[R(t)\frac{x^2}{2} + \frac{z^2}{2}\right]/R^{1/2}(t)$$
$$\le \left[R(t)\left(\frac{x^{2k}}{2k} + C_1\right) + \frac{z^2}{2}\right]/R^{1/2}(t) \quad (10)$$
$$\le V(s)/R^{1/2}(t) + C_1R^{1/2}(t)$$

for some $C_1 \ge 0$, a constant. Therefore,

$$(N^\alpha V)(s) \le \gamma(N^\alpha P(t))(s)V(s)/R^{1/2}(t) + \gamma|(N^\alpha P(t))(s)|C_1R^{1/2}(t).$$

Now if $\tau(s)$ denotes the inverse function of $s(t)$,

$$\left({}_NJ^\alpha_{t_0}\left\{|(N^\alpha P(\tau))(s)|/R^{\frac{1}{2}}(\tau)\right\}\right)(s) = \left({}_NJ^\alpha_{t_0}\left\{|\{(ar)'/a^\gamma r^{\gamma+1}\}'|/(ar)^{(\omega-\gamma)/2}\right\}\right)(s)$$

and

$$\left({}_NJ^\alpha_{t_0}\left|(N^\alpha P(\tau))\right|R^{\frac{1}{2}}(\tau)\right)\right)(s) = \left({}_NJ^\alpha_{t_0}|\left\{(ar)'/a^\gamma r^{\gamma+1}\right\}'|(ar)^{(\omega-\gamma)/2}\right)(t).$$

Integrating $(N^\alpha V)(s)$ gives

$$V(s) \le V(t_0) + \gamma\left({}_NJ^\alpha_{t_0}\left|N^\alpha P(\tau)\right|V/R^{\frac{1}{2}}(\tau)\right)(s) + C_1\gamma\left({}_NJ^\alpha_{t_0}\left|N^\alpha P(\tau)\right|R^{\frac{1}{2}}(\tau)\right)(s)$$
$$= V(t_0) + \gamma\left({}_NJ^\alpha_{t_0}\left\{|\{(ar)'/a^\gamma r^{\gamma+1}\}'|/(ar)^{(\omega-\gamma)/2}\right\}\right)(s)$$
$$+ C_1\gamma\left({}_NJ^\alpha_{t_0}|\left\{(ar)'/a^\gamma r^{\gamma+1}\right\}'|(ar)^{(\omega-\gamma)/2}\right)(s). \quad (11)$$

We can now formulate our limit-circle result.

Theorem 3.1 *Assume that*

$$\left({}_NJ^\alpha_{t_0}\left\{|\{ar)'/a^\gamma r^{\gamma+1}\}'|/(ar)^{(\omega-\gamma)/2}\right\}\right)(\infty) < \infty \quad (12)$$

and

$$\left({}_N J_{t_0}^{\alpha}\left\{|(ar)' a^{\alpha} r^{\alpha+1}\right\}' |(ar)^{(\beta-\alpha)/2}\right)(\infty) < \infty. \tag{13}$$

If

$$\left({}_N J_{t_0}^{\alpha} \frac{1}{(ar)^{\gamma-\omega}}\right)(\infty) < \infty,$$

then any solution y of equation (NF) *is of the nonlinear limit-circle type, that is,*

$$\left({}_N J_{t_0}^{\alpha} y^{2k}\right)(\infty) < \infty.$$

Proof. From the analysis above, we arrive at (11). We see that condition (12) ensures that the second term on the right-hand side of (11) is bounded, so by Lemma 1.4, for some constant $C_2 > 0$,

$$V(s) \le C_2 \exp\left({}_N J_{t_0}^{\alpha} |(N^{\alpha} P(\tau))| R^{\frac{1}{2}}(\tau)\right)(s).$$

Condition (13) then shows that $V(s)$ is bounded, say, $V(s) \le C_3$ for some $C_3 > 0$. Therefore,

$$(a(t)r(t))^{\omega-\gamma} y^{2k}(t) = (a(t)r(t))^{\omega-\gamma} x^{2k}(s) \le 2kC_3,$$

and so it follows that

$$\left({}_N J_{t_0}^{\alpha} y^{2k}(t)\right) \le 2kC_3 \left({}_N J_{t_0}^{\alpha}[1/(a(u))r(u))^{\omega-\gamma}]\right)(\infty) < \infty$$

by condition (14), and so all solutions of equation (NF) are of the nonlinear limit–circle type. □

Notice that if we are in the linear case (i.e., $k = 1$), then in reconstructing $V(s)$ in (10), the constant $C_1 \equiv 0$, and so condition (13) is not needed in the theorem.

Next, we wish to formulate and prove a limit-point result for equation (NF).

Theorem 3.2 *In addition to conditions* (12) *and* (13)*, assume that there are constants D_1, $D_2 > 0$ such that*

$$\left|(N^{\alpha}(ar))(t)/a^{1/2}(t) r^{3/2}(t)\right| \le D_1 \tag{14}$$

and

$$|a^{\frac{1}{2}}(t)(N^{\alpha} r)(t)/r^{\frac{3}{2}}(t)| \le D_2. \tag{15}$$

In addition, assume that

$$\left({}_N J_{t_0}^{\alpha}\left\{\left[(N^{\alpha}(ar))(t)\right]^2/ar^3\right\}\right)(\infty) < \infty \tag{16}$$

and

$$\left({}_N J_{t_0}^{\alpha}\{a[(N^{\alpha} r)(t)]^2/r^3\}\right)(\infty) < \infty. \tag{17}$$

If

$$\left({}_N J_{t_0}^{\alpha}[1/(ar)^{\omega-\gamma}]\right)(\infty) = \infty, \tag{18}$$

then equation (NF) *is of the nonlinear limit-point type, that is, there is a solution y of* (NF) *such that*

$$\left({}_N J_{t_0}^{\alpha} y^{2k}\right)(\infty) = \infty.$$

Proof. Suppose that equation (NF) is of the nonlinear limit-circle type, and let y be one such solution. Then, since $y^2 \le y^{2k} + 1$ for all $y \in \mathbb{R}$ and (17) holds,

$$\left({}_N J^{\alpha}_{t_0}\{[(N^{\alpha}(ar)(t)]^2 y^2/ar^3\}\right)(s) \le D_1^2 \left({}_N J^{\alpha}_{t_0} y^{2k}\right)(t) + \left({}_N J^{\alpha}_{t_0}\{[(N^{\alpha}(ar)(t)]^2/ar^3\}\right)(s) < \infty. \quad (19)$$

Now if we multiply equation (NF) by $y(t)/r(t)$, use the identity $y(t)(N^{\alpha}(a(t)(N^{\alpha}y)(t)))(t) = y(t)(N^{\alpha}(a(t)(N^{\alpha}y)))(t) - a(t)[(N^{\alpha}y)(t)]^2$, and integrate by parts, we then obtain

$$a(t)\,(N^{\alpha}y)(t)y/r)\,(t) - a(t_1)(N^{\alpha}y)(t_1)y(t_1)/r(t_1) + \left({}_N J^{\alpha}_{t_1}[a(t)(N^{\alpha}y)(t)y(t)(N^{\alpha}r)(t)/r^2]\right)(t) + \left({}_N J^{\alpha}_{t_1} y^{2k}\right)(t) - \left({}_N J^{\alpha}_{t_1}\{a[(N^{\alpha}y)(t)]^2/r\}\right)(t) = 0 \quad (20)$$

for any $t_1 \ge t_0$. An application of the Schwarz inequality gives

$$\left|\left({}_N J^{\alpha}_{t_1}[a(N^{\alpha}y)(t)y(N^{\alpha}r)(t)/r^2]\right)(t)\right| \le \left[\left({}_N J^{\alpha}_{t_1}\{a[(N^{\alpha}y)(t)]^2/r\}\right)(t)\right]^{\frac{1}{2}} \left[\left({}_N J^{\alpha}_{t_1}[ay^2/(N^{\alpha}r)(t)]^2/r^3\}\right)(t)\right]^{\frac{1}{2}}.$$

From (15), we have

$$a(t)y^2(t)[(N^{\alpha}r)(t)]^2/r^3(t) \le \{a(t)[(N^{\alpha}r)(t)]^2/r^3(t)\}[y^{2k}(t)+1] \le D_2^2 y^{2k}(t) + a(t)[(N^{\alpha}r)(t)]^2/r^3(t),$$

so, integrating this expression, applying (17), and using the fact that y is a nonlinear limit circle solution give

$$\left({}_N J^{\alpha}_{t_1}\{ay^2[(N^{\alpha}r)(t)]^2/r^3\}\right)(\infty) \le C_4 < \infty$$

for some $C_4 > 0$. If y is not eventually monotonic, let $\{t_j\} \to \infty$ be an increasing sequence of zeros of $(N^{\alpha}y)(t)$. Then from (20), we have

$$C_4 H^{\frac{1}{2}}(t_j) + C_5 \ge H(t_j),$$

where

$$H(t) = \left({}_N J^{\alpha}_{t_1}\{a[(N^{\alpha}y)(t)]^2/r\}\right)(t)$$

and $C_5 > 0$ is a constant. It follows that $H(t_j) \le C_6 < \infty$ for all j and some constant $C_6 > 0$, so

$$\left({}_N J^{\alpha}_{t_0}\left\{a[(N^{\alpha}y)(t)]^2/r\right\}\right)(\infty) < \infty. \quad (21)$$

If $y(t)$ is eventually monotonic, then $y(t)(N^{\alpha}y)(t) \le 0$ for $t \ge t_1$ for sufficiently large $t_1 \ge t_0$ since y is a nonlinear limit-circle type solution. Using this in (20), we can repeat the style of argument used above to again see that (21) holds.

Finally, we define $V(s)$ as we did in the proof of Theorem 3.1, namely,

$$V(s) = z^2/2 + (a(t)r(t))^{\omega-\gamma} x^{2k}/2k;$$

then

$$(N^{\alpha}V)(s) \ge -\gamma|(N^{\alpha}P)(s)|V(s)/R^{\frac{1}{2}}(t) - \gamma|(N^{\alpha}P)(t)|C_1 R^{\frac{1}{2}}(t),$$

so

$$(N^\alpha V)(s) + \gamma|(N^\alpha P)(s)|V(s)/R^{\frac{1}{2}}(t) \geq -\gamma|(N^\alpha P)(t)|C_1 R^{\frac{1}{2}}(t). \tag{22}$$

If we let G and $g : \mathbb{R}_+ \to \mathbb{R}$ be given by

$$G(t) = \gamma|(N^\alpha P(t))(s)|/R^{\frac{1}{2}}(t)$$

and

$$g(t) = \gamma|(N^\alpha P(t))(s)|C_1 R^{\frac{1}{2}}(t),$$

(22) can be written as

$$(N^\alpha V)(s) + G(t)V(s) \geq -g(t).$$

Therefore,

$$\left(N^\alpha \left(V \exp\left({}_N J^\alpha_{t_0} G(\tau)\right)(s)\right)\right) \geq -g(t) \exp\left({}_N J^\alpha_{t_0} G(\tau)\right)(s). \tag{23}$$

Condition (12) ensures that

$$\exp\left({}_N J^\alpha_{t_0} G(\tau)\right)(\infty) \leq C_7 < \infty$$

for some constant $C_7 > 0$, and condition (13) implies that

$$C_7 \left({}_N J^\alpha_{t_0} g(\tau)\right)(\infty) \leq C_8 < \infty$$

for some $C_8 > 0$.

Let $y(t)$ be any solution of (NF) such that $V(t_0) = V(x(t_0), z(t_0), t_0) > C_8 + 1$. Integrating (23), we have

$$V(s) \exp\left({}_N J^\alpha_{t_0} G(\tau)\right)(s) \geq V(t_0) - C_8 > 1,$$

and so

$$V(s) \geq 1/C_8$$

for $s \geq 0$. Dividing both members of this last inequality by $(a(t)r(t))^{\omega-\gamma}$ and rewriting the left-hand side in terms of t, we have

$$\begin{aligned} a(t)[(N^\alpha y)(t)]^2/2r + \gamma(a(t)r(t))' y(t)y'(t)/r^2(t) \\ + \gamma^2[(a(t)r(t))']^2 y^2(t)/2a(t)r^3(t) + y^{2k}(t)/2k \geq 1/C_8(a(t)r(t))^{\omega-\gamma}. \end{aligned} \tag{24}$$

If $y(t)$ is a nonlinear limit–circle solution of (NF), then (19) and (21) hold. By the Schwarz inequality,

$$\begin{aligned} &\left|\left({}_N J^\alpha_{t_0}\left\{(N^\alpha(ar))(t)y(N^\alpha y)(t)/r^2\right\}\right)(\infty)\right| \\ &\qquad \leq \left[\left({}_N J^\alpha_{t_0}\left\{[N^\alpha(ar)(t)]^2 y^2/ar^3)\right\}(\infty)\right)\right]^{\frac{1}{2}} \\ &\qquad\qquad \left[\left({}_N J^\alpha_{t_0}\left\{a[(N^\alpha y)(t)]^2/r)\right\}\right)(\infty)\right]^{\frac{1}{2}} < \infty \end{aligned}$$

by (19) and (21). Since $y(t)$ is a nonlinear limit-circle type solution, an integration of (24) contradicts (18). □

Remark 3.1 From the proof of Theorem 3.2, we can see that if conditions (14) and (16) hold, then (19) is a necessary condition for the existence of a nonlinear limit-circle solution of equation (NF). The same thing can be said about (21) if (15) and (17) hold.

Based on Theorems 3.1 and 3.2, we have the following necessary and sufficient condition for equation (NF) to be of the nonlinear limit-circle type.

Theorem 3.3 *Let conditions* (12)–(17) *hold. Then equation* (NF) *is of the nonlinear limit-circle type if and only if*

$$\left({}_N J_{t_0}^{\alpha}[1/(ar)^{\omega-\gamma}]\right)(\infty) = \left({}_N J_{t_0}^{\alpha}[1/(ar)^{k/(k+1)}]\right)(\infty) < \infty. \tag{25}$$

We conclude this paper with a brief discussion of some possible directions for further research. One somewhat obvious possibility is to explore sublinear equations, that is, equations of the form

$$(N^{\alpha}(a(t)(N^{\alpha}y)(t)))(t) + r(t)y^{\delta}(t) = 0,$$

where $0 < \delta < 1$. Of course, equations with more general nonlinear terms such as $f(y)$ instead of y^{2k-1} in (NF), is another possible direction for further research. Adding a forcing term to equation (NF) should not cause major difficulties. Exploring similar results to those in this paper for equations with a delay argument or for equations with a neutral term, would also be of interest.

Another interesting possible direction would be to look at the relationship between limit-point and limit-circle solutions of (NF) and other asymptotic properties of solutions such as boundedness, oscillation, convergence to zero, stability, etc.

Equations of higher order are another possible direction of interest. This would require the notion of deficiency indicies; in this regard, the works of Devinatz [8], Dunford and Schwartz [9], Everitt [11], Fedorjuk [12], and Naimark [22] would be useful. As a final suggestion, equation (NF) with $r(t) < 0$ is another possibility, but in that case, the continuability of solutions becomes an issue.

References

[1] F. V. Atkinson. Nonlinear extensions of limit–point criteria. *Math. Z.* **130** (1973) 297–312.

[2] M. Bartušek, Z. Došlá and J. R. Graef. *The Nonlinear Limit–Point/Limit–Circle Problem.* Birkhäuser, Boston, 2004.

[3] M. Bartušek and J. R. Graef. *The Strong Nonlinear Limit-Point/Limit-Circle Problem.* Trends in Abstract and Applied Analysis, Vol. **6**, World Scientific, Singapore, 2018.

[4] J. Burlak. On the non–existence of L_2-solutions of nonlinear differential equations. *Proc. Edinburgh Math. Soc.* **14** (1965) 257–268.

[5] T. A. Burton and W. T. Patula. Limit circle results for second order equations. *Monatsh. Math.* **81** (1976) 185–194.

[6] E. A. Coddington and N. Levinson. *Theory of Ordinary Differential Equations.* McGraw–Hill, New York, 1955.

[7] J. Detki. The solvability of a certain second order nonlinear ordinary differential equation in $L^p(0,\infty)$. *Math. Balk.* **4** (1974) 115–119. (In Russian).

[8] A. Devinatz. The deficiency index problem for ordinary self adjoint differential operators. *Bull. Amer. Math. Soc.* **79** (1973), 1109–1127.

[9] N. Dunford and J. T. Schwartz. *Linear Operators; Part II: Spectral Theory.* Wiley, New York, 1963.

[10] J. Elias. On the solutions of n-th order differential equation in $L^2(0,\infty)$. In: *Qualitative Theory of Differential Equations Szeged (Hungary), 1979*, ed. M. Farkas. Colloquia Mathematica Societatis János Bolyai, Vol. **30**, North-Holland, Amsterdam, 181–191 (1981).

[11] W. N. Everitt. On the deficiency index problem for ordinary differential operators 1910–1976. *Differential Equations, Proceedings Uppsala 1977*, Almqvist & Wiksell, Stockholm, 62–81 (1977).

[12] M. V. Fedorjuk. Asymptotics of solutions of ordinary linear differential equations of n-th order. *Dokl. Akad. Nauk SSSR* **165** (1965) 777–779.

[13] J. R. Graef. Limit circle criteria and related properties for nonlinear equations. *J. Differential Equations* **35** (1980) 319–338.

[14] J. R. Graef. Limit circle type results for sublinear equations. *Pacific J. Math.* **104** (1983) 85–94.

[15] J. R. Graef and P. W. Spikes. On the nonlinear limit–point/limit–circle problem. *Nonlinear Anal.* **7** (1983) 851–871.

[16] J. R. Graef. Asymptotic properties of general nonlinear differential equations containing nonconformable fractional derivatives. *J. Math. Appl.* **47** (2024), 23–37.

[17] P. M. Guzmán, G. Langton, L. M. L. M. Bittencurt, J. Medina, and J. E. Nápoles Valdes. A new definition of a fractional derivative of local type. *J. Math. Anal.* **9** (2018) 88–98.

[18] T. G. Hallam. On the nonexistence of L^p solutions of certain nonlinear differential equations. *Glasgow Math. J.* **8** (1967) 133–138.

[19] F. Martínez and J. E. Nápoles Valdes. Towards a non-conformable fractional calculus of n-variables. *J. Math.* **43** (2020) 87–98.

[20] J. E. Nápoles Valdes, P. M. Guzman, and L. M. Lugo. On the stability of solutions of nonconformable differential equations. *Stud. Univ. Babeş-Bolyai Math.*, to appear.

[21] J. E. Nápoles Valdes and C. Tunç. On the boundedness and oscillation of non-conformable Liénard equation. *J. Fract. Calc. Appl.* **11** (2020) 92–101.

[22] M. A. Naimark. *Linear Differential Operators, Part II.* George Harrap & CO., LTD, London, 1968.

[23] P. W. Spikes. Criteria of limit circle type for nonlinear differential equations. *SIAM J. Math. Anal.* **10** (1979) 456–462.

[24] L. Suyemoto and P. Waltman. Extension of a theorem of A. Winter. *Proc. Amer. Math. Soc.* **14** (1963) 970–971.

[25] E. C. Titchmarsh. *Eigenfunction Expansions Associated with Second-Order Differential Equations*, Part I. Oxford Univ. Press, Oxford (1962).

[26] E. C. Titchmarsh. On the uniqueness of the Green's function associated with a second-order differential equation. *Canad. J. Math.* **1** (1949) 191–198.

[27] H. Weyl. Über gewöhnliche Differentialgleichungen mit Singularitäten und die zugehörige Entwicklung willkürlicher Funktionen. *Math. Ann.* **68** (1910) 220–269.

[28] J. S. W. Wong. Remark on a theorem of A. Wintner. *Enseignement Math.* (2) **13** (1967) 103–106.

Nonlinear Dynamics and Systems Theory, **25** (4) (2025) 410–423

Transformation and Generalised H_∞ Optimization of Descriptor Systems

A. G. Mazko *

Institute of Mathematics of the National Academy of Sciences of Ukraine, 3 Tereshchenkivska St., Kyiv, 01024, Ukraine

Received: December 22, 2024; Revised: July 7, 2025

Abstract: The generalized type H_∞ control problem is investigated for a class of linear descriptor systems with nonzero initial state. A generalized performance measure is used, which characterizes the weighted damping level of external and initial disturbances. A non-degenerate transformation of the system is proposed, which allows to apply known evaluation methods and achieve desired performance measures for ordinary lower-order systems. A numerical example of the descriptor control system is given to show the effectiveness of the obtained results.

Keywords: *descriptor system; exogenous disturbances; weighted performance measure; H_∞ control; LMI.*

Mathematics Subject Classification (2020): 34A09, 34D10, 93B17, 93B36, 93C05, 93D09, 93D15.

1 Introduction

In modern control theory, great attention is paid to descriptor (differential-algebraic) systems, which are used in modeling the motion of objects in mechanics, robotics, energy, electrical engineering, economics, etc. (see, e.g., [1–5]). Equations of motion, inputs and outputs of controlled objects may contain uncertain elements (parameters, external disturbances, measurement inaccuracies, etc.) that necessitate solving the problems of robust stabilization and minimize the impact of bounded disturbances on the quality of transient processes (H_∞ *optimization*).

A typical performance measure in the H_∞ optimization problem for systems with zero initial state is a damping level of external (exogenous) disturbances, which corresponds

* Corresponding author: mailto:mazkoag@gmail.com

to the maximum value of the ratio for L_2-norms of controlled output and disturbances. For a class of the linear descriptor systems

$$E\dot{x} = Ax + Bw, \quad z = Cx + Dw, \tag{1}$$

this characteristic coincides with the H_∞-norm of the matrix transfer function

$$\|\mathcal{H}\|_\infty = \sup_{\omega\in\mathbb{R}} \sqrt{\lambda_{\max}(\mathcal{H}^\top(-i\omega)\mathcal{H}(i\omega))}, \quad \mathcal{H}(\lambda) = C(\lambda E - A)^{-1}B + D,$$

where $x \in \mathbb{R}^n$ is the state, $z \in \mathbb{R}^k$ is the controlled output and $w \in \mathbb{R}^s$ represents the exogenous input (external disturbances), E, A, B, C and D are the constant matrices with compatible dimensions, $\lambda_{\max}(\cdot)$ denotes the maximum eigenvalue of a matrix.

In practice, it is advisable to apply generalized performance measures of the form [6,7]

$$J_0 = \sup_{0<\|w\|_P<\infty} \frac{\|z\|_Q}{\|w\|_P}, \quad J = \sup_{\{w,x_0\}\in\mathcal{W}} \frac{\|z\|_Q}{\sqrt{\|w\|_P^2 + x_0^\top X_0 x_0}}. \tag{2}$$

Here, $\|z\|_Q$ and $\|w\|_P$ are the weighted L_2-norms of z and w, respectively,

$$\|z\|_Q = \sqrt{\int_0^\infty z^\top Q z\, dt}, \quad \|w\|_P = \sqrt{\int_0^\infty w^\top P w\, dt},$$

$\mathcal{W}$ is a set of admissible pairs $\{w, x_0\}$ of the system such that $0 < \|w\|_P^2 + x_0^\top X_0 x_0 < \infty$, $P = P^\top > 0$, $Q = Q^\top > 0$ and $X_0 = E^\top H E$ are the weight matrices, $H = H^\top > 0$ and the initial vector $x_0 = x(0_-)$ (see also [8, 9]). It is obvious that $J_0 \le J$. If $P = I_s$ and $Q = I_k$, then $J_0 = \|\mathcal{H}\|_\infty$. The value of J characterizes the weighted damping level of external disturbances, as well as initial disturbances caused by the nonzero initial vector.

Well-known H_∞ control design methods are based on the statements of the Bounded Real Lemma type [10–12], which represent necessary and sufficient conditions for achieving the upper estimates of the performance measures used. These statements are formulated in terms of quadratic matrix equations and linear matrix inequalities (LMIs). For a class of linear descriptor systems, similar statements were established in [13–16]. For the available H_∞ optimization methods for such systems, see, e.g., [3, 5, 7, 13, 15, 17].

This paper proposes new methods for solving the generalized H_∞ control problem for linear descriptor systems with performance measures of the form (2) based on a nonsingular transformation of such systems into ordinary ones and the application of well-known methods for synthesis of static and dynamic controllers. As a result, in a number of cases, the corresponding control synthesis algorithms are based on LMIs solving without additional rank constraints. In particular, the order of the desired dynamic controller in such synthesis algorithms does not exceed the rank of the coefficient matrix at the state derivative in the original system. Also, a distinctive feature of the obtained results compared to known results is the application of weighted performance measures, which provide new opportunities for achieving the desired characteristics of descriptor control systems. By using weight coefficients in these performance criteria, we can establish priorities between the components of controlled output and the unknown disturbances in the control system.

Note that quite effective computer tools have been created for solving LMIs, for example, the LMI Toolbox of MATLAB software [18]. The LMIRank and YALMIP

tools with MATLAB [19, 20] as well as the Solve Block in Mathcad Prime software [21] can be used to solve LMIs with rank constraints.

Notations: I_n is the identity $n\times n$ matrix; $0_{n\times m}$ is the zero $n\times m$ matrix; $X = X^\top > 0$ (≥ 0) is a positive (nonnegative) definite symmetric matrix; $\sigma(A)$ is the spectrum of A; $A^{-1}(A^+)$ is the inverse (pseudo-inverse) of A; $\operatorname{Ker} A$ is the kernel of A; W_A is the right null matrix of $A \in \mathbb{R}^{m\times n}$, that is, $AW_A = 0$, $W_A \in \mathbb{R}^{n\times(n-r)}$, $\operatorname{rank} W_A = n - r$, where $r = \operatorname{rank} A < n$ ($W_A = 0$ if $r = n$); $\|w\|_P$ is the weighted L_2-norm of a vector function $w(t)$; $\mathbb{C}^-$ is the open half-plane $\mathrm{Re}\lambda < 0$.

2 Definitions and Auxiliary Statements

Consider the descriptor system (1) with $\operatorname{rank} E = r < n$ and the performance measures (2). The system is said to be *admissible* if the pair of matrices $\{E, A\}$ is *regular*, *stable* and *impulse-free* [1], i.e., $\det F(\lambda) \not\equiv 0$ ($\lambda \in \mathbb{C}$), $\sigma(F) \subset \mathbb{C}^-$ and $\deg\{\det F(\lambda)\} = r$, respectively. Here, $\sigma(F)$ is the finite spectrum of the matrix pencil $F(\lambda) = A - \lambda E$. The system (1) is called *internally stable* if it is stable without disturbances ($w \equiv 0$).

The pair of matrices $\{E, A\}$ is regular if and only if there exist nonsingular matrices L and R that transform it to the canonical Weierstrass form [22]. System (1) is impulse-free if and only if [2]

$$\operatorname{rank}\begin{bmatrix} E & 0 \\ A & E \end{bmatrix} = n + r. \tag{3}$$

Let $E = E_1E_2^\top$ be the skeletal decomposition of E, where $E_1, E_2 \in \mathbb{R}^{n\times r}$ are matrices of full rank r. Denote the corresponding orthogonal complements by $E_1^\perp, E_2^\perp \in \mathbb{R}^{n\times(n-r)}$ such that $E_i^\top E_i^\perp = 0$ and $\det\begin{bmatrix} E_i & E_i^\perp \end{bmatrix} \neq 0$, $i = 1, 2$.

Define a nonsingular transformation of system (1) by

$$LER = \begin{bmatrix} I_r & 0 \\ 0 & 0 \end{bmatrix},\ LAR = \begin{bmatrix} A_1 & A_2 \\ A_3 & A_4 \end{bmatrix},\ x = R\begin{bmatrix} \xi_1 \\ \xi_2 \end{bmatrix},\ \xi_1 \in \mathbb{R}^r,\ \xi_2 \in \mathbb{R}^{n-r}, \tag{4}$$

where

$$L = \begin{bmatrix} E_1^+ \\ E_1^{\perp+} \end{bmatrix},\quad E_1^+ = (E_1^\top E_1)^{-1}E_1^\top,\quad E_1^{\perp+} = (E_1^{\perp\top}E_1^\perp)^{-1}E_1^{\perp\top},$$

$$R = \begin{bmatrix} E_2^{+\top} & E_2^{\perp+\top} \end{bmatrix},\quad E_2^+ = (E_2^\top E_2)^{-1}E_2^\top,\quad E_2^{\perp+} = (E_2^{\perp\top}E_2^\perp)^{-1}E_2^{\perp\top},$$

$$A_1 = E_1^+AE_2^{+\top},\quad A_2 = E_1^+AE_2^{\perp+\top},\quad A_3 = E_1^{\perp+}AE_2^{+\top},\quad A_4 = E_1^{\perp+}AE_2^{\perp+\top}.$$

Note that

$$L^{-1} = \begin{bmatrix} E_1 & E_1^\perp \end{bmatrix},\quad R^{-1} = \begin{bmatrix} E_2^\top \\ E_2^{\perp\top} \end{bmatrix},\quad \xi_1 = E_2^\top x,\quad \xi_2 = E_2^{\perp\top}x.$$

It is easy to establish that (3) is equivalent to the inequality $\det A_4 \neq 0$, i.e.,

$$\det(E_1^{\perp\top}AE_2^\perp) \neq 0. \tag{5}$$

Eliminating the variable $\xi_2 = -A_4^{-1}\big(A_3\xi_1 + B_2w\big)$ under the condition (5), based on the transformation (4), we obtain the ordinary system

$$\dot\xi_1 = \bar A\xi_1 + \bar Bw,\quad z = \bar C\xi_1 + \bar Dw,\quad \xi_1(0) = \xi_{10}, \tag{6}$$

where

$$\bar{A} = A_1 - A_2A_4^{-1}A_3,\ \bar{B} = B_1 - A_2A_4^{-1}B_2,\ \bar{C} = C_1 - C_2A_4^{-1}A_3,\ \bar{D} = D - C_2A_4^{-1}B_2,$$

$$LB = \begin{bmatrix} B_1 \\ B_2 \end{bmatrix}, \quad CR = \begin{bmatrix} C_1 & C_2 \end{bmatrix}.$$

The spectrum of matrix $\bar{A}$ coincides with $\sigma(F)$ and the performance measures J_0 and J of impulse-free system (1) do not depend on ξ_2 and are determined by system (6) since

$$\begin{bmatrix} I_r & -A_2A_4^{-1} \\ 0 & I_{n-r} \end{bmatrix} LF(\lambda)R \begin{bmatrix} I_r & 0 \\ -A_4^{-1}A_3 & I_{n-r} \end{bmatrix} = \begin{bmatrix} \bar{A} - \lambda I_r & 0 \\ 0 & A_4 \end{bmatrix},$$

$$x_0^\top X_0 x_0 = \begin{bmatrix} \xi_{10}^\top & \xi_{20}^\top \end{bmatrix} R^\top E^\top L^\top L^{-1\top} H L^{-1} LER \begin{bmatrix} \xi_{10} \\ \xi_{20} \end{bmatrix} = \xi_{10}^\top \bar{H} \xi_{10},$$

where $\bar{H} = E_1^\top H E_1$. Therefore, applying Lemma 4.1 from [23] to system (6), we have the following statement.

Lemma 2.1 *System* (1) *is admissible with* $J_0 < \gamma$ *if and only if* (5) *holds and there exists a matrix* $X = X^\top > 0$ *such that*

$$\bar{\Phi}(X) = \begin{bmatrix} \bar{A}^\top X + X\bar{A} + \bar{C}^\top Q \bar{C} & X\bar{B} + \bar{C}^\top Q\bar{D} \\ \bar{B}^\top X + \bar{D}^\top Q\bar{C} & \bar{D}^\top Q\bar{D} - \gamma^2 P \end{bmatrix} < 0. \tag{7}$$

The system is admissible with $J < \gamma$ *if and only if* (5) *holds and the LMIs* (7) *and*

$$0 < X < \gamma^2 \bar{H} \tag{8}$$

are feasible.

Lemma 2.1 can be used to calculate the characteristics J_0 and J of system (1) based on solving the corresponding optimization problems. At the same time, the restrictions in these problems are used exclusively in terms of LMIs:

$$J_0 = \inf\big\{\gamma :\ \bar{\Phi}(X) < 0,\ X > 0\big\}, \quad J = \inf\big\{\gamma :\ \bar{\Phi}(X) < 0,\ 0 < X < \gamma^2\bar{H}\big\}.$$

For the *worst-case* perturbation vector $w(t)$ with respect to J_0, in (2), the supremum is reached, i.e., $\|z\|_Q = J_0\|w\|_P$. If $\|z\|_Q^2 = J^2\big(\|w\|_P^2 + x_0^\top X_0 x_0\big)$, then $\{w(t), x_0\}$ is the *worst-case* pair with respect to J in system (1). The methods of finding such vectors in individual cases are proposed in [8, 24, 25]. For example, if system (1) is admissible and there exists a matrix X such that

$$A_0^\top X + X^\top A_0 + X^\top R_0 X + Q_0 = 0, \quad 0 \le E^\top X = X^\top E \le J^2 X_0,$$

where $A_0 = A + BR_1^{-1}D^\top QC$, $R_0 = BR_1^{-1}B^\top$, $Q_0 = C^\top\big(Q + QDR_1^{-1}D^\top Q\big)C$, $R_1 = J^2P - D^\top QD > 0$, then the worst-case pair $\{w(t), x_0\}$ with respect to J can be defined as $w = K_* x$ with $K_* = R_1^{-1}(B^\top X + D^\top QC)$ and $x_0 \in \operatorname{Ker}(E^\top X - J^2 X_0)$ [25].

We present another method of finding the worst-case pair $\{w(t), x_0\}$ with respect to J for impulse-free system (1) based on the transformation (4). Under condition (5), we construct the worst-case initial vector in the form

$$x_0 = R \begin{bmatrix} \xi_{10} \\ -A_4^{-1}\big(A_3\xi_{10} + B_2 w(0)\big) \end{bmatrix}, \tag{9}$$

where $\{w(t), \xi_{10}\}$ is the worst-case pair of system (6) with respect to J.

According to the Schur complement lemma [10], the condition (7) is equivalent to the Riccati matrix inequality

$$\bar{A}_0^\top X + X\bar{A}_0 + X\bar{R}_0 X + \bar{Q}_0 < 0, \tag{10}$$

where $\bar{A}_0 = \bar{A} + \bar{B}\,\bar{R}_1^{-1}\bar{D}^\top Q\bar{C}$, $\bar{R}_0 = \bar{B}\,\bar{R}_1^{-1}\bar{B}^\top$, $\bar{Q}_0 = \bar{C}^\top\big(Q + Q\bar{D}\,\bar{R}_1^{-1}\bar{D}^\top Q\big)\bar{C}$, $\bar{R}_1 = \gamma^2 P - \bar{D}^\top Q\bar{D} > 0$. If the pair $\{\bar{A}, \bar{B}\}$ is controllable, the pair $\{\bar{A}, \bar{C}\}$ is observable, and $J_0 < \gamma$, then the corresponding Riccati matrix equation

$$\bar{A}_0^\top X + X\bar{A}_0 + X\bar{R}_0 X + \bar{Q}_0 = 0 \tag{11}$$

has the solutions X_- and X_+ such that $\sigma(\bar{A}_0 + \bar{R}_0 X_\pm) \subset \mathbb{C}^\pm$, $0 < X_- < X_+$, and every solution of inequality (10) belongs to the interval $X_- < X < X_+$ (see [26, 27]). Moreover, if $J < \gamma$ ($J \le \gamma$) and X satisfies (11), then $X < \gamma^2\bar{H}$ ($X \le \gamma^2\bar{H}$). Indeed, setting $v(\xi_1) = \xi_1^\top X\xi_1$ and

$$w = \bar{K}_*\xi_1, \quad \bar{K}_* = \bar{R}_1^{-1}\big(\bar{B}^\top X + \bar{D}^\top Q\bar{C}\big), \tag{12}$$

we get $\dot{v} + z^\top Qz - \gamma^2 w^\top Pw = 0$, where $\dot{v}$ is the derivative of the Lyapunov function v along the trajectory of system (6). Integrating the above equality from zero to infinity under the condition $J < \gamma$, we get $\|z\|_Q^2 - \gamma^2\|w\|_P^2 = \xi_{10}^\top X\xi_{10} < \gamma^2\xi_{10}^\top\bar{H}\xi_{10}$ for any $\xi_{10} \neq 0$, otherwise $J \ge \gamma$. If $J = \gamma$, then under conditions (11) and (12), the equality $\xi_{10}^\top X\xi_{10} = \gamma^2\xi_{10}^\top\bar{H}\xi_{10}$ or its equivalent $(X - \gamma^2\bar{H})\xi_{10} = 0$ is possible for some $\xi_{10} \neq 0$. At the same time, $\|z\|_Q^2 = J^2(\|w\|_P^2 + \xi_{10}^\top\bar{H}\xi_{10})$, i.e., in (2), the supremum is reached. Hence, the following statement holds.

Lemma 2.2 *Let $X > 0$ be the stabilizing solution of the Riccati equation (11) with $\gamma = J$. Then the structured vector of external disturbances (12), where ξ_1 is a solution of the system*

$$\dot{\xi}_1 = (\bar{A} + \bar{B}\bar{K}_*)\xi_1, \quad \xi_1(0) = \xi_{10}, \tag{13}$$

and the vector (9) with $\xi_{10} \in \operatorname{Ker}(X - J^2\bar{H})$ present the worst-case pair $\{w(t), x_0\}$ with respect to J in system (1). If $X > 0$ is the stabilizing solution of (11) with $\gamma = J_0$ and $\xi_1 = \xi_1(t, \xi_{10})$ is a solution of (13) at $\xi_{10} = 0$, then (12) are the worst-case disturbances with respect to J_0 in system (1).

3 Main Results

Consider a class of linear descriptor control system described by

$$\begin{aligned} E\dot{x} &= Ax + B_1 w + B_2 u, \quad x(0_-) = x_0, \\ z &= C_1 x + D_{11} w + D_{12} u, \\ y &= C_2 x + D_{21} w + D_{22} u, \end{aligned} \tag{14}$$

where $x \in \mathbb{R}^n$ is the state, $u \in \mathbb{R}^m$ is the control input, $w \in \mathbb{R}^s$ represents the exogenous input, $z \in \mathbb{R}^k$ is the controlled output and $y \in \mathbb{R}^l$ is the measured output. In (14), all matrix coefficients are constant, $\operatorname{rank} E = r < n$ and the pair $\{E, A\}$ is regular and impulse-free. The components of $w(t)$ can be both external disturbances acting on the system and errors of the measured output. This vector must be bounded by the weighted

norm. The initial perturbations in the system are caused by the unknown initial vector x_0.

We are interested in the stabilizing control laws that guarantee the internal stability of the closed-loop system and the desired upper estimates of performance measure (2) for the system with respect to the controlled output z. Static and dynamic controllers that minimize the performance measure J are called *J-optimal*. For the identity weight matrices P and Q, the J_0-optimal control is called *H_∞-optimal*. The search for J_0- and J-optimal controllers can be performed based on achieving the corresponding estimates $J_0 < \gamma$ and $J < \gamma$ for the minimum possible value of γ.

When studying the class of systems (14), their properties such as C-, R- and I-controllability, as well as the dual properties C-, R- and I-observability, are used [3, 5]. In particular, for solvability of the generalized H_∞ optimization problems, the triple $\{E, A, B_2\}$ must be stabilizable and I-controllable. This is equivalent to the existence of a matrix K such that the pair $\{E, A + B_2K\}$ is stable and impulse-free, i.e., admissible. The I-controllability of the triple $\{E, A, B_2\}$ and I-observability of the triple $\{E, A, C_2\}$ are equivalent to the corresponding equalities [28]

$$\operatorname{rank}\begin{bmatrix} E & 0 & 0 \\ A & E & B_2 \end{bmatrix} = n + r, \quad \operatorname{rank}\begin{bmatrix} E & A \\ 0 & E \\ 0 & C_2 \end{bmatrix} = n + r. \tag{15}$$

We apply the equivalent transformation (4) to system (14). Excluding the variable $\xi_2 = -A_4^{-1}\big(A_3\xi_1 + B_{12}w + B_{22}u\big)$ under condition (5), we get the ordinary system

$$\dot\xi_1 = \bar A\xi_1 + \bar B_1 w + \bar B_2 u, \quad z = \bar C_1\xi_1 + \bar D_{11}w + \bar D_{12}u, \quad y = \bar C_2\xi_1 + \bar D_{21}w + \bar D_{22}u, \tag{16}$$

where $\bar A = A_1 - A_2A_4^{-1}A_3$, $\bar B_1 = B_{11} - A_2A_4^{-1}B_{12}$, $\bar B_2 = B_{21} - A_2A_4^{-1}B_{22}$,
$\bar C_1 = C_{11} - C_{12}A_4^{-1}A_3$, $\bar D_{11} = D_{11} - C_{12}A_4^{-1}B_{12}$, $\bar D_{12} = D_{12} - C_{12}A_4^{-1}B_{22}$,
$\bar C_2 = C_{21} - C_{22}A_4^{-1}A_3$, $\bar D_{21} = D_{21} - C_{22}A_4^{-1}B_{12}$, $\bar D_{22} = D_{22} - C_{22}A_4^{-1}B_{22}$,

$$LB_1 = \begin{bmatrix} B_{11} \\ B_{12} \end{bmatrix}, \quad LB_2 = \begin{bmatrix} B_{21} \\ B_{22} \end{bmatrix}, \quad C_1R = \begin{bmatrix} C_{11} & C_{12} \end{bmatrix}, \quad C_2R = \begin{bmatrix} C_{21} & C_{22} \end{bmatrix}.$$

Defining the performance measure (2) for this system, we use the expression $x_0^\top X_0 x_0 = \xi_{10}^\top \bar H \xi_{10}$, where $\xi_{10} = \xi_1(0)$, $\bar H = E_1^\top H E_1$ (see the previous section).

Thus, the J_0- and J-optimization problems for descriptor system (14) with the impulse-free pair $\{E, A\}$ are reduced to the application of well-known methods for solving similar problems for system (16).

3.1 Static controller

When using for system (16) the static output-feedback controller

$$u = Ky, \quad \det(I_m - K\bar D_{22}) \neq 0, \tag{17}$$

the closed-loop system has the form

$$\dot\xi_1 = A_*\xi_1 + B_*w, \quad z = C_*\xi_1 + D_*w, \tag{18}$$

where $A_* = \bar A + \bar B_2K_0\bar C_2$, $B_* = \bar B_1 + \bar B_2K_0\bar D_{21}$, $C_* = \bar C_1 + \bar D_{12}K_0\bar C_2$, $D_* = \bar D_{11} + \bar D_{12}K_0\bar D_{21}$ and $K_0 = (I_m - K\bar D_{22})^{-1}K$. The controller (17) will also be used for the original system (14).

Applying the Schur complement lemma [10], we rewrite the inequality (7) in Lemma 2.1 for system (18) as the LMI with respect to K_0:

$$\begin{bmatrix} A_*^\top X + X A_* & X B_* & C_*^\top \\ B_*^\top X & -\gamma^2 P & D_*^\top \\ C_* & D_* & -Q^{-1} \end{bmatrix} = L_0^\top K_0 R_0 + R_0^\top K_0^\top L_0 + \Omega < 0, \tag{19}$$

where $R_0 = \begin{bmatrix} \bar{C}_2 & \bar{D}_{21} & 0_{l\times k} \end{bmatrix}$, $L_0 = \begin{bmatrix} \bar{B}_2^\top X & 0_{m\times s} & \bar{D}_{12}^\top \end{bmatrix}$ and

$$\Omega = \begin{bmatrix} \bar{A}^\top X + X\bar{A} & X\bar{B}_1 & \bar{C}_1^\top \\ \bar{B}_1^\top X & -\gamma^2 P & \bar{D}_{11}^\top \\ \bar{C}_1 & \bar{D}_{11} & -Q^{-1} \end{bmatrix}.$$

Based on Lemma 2.1 and Theorem 5.1 from [7], we have the following result.

Theorem 3.1 *For system* (14)*, there is a static output-feedback controller* (17) *such that the closed-loop system is admissible and $J < \gamma$ if and only if* (8) *and*

$$W_{\bar{R}}^\top \begin{bmatrix} \bar{A}^\top X + X\bar{A} + \bar{C}_1^\top Q \bar{C}_1 & X\bar{B}_1 + \bar{C}_1^\top Q \bar{D}_{11} \\ \bar{B}_1^\top X + \bar{D}_{11}^\top Q \bar{C}_1 & \bar{D}_{11}^\top Q \bar{D}_{11} - \gamma^2 P \end{bmatrix} W_{\bar{R}} < 0, \tag{20}$$

$$W_{\bar{L}}^\top \begin{bmatrix} \bar{A}Y + Y\bar{A}^\top + \bar{B}_1 P^{-1} \bar{B}_1^\top & Y\bar{C}_1^\top + \bar{B}_1 P^{-1} \bar{D}_{11}^\top \\ \bar{C}_1 Y + \bar{D}_{11} P^{-1} \bar{B}_1^\top & \bar{D}_{11} P^{-1} \bar{D}_{11}^\top - \gamma^2 Q^{-1} \end{bmatrix} W_{\bar{L}} < 0, \tag{21}$$

$$W = \begin{bmatrix} X & \gamma I_r \\ \gamma I_r & Y \end{bmatrix} \geq 0, \quad \operatorname{rank} W = r, \tag{22}$$

where $\bar{R} = \begin{bmatrix} \bar{C}_2 & \bar{D}_{21} \end{bmatrix}$ and $\bar{L} = \begin{bmatrix} \bar{B}_2^\top & \bar{D}_{12}^\top \end{bmatrix}$, are feasible for some X and Y.

The gain matrix of the controller can be found as $K = K_0(I_l + \bar{D}_{22} K_0)^{-1}$, where K_0 is a solution of (19)*.*

Note that (22) hold if and only if $X = X^\top > 0$, $Y = Y^\top > 0$ and $XY = \gamma^2 I_r$. In what follows, we present the corollaries of Lemma 2.1 and Theorem 3.1 for

$$\operatorname{rank} \bar{C}_2 = r \leq l, \quad \bar{D}_{21} = 0, \quad \bar{D}_{22} = 0, \tag{23}$$

$$\bar{D}_{11}^\top Q \bar{D}_{11} < \gamma^2 P. \tag{24}$$

Conditions (23) are satisfied if, for example,

$$\operatorname{rank}(C_2 E_2) = r, \quad C_2 E_2^\perp = 0, \quad D_{21} = 0, \quad D_{22} = 0.$$

Theorem 3.2 *Suppose* (23) *and* (24) *hold. The following statements are equivalent:*

1) *for system* (14)*, there is a static state-feedback controller* (17)*, for which the closed-loop system is admissible and $J < \gamma$;*

2) *there is a matrix $Y > \bar{H}^{-1}$ that satisfies* (21)*;*

3) *there exist matrices $Y > \bar{H}^{-1}$ and Z satisfying the LMI*

$$\begin{bmatrix} \gamma^2(\bar{A}Y + Y\bar{A}^\top + \bar{B}_2 Z + Z^\top \bar{B}_2^\top) & \gamma^2 \bar{B}_1 & Y\bar{C}_1^\top + Z^\top \bar{D}_{12}^\top \\ \gamma^2 \bar{B}_1^\top & -\gamma^2 P & \bar{D}_{11}^\top \\ \bar{C}_1 Y + \bar{D}_{12} Z & \bar{D}_{11} & -Q^{-1} \end{bmatrix} < 0. \tag{25}$$

When statement 2) *holds, the desired gain matrix $K = K_0$ of controller* (17) *in statement* 1) *can be found as a solution of* (19) *with $X = \gamma^2 Y^{-1}$. If statement* 3) *holds, then this matrix can be defined as a solution of the linear equation $K\bar{C}_2 Y = Z$.*

Proof. Given the conditions (23), we have $y = \bar{C}_2\xi_1 = \bar{C}_2E_2^\top x$ and $l \geq r$. The equivalence of statements 1) and 2) follows from Theorem 3.1 since $W_{\bar{R}} = \begin{bmatrix} 0 & I_s \end{bmatrix}^\top$ under conditions (23). In this case, the inequality (20) takes the form (24) and does not depend on X. The desired matrix in (21) has the form $Y = \gamma^2 X^{-1}$. Therefore, instead of (8), we have the equivalent condition $Y > \bar{H}^{-1}$. Given (23), the matrix K of the controller (17) satisfying statement 1) can be an arbitrary solution K_0 of the LMI (19).

The equivalence of statements 1) and 3) follows from Lemma 2.1 for the closed-loop system (18), where $K_0 = K$. At the same time, the inequality (25) in statement 3) arises as a result of multiplying the first block row on the left-hand side and the first block column on the right-hand side of (19) by $Y = \gamma^2 X^{-1}$, taking into account (23) and the notation $Z = K\bar{C}_2Y$. The last correlation can be solved with respect to K:

$$K = \begin{cases} Z(\bar{C}_2Y)^{-1}, & l = r, \\ ZY^{-1}\bar{C}_2^{+} + T\bar{C}_2^{\perp\top}, & l > r, \end{cases}$$

where T is an arbitrary $m \times (l - r)$ matrix. □

Remark 3.1 Consider the case when the pair $\{E, A\}$ in system (14) is not impulse-free, but there exists a matrix $K_1 \in \mathbb{R}^{m\times l}$ such that

$$\det(I_m - K_1D_{22}) \neq 0, \quad \det\left[E_1^{\perp\top}(A + B_2K_{10}C_2)E_2^{\perp}\right] \neq 0, \tag{26}$$

where $K_{10} = K_{11}K_1$ and $K_{11} = (I_m - K_1D_{22})^{-1}$. It can be established that under conditions (26), the rank relations (15) are satisfied, i.e., the system is I-controllable and I-observable.

Under the above assumptions, instead of (17), we use the controller $u = K_1y + v$, where v is a new control in the system

$$E\dot{x} = \widetilde{A}x + \widetilde{B}_1w + \widetilde{B}_2v, \quad z = \widetilde{C}_1x + \widetilde{D}_{11}w + \widetilde{D}_{12}v, \quad y = \widetilde{C}_2x + \widetilde{D}_{21}w + \widetilde{D}_{22}v. \tag{27}$$

Here, under condition (26), the pair $\{E, \widetilde{A}\}$ is impulse-free and

$$\widetilde{A} = A + B_2K_{10}C_2, \quad \widetilde{B}_1 = B_1 + B_2K_{10}D_{21}, \quad \widetilde{B}_2 = B_2K_{11},$$

$$\widetilde{C}_1 = C_1 + D_{12}K_{10}C_2, \quad \widetilde{D}_{11} = D_{11} + D_{12}K_{10}D_{21}, \quad \widetilde{D}_{12} = D_{12}K_{11},$$

$$\widetilde{C}_2 = C_2 + D_{22}K_{10}C_2, \quad \widetilde{D}_{21} = D_{21} + D_{22}K_{10}D_{21}, \quad \widetilde{D}_{22} = D_{22}K_{11}.$$

We perform an equivalent transformation of system (27) based on the relations

$$LER = \begin{bmatrix} I_r & 0 \\ 0 & 0 \end{bmatrix}, \quad L\widetilde{A}R = \begin{bmatrix} \widetilde{A}_1 & \widetilde{A}_2 \\ \widetilde{A}_3 & \widetilde{A}_4 \end{bmatrix}, \quad L\widetilde{B}_1 = \begin{bmatrix} \widetilde{B}_{11} \\ \widetilde{B}_{12} \end{bmatrix}, \quad L\widetilde{B}_2 = \begin{bmatrix} \widetilde{B}_{21} \\ \widetilde{B}_{22} \end{bmatrix},$$

$$\widetilde{C}_1R = \begin{bmatrix} \widetilde{C}_{11} & \widetilde{C}_{12} \end{bmatrix}, \quad \widetilde{C}_2R = \begin{bmatrix} \widetilde{C}_{21} & \widetilde{C}_{22} \end{bmatrix},$$

$$x = R\begin{bmatrix} \xi_1 \\ \xi_2 \end{bmatrix}, \quad \xi_1 = E_2^\top x, \quad \xi_2 = -\widetilde{A}_4^{-1}\big(\widetilde{A}_3\xi_1 + \widetilde{B}_{12}w + \widetilde{B}_{22}v\big),$$

where L and R are nonsingular matrices defined in (4). Then we can formulate analogues of Theorems 3.1 and 3.2 using the static controller $v = Ky$ for the ordinary system

$$\dot{\xi}_1 = \bar{A}\xi_1 + \bar{B}_1w + \bar{B}_2v, \quad z = \bar{C}_1\xi_1 + \bar{D}_{11}w + \bar{D}_{12}v, \quad y = \bar{C}_2\xi_1 + \bar{D}_{21}w + \bar{D}_{22}v, \tag{28}$$

where

$$\bar{A} = \widetilde{A}_1 - \widetilde{A}_2\widetilde{A}_4^{-1}\widetilde{A}_3, \quad \bar{B}_1 = \widetilde{B}_{11} - \widetilde{A}_2\widetilde{A}_4^{-1}\widetilde{B}_{12}, \quad \bar{B}_2 = \widetilde{B}_{21} - \widetilde{A}_2\widetilde{A}_4^{-1}\widetilde{B}_{22},$$

$$\bar{C}_1 = \widetilde{C}_{11} - \widetilde{C}_{12}\widetilde{A}_4^{-1}\widetilde{A}_3, \quad \bar{D}_{11} = \widetilde{D}_{11} - \widetilde{C}_{12}\widetilde{A}_4^{-1}\widetilde{B}_{12}, \quad \bar{D}_{12} = \widetilde{D}_{12} - \widetilde{C}_{12}\widetilde{A}_4^{-1}\widetilde{B}_{22},$$

$$\bar{C}_2 = \widetilde{C}_{21} - \widetilde{C}_{22}\widetilde{A}_4^{-1}\widetilde{A}_3, \quad \bar{D}_{21} = \widetilde{D}_{21} - \widetilde{C}_{22}\widetilde{A}_4^{-1}\widetilde{B}_{12}, \quad \bar{D}_{22} = \widetilde{D}_{22} - \widetilde{C}_{22}\widetilde{A}_4^{-1}\widetilde{B}_{22}.$$

As a result, the original system (14) with the control

$$u = \big(K_{10}C_2 + K_{11}K_0\bar{C}_2E_2^\top\big)x + \big(K_{10}D_{21} + K_{11}K_0\bar{D}_{21}\big)w$$

takes the form

$$E\dot{x} = A_0x + B_0w, \quad z = C_0x + D_0w, \tag{29}$$

where $K_0 = (I_m - K\bar{D}_{22})^{-1}K$, $\det(I_m - K\bar{D}_{22}) \neq 0$,

$$A_0 = A + B_2\big(K_{10}C_2 + K_{11}K_0\bar{C}_2E_2^\top\big), \quad B_0 = B_1 + B_2\big(K_{10}D_{21} + K_{11}K_0\bar{D}_{21}\big),$$

$$C_0 = C_1 + D_{12}\big(K_{10}C_2 + K_{11}K_0\bar{C}_2E_2^\top\big), \quad D_0 = D_{11} + D_{12}\big(K_{10}D_{21} + K_{11}K_0\bar{D}_{21}\big).$$

3.2 Dynamic controller

When using for system (16) the dynamic controller of the order p

$$\dot{\eta} = Z\eta + Vy, \quad u = U\eta + Ky, \quad \eta(0) = 0, \tag{30}$$

the closed-loop system in an extended phase space $\mathbb{R}^{r+p}$ has the form

$$\dot{\widehat{x}} = \widehat{A}_*\widehat{x} + \widehat{B}_*w, \quad z = \widehat{C}_*\widehat{x} + \widehat{D}_*w, \quad \widehat{x}(0) = \widehat{x}_0, \tag{31}$$

where

$$\widehat{A}_* = \widehat{A} + \widehat{B}_2\widehat{K}_0\widehat{C}_2,\ \widehat{B}_* = \widehat{B}_1 + \widehat{B}_2\widehat{K}_0\widehat{D}_{21},\ \widehat{C}_* = \widehat{C}_1 + \widehat{D}_{12}\widehat{K}_0\widehat{C}_2,\ \widehat{D}_* = \bar{D}_{11} + \widehat{D}_{12}\widehat{K}_0\widehat{D}_{21},$$

$$\widehat{x} = \begin{bmatrix} \xi_1 \\ \eta \end{bmatrix}, \quad \widehat{A} = \begin{bmatrix} \bar{A} & 0_{r\times p} \\ 0_{p\times r} & 0_{p\times p} \end{bmatrix}, \quad \widehat{B}_1 = \begin{bmatrix} \bar{B}_1 \\ 0_{p\times s} \end{bmatrix}, \quad \widehat{B}_2 = \begin{bmatrix} \bar{B}_2 & 0_{r\times p} \\ 0_{p\times m} & I_p \end{bmatrix},$$

$$\widehat{C}_1 = \begin{bmatrix} \bar{C}_1 & 0_{k\times p} \end{bmatrix}, \ \widehat{C}_2 = \begin{bmatrix} \bar{C}_2 & 0_{l\times p} \\ 0_{p\times r} & I_p \end{bmatrix}, \ \widehat{D}_{12} = \begin{bmatrix} \bar{D}_{12} & 0_{k\times p} \end{bmatrix}, \ \widehat{D}_{21} = \begin{bmatrix} \bar{D}_{21} \\ 0_{p\times s} \end{bmatrix},$$

$$\widehat{K}_0 = \begin{bmatrix} K_0 & U_0 \\ V_0 & Z_0 \end{bmatrix} = \left[\begin{array}{c|c} (I_m - K\bar{D}_{22})^{-1}K & (I_m - K\bar{D}_{22})^{-1}U \\ \hline V(I_l - \bar{D}_{22}K)^{-1} & Z + V\bar{D}_{22}(I_m - K\bar{D}_{22})^{-1}U \end{array}\right].$$

We define a performance measure $\widehat{J}$ for system (31) of the form (2) with the weight matrices P, Q and $\widehat{X}_0$, where $\widehat{X}_0$ is some block $(r+p)\times(r+p)$ matrix, whose first diagonal block is $\bar{H}$. The value of $\widehat{J}$ coincides with J since $\eta(0) = 0$.

Lemma 3.1 [23]. *Given positive definite matrices $X, Y \in R^{r\times r}$ and a number $\gamma > 0$, there are matrices $X_1 \in \mathbb{R}^{p\times r}$, $X_2 \in \mathbb{R}^{p\times p}$, $Y_1 \in \mathbb{R}^{p\times r}$ and $Y_2 \in \mathbb{R}^{p\times p}$ such that*

$$\widehat{X} = \begin{bmatrix} X & X_1^\top \\ X_1 & X_2 \end{bmatrix} > 0, \quad \widehat{Y} = \begin{bmatrix} Y & Y_1^\top \\ Y_1 & Y_2 \end{bmatrix} > 0, \quad \widehat{X}\widehat{Y} = \gamma^2 I_{r+p} \tag{32}$$

if and only if

$$W = \begin{bmatrix} X & \gamma I_r \\ \gamma I_r & Y \end{bmatrix} \geq 0, \quad \operatorname{rank} W \leq r + p. \tag{33}$$

Theorem 3.3 *For system* (14)*, there is a dynamic controller* (30) *of order* $p \le r$*, such that a closed-loop system is admissible and* $J < \gamma$ *if and only if* (8)*,* (20)*,* (21) *and* (33) *are feasible with respect to* X *and* Y*. The matrices of such controller can be defined as*

$$\begin{bmatrix} K & U \\ V & Z \end{bmatrix} = (I_{m+p} + \widehat{K}_0 \widehat{D}_{22})^{-1} \widehat{K}_0, \quad \widehat{D}_{22} = \begin{bmatrix} \bar{D}_{22} & 0_{l\times p} \\ 0_{p\times m} & 0_{p\times p} \end{bmatrix}, \tag{34}$$

where $\widehat{K}_0$ *is a solution of the LMI*

$$\widehat{L}^\top \widehat{K}_0 \widehat{R} + \widehat{R}^\top \widehat{K}_0^\top \widehat{L} + \widehat{\Omega} < 0, \tag{35}$$

$$\widehat{R} = \begin{bmatrix} \widehat{C}_2 & \widehat{D}_{21} & 0_{(l+p)\times k} \end{bmatrix}, \quad \widehat{L} = \begin{bmatrix} \widehat{B}_2^\top \widehat{X} & 0_{(m+p)\times s} & \widehat{D}_{12}^\top \end{bmatrix},$$

$$\widehat{\Omega} = \begin{bmatrix} \widehat{A}^\top \widehat{X} + \widehat{X}\widehat{A} & \widehat{X}\widehat{B}_1 & \widehat{C}_1^\top \\ \widehat{B}_1^\top \widehat{X} & -\gamma^2 P & \widehat{D}_{11}^\top \\ \widehat{C}_1 & \widehat{D}_{11} & -Q^{-1} \end{bmatrix}.$$

The block matrix $\widehat{X}$ *in* (35) *is formed on the basis of Lemma* 3.1 *according to* (32)*, where* X *and* Y *satisfy* (8)*,* (20)*,* (21) *and* (33)*.*

Taking into account the structure of matrices in (31), the system (16) with a dynamic controller (30) can be represented as a system in the space $\mathbb{R}^{r+p}$ with a static controller:

$$\dot{\widehat{x}} = \widehat{A}\,\widehat{x} + \widehat{B}_1\, w + \widehat{B}_2\, \widehat{u}, \quad z = \widehat{C}_1\, \widehat{x} + \widehat{D}_{11}\, w + \widehat{D}_{12}\, \widehat{u}, \quad \widehat{y} = \widehat{C}_2\, \widehat{x} + \widehat{D}_{21}\, w,$$

$$\widehat{x} = \begin{bmatrix} \xi_1 \\ \eta \end{bmatrix}, \quad \widehat{y} = \begin{bmatrix} y - \bar{D}_{22} u \\ \eta \end{bmatrix}, \quad \widehat{u} = \begin{bmatrix} u \\ \dot{\eta} \end{bmatrix}, \quad \widehat{u} = \widehat{K}_0 \widehat{y}.$$

Therefore, Theorem 3.3 can be proved as a corollary of Theorem 3.1 and Lemma 3.1.

Note that Theorems 3.1 and 3.3, without using the constraint $X < \gamma^2 \bar{H}$, give the existence criteria and methods for constructing stabilizing controllers that provide the estimate $J_0 < \gamma$ for the corresponding closed-loop systems. In the case $p = 0$, Theorem 3.3 yields a criterion for the existence of a static controller (17) with the properties specified in Theorem 3.1. The construction of dynamic controllers of the order $p = r$ satisfying Theorem 3.3 reduces to the solution of the LMI system without additional constraints. In this case, the rank constraint in (33) holds automatically.

We present the following algorithm for constructing a dynamic controller (30), which satisfies Theorem 3.3.

Algorithm 3.1

1) Calculating the transforming matrices (4) and coefficient matrices of system (16);
2) calculating $W_{\bar{R}}$ and $W_{\bar{L}}$, where $\bar{R} = \begin{bmatrix} \bar{C}_2 & \bar{D}_{21} \end{bmatrix}$, $\bar{L} = \begin{bmatrix} \bar{B}_2^\top & \bar{D}_{12}^\top \end{bmatrix}$;
3) finding matrices X and Y that satisfy (8), (20), (21) and (33);
4) constructing the decomposition $\Delta = Y - \gamma^2 X^{-1} = S^\top S \ge 0$, where $S \in \mathbb{R}^{p\times r}$, $\ker S = \ker \Delta$, and forming the block matrix

$$\widehat{X} = \begin{bmatrix} X & X_1^\top \\ X_1 & X_2 \end{bmatrix} > 0, \quad X_1 = \frac{1}{\gamma} SX, \quad X_2 = \frac{1}{\gamma^2} SXS^\top + I_p;$$

5) solving the LMI (35) with respect to $\widehat{K}_0$ taking into account $\det(I_m + K_0 \bar{D}_{22}) \neq 0$;
6) calculating the controller matrices according to (34).

Remark 3.2 Algorithm 3.1 can be implemented, e.g., by means of the MATLAB software. If $\Delta = 0$ in step 4) of the algorithm, i.e., $\operatorname{rank} W = r$, then solving the LMI (19), we obtain the gain matrix of static controller (17), which satisfies Theorem 3.1.

Remark 3.3 If the pair $\{E, A\}$ in system (14) is not impulse-free, but there is a matrix $K_1 \in \mathbb{R}^{m\times l}$ satisfying (26), then we set $u = K_1 y + v$, where v is a new control generated by

$$\dot\eta = Z\eta + Vy, \quad v = U\eta + Ky, \quad \eta(0) = 0,$$

which solves the problem for the ordinary system (28) formed on the basis of equivalent transformation of system (27) (see the previous subsection). As a result, the closed-loop descriptor system in the extended phase space has the form

$$\widehat E\dot{\widehat x} = \widehat A_0\widehat x + \widehat B_0 w, \quad z = \widehat C_0\widehat x + \widehat D_0 w, \quad \widehat x(0) = \widehat x_0, \tag{36}$$

where

$$\widehat E = \begin{bmatrix} E & 0 \\ 0 & I_p \end{bmatrix}, \quad \widehat x = \begin{bmatrix} x \\ \eta \end{bmatrix}, \quad \widehat x_0 = \begin{bmatrix} x_0 \\ 0 \end{bmatrix},$$

$$\widehat A_0 = \begin{bmatrix} A + B_2(K_{10}C_2 + K_{11}G_1) & B_2K_{11}G_2 \\ V(\bar C_2E_2^\top + \bar D_{22}G_1) & Z + V\bar D_{22}G_2 \end{bmatrix}, \widehat B_0 = \begin{bmatrix} B_1 + B_2(K_{10}D_{21} + K_{11}G_3) \\ V(\bar D_{21} + \bar D_{22}G_3) \end{bmatrix},$$

$$\widehat C_0 = \begin{bmatrix} C_1 + D_{12}(K_{10}C_2 + K_{11}G_1) & D_{12}K_{11}G_2 \end{bmatrix}, \ \widehat D_0 = D_{11} + D_{12}(K_{10}D_{21} + K_{11}G_3),$$

$$G_1 = K_0\bar C_2E_2^\top, \ \ G_2 = (I_m - K\bar D_{22})^{-1}U, \ \ G_3 = K_0\bar D_{21}, \ \ K_0 = (I_m - K\bar D_{22})^{-1}K.$$

4 Example

Consider an electric circuit control system of the form described in (14), where [29]

$$E = \begin{bmatrix} L & 0 & 0 \\ 0 & C & 0 \\ 0 & 0 & 0 \end{bmatrix}, \quad A = \begin{bmatrix} -R_1 & -1 & 1 \\ 0 & -1/R_2 & 0 \\ 1 & 0 & 0 \end{bmatrix}, \quad B_1 = B_2 = \begin{bmatrix} 0 \\ 1 \\ -1 \end{bmatrix},$$

$$C_1 = C_2 = \begin{bmatrix} 0 & 1 & 0 \\ 0 & 0 & 1 \end{bmatrix}, \ \ D_{12} = \begin{bmatrix} 0 \\ 1 \end{bmatrix}, \ \ D_{11} = D_{21} = D_{22} = 0_{2\times 1},$$

$x = \begin{bmatrix} i & v_2 & v_1 \end{bmatrix}^\top$, $z = \begin{bmatrix} v_2 & v_1 + u \end{bmatrix}^\top$, $y = \begin{bmatrix} v_2 & v_1 \end{bmatrix}^\top$, $L = 3$ is the inductance, $C = 2$ is the capacitance, $R_1 = 2$ and $R_2 = 1$ are the resistances, i is the current, v_1 and v_2 are the voltages, u is the control signal of a current source with bounded disturbance w (see Fig. 1). In this system, the pair $\{E, A\}$ is not impulse-free, the triples $\{E, A, B_2\}$ and $\{E, A, C_2\}$ are I-controllable and I-observable, respectively.

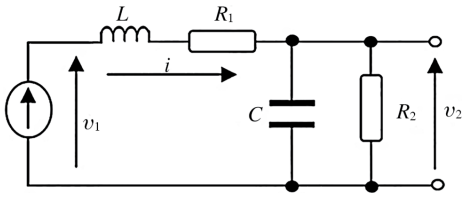

Figure 1: The electrical circuit.

We choose $K_1 = \begin{bmatrix} 0 & 1 \end{bmatrix}$ satisfying (26) and the weight matrices for performance measures (2): $P = 1$, $Q = I_2$, $X_0 = E^\top HE$, $H = 3I_3$. Using Theorem 3.1 for system (27) with $\gamma = 1,03624$, we find the controller

$$v = Ky, \quad K = \begin{bmatrix} 0.22439 & -17.998625 \end{bmatrix},$$

such that the closed-loop system is admissible and $J = 0.94402 < \gamma$. At the same time, the finite spectrum of the system coincides with $\sigma(\bar{A}) = \{-0.59314 \pm 0.39471\, i\}$, where $\bar{A}$ is a system matrix of (28). Applying Lemma 2.2 for closed-loop system (29), the worst-case pair $\{w, x_0\}$ with respect to J is found as follows:

$$w = \bar{K}_* \xi_1, \quad \bar{K}_* = \begin{bmatrix} -26.31483 & -4.74882 \end{bmatrix}, \tag{37}$$

$$x_0 = \begin{bmatrix} -0.32886 & 0.08162 & 1.50212 \end{bmatrix}^\top. \tag{38}$$

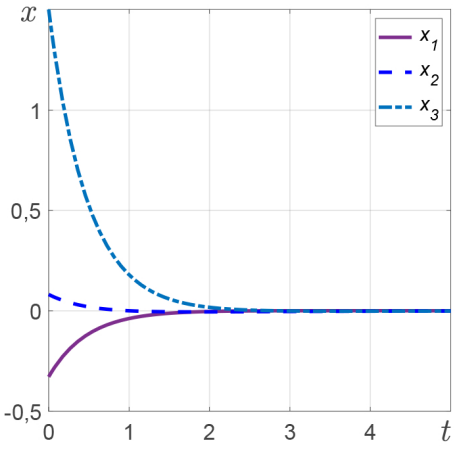

Figure 2: Behavior of a closed-loop system.

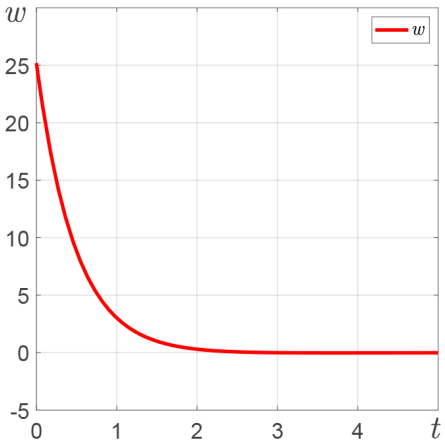

Figure 3: The worst-case perturbation with respect to J.

Fig.2 shows the behavior of the solution of the closed-loop system under the worst-case conditions (37) and (38), and Fig.3 shows the behavior of the worst-case disturbance (37).

Next, applying Algorithm 3.1, the matrices of the approximate J-optimal dynamic controller (30) of the order $p = 2$ are found for system (27) as follows:

$$\begin{bmatrix} K & U \\ V & Z \end{bmatrix} = \left[\begin{array}{cc|cc} 0.16824 & -2.24725 & -0.00072 & -0.15173 \\ -0.00256 & 0.00014 & -0.00063 & 0.00259 \\ \hline -0.10392 & 0.09342 & -0.01008 & -0.77037 \end{array}\right],$$

for which the closed-loop system (36) is admissible with the finite spectrum

$$\{-0.72210 \pm 0.30576\, i,\ -0.77143,\ -0.00067\}$$

and has the minimum value of the performance measure $J = 0.28356$.

5 Conclusion

Constructive methods for evaluating and achieving the desired damping level of external and initial disturbances in descriptor control systems have been developed. The practical implementation of these methods is based on the equivalent transformation of descriptor systems and application of well-known methods of H_∞ control theory for ordinary lower-order systems. Thus, the existence conditions and algorithms for constructing a dynamic controller of the order $p = \operatorname{rank} E$, for which the closed-loop system is admissible with weighted performance measures $J_0 < \gamma$ or $J < \gamma$, reduce to solving LMIs without additional rank constraints. In the case, when the original descriptor system is not impulse-free, it is proposed to search for an additional control that provides the specified property of this system. The equivalent transformation of the descriptor system to the ordinary one was also applied to find the worst-case external and initial disturbances with respect to the weighted performance measures. Studying the behavior of a closed-loop system under such worst-case conditions can be important in the design and testing of real controlled objects.

Acknowledgment

This work was supported by a grant from the Simons Foundation (SFI-PD-Ukraine-00014586, A.G.M.).

References

[1] L. Dai. *Singular Control Systems*. Springer, New York, 1989.

[2] Guang-Ren Duan. *Analysis and Design of Descriptor Linear Systems*. Springer, New York etc., 2010.

[3] Yu Feng and Mohamed Yagoubi. *Robust Control of Linear Descriptor Systems*. Springer Nature Singapore Pte Ltd., 2017.

[4] S. Campbell, A. Ilchmann, V. Mehrmann and T. Reis (Eds.). *Applications of Differential-Algebraic Equations: Examples and Benchmarks*. Differential-Algebraic Equations Forum, Springer Nature, Switzerland AG, 2019.

[5] A. A. Belov and A. P. Kurdyukov. *Descriptor Systems and Control Problems*. Fizmatlit, Moscow, 2015. [Russian]

[6] A. G. Mazko. *Robust Stability and Stabilization of Dynamic Systems. Methods of Matrix and Cone Inequalities*. Proc. of the Institute of Mathematics, National Academy of Sciences of Ukrain, Vol. 102, 2016. [Russian]

[7] A. G. Mazko. *Matrix Methods for the Analysis and Synthesis of Dynamical Systems*. Kyiv, Naukova Dumka, 2023. https://doi.org/10.37863/6103136622-55. [Ukrainian]

[8] D. V. Balandyn and M. M. Kogan. Generalized H_∞ optimal control as a trade-off between the H_∞ optimal and γ-optimal controls. *Automation and Remote Control* **71** (6) (2010) 993 – 1010. https://doi.org/10.1134/S0005117910060020.

[9] Z. Feng, J. Lam, S. Xu and S. Zhou. H_∞ control with transients for singular systems. *Asian Journal of Control 18* (3) (2016) 817 – 827.

[10] S. Boyd, L. El Ghaoui, E. Feron and V. Balakrishman. *Linear Matrix Inequalities in System and Control Theory*. SIAM Stud. Appl. Math., **15**, 1994.

[11] P. Gahinet and P. Apkarian. A linear matrix inequality approach to H_∞ control. *Intern. J. of Robust and Nonlinear Control* **4** (1994) 421 – 448.

[12] S. Xu, J. Lam and Y. Zou. New versions of bounded real lemmas for continuous and discrete uncertain systems. *Circuits, Systems and Signal Process* **26** (2007) 829 – 838.

[13] M. Chadli, P. Shi, Z. Feng and J. Lam. New bounded real lemma formulation and H_∞ control for continuous-time descriptor systems. *Asian J. Control* **20** (1) (2018) 1 – 7.

[14] F. Gao, W. Q. Liu, V. Sreeram and K. L. Teo. Bounded real lemma for descriptor systems and its application. In: *IFAC 14th Triennial World Congress*. Beijing, P.R., China, 1999, 1631 – 1636.

[15] I. Masubushi, Y. Kamitane, A. Ohara and N. Suda. H_∞ Control for descriptor systems: a matrix inequalities approach. *Automatica* **33** (4) (1997) 669 – 673.

[16] A. G. Mazko. Evaluation of the weighted level of damping of bounded disturbances in descriptor systems. *Ukrainian Mathematical Journal* **70** (11) (2019) 1777 – 1790, https://doi.org/10.1007/s11253-019-01606-x.

[17] Masaki Inoue, Teruyo Wada, Masao Ikeda and Eiho Uezato. Robust state-space H_∞ controller design for descriptor systems. *Automatica* **59** (2015) 164 – 170.

[18] P. Gahinet, A. Nemirovski, A. J. Laub and M. Chilali. *The LMI Control Toolbox. For Use with Matlab. User's Guide*. Natick, MA, The MathWorks, Inc., 1995.

[19] R. Orsi, U. Helmke and J. B. Moore. A Newton-like method for solving rank constrained linear matrix inequalities. *Automatica* **42** (11) (2006) 1875 – 1882.

[20] J. Löfberg. YALMIP: A toolbox for modeling and optimization in MATLAB. In: *IEEE International Symposium on Computer Aided Control Systems Design*. Taipei, Taiwan, 2004, 284–289.

[21] Yu. E. Voskoboynikov and A. F. Zadorozhny. *Basic Computing and Programming in the MathCAD PRIME Package: Teaching Manual*. St. Petersburg, "Lan" Publishing House, 2016.

[22] F. R. Gantmacher. *Matrix Theory*. Moscow, Nauka, 1988. [Russian]

[23] A. G. Mazko. Robust output feedback stabilization and optimization of control systems. *Nonlinear Dynamics and Systems Theory* **17** (1) (2017) 42–59.

[24] A. G. Mazko and S. M. Kusii. Weighted damping of limited disturbances in the aircraft control system in landing mode. *Proc. of the Institute of Mathematics, Ukrainian National Academy of Sciences* **15** (1) (2018) 88 – 99. [Ukrainian]

[25] A. G. Mazko and T. O. Kotov. Robust stabilization and weighted damping of bounded disturbances in descriptor control systems. *Ukrainian Mathematical Journal* **71** (10) (2020) 1572 – 1589, DOI 10.1007/s11253-020-01732-x.

[26] K. Zhou, J. C. Doyle and K. Glover. *Robust and Optimal Control*. Englewood, Prentice-Hall, Inc., 1996.

[27] G. E. Dullerud and F. G. Paganini. *A Course in Robust Control Theory. A Convex Approach*. Berlin, Springer-Verlag, 2000.

[28] D. Cobb. Controllability, observability and duality in singular systems. *IEEE Transactions on Automatic Control* **29** (1984) 1076 – 1082.

[29] K. Takaba. Robust H^2 control of descriptor system with time-varying uncertainty. *Intern. J. of Robust and Nonlinear Control* **71** (4) (1998) 559 – 579.

Nonlinear Dynamics and Systems Theory, **25** (4) (2025) 424–433

Bright and Dark Solitons via Homoclinic Dynamics in Helmholtz-Type DNLS Equations

A. Mehazzem [1*], M. S. Abdelouahab [1] and R. Amira [2]

[1] *Department of Mathematics and Computer Science, Abdelhafid Boussouf University Center of Mila, Mila, Algeria.*

[2] *Laboratory of Mathematics, Informatics and Systems (LAMIS), Echahid Cheikh Larbi Tebessi University, Tebessa, Algeria.*

Received: October 29, 2024; Revised: July 13, 2025

Abstract: The existence of homoclinic orbits in a dynamical system has interesting consequences for its behavior. This is the case in this paper, where we present a model of the discrete nonlinear Schrödinger equation under the Helmholtz operator. We give the fundamental theorem of the existence of a homoclinic (heteroclinic) orbit for a particular class of reversible planar maps. Homoclinic structures are known to be sources of sensitivity that, under small perturbations, can bifurcate solutions. The problem of the existence of solitons has therefore been replaced by that of the existence of homoclinic solutions. We prove the existence of bright and dark solitons in a certain case of nonlinearity.

Keywords: *discrete Schrödinger equation; Helmholtz operator; homoclinic orbits; heteroclinic orbits; reversible planar maps.*

Mathematics Subject Classification (2020): 35Q55, 35Q51, 37K60, 70K44, 93-02.

1 Introduction

Over the last decade, the existence of discrete solitons in DNLS equations has become a hot topic of many studies, to mention just a few, refer to [7, 11–13, 15–17]. These include variational methods, central manifold reduction, and the Nehari manifold approach. A good number of these papers take into account DNLS equations with constant coefficients, and their conclusions have been presented in [7, 12, 15, 16, 19]. DNLS equations with periodic coefficients have recently appeared in the physics literature, and this phenomenon can be identified by numerical simulations [11, 13].

* Corresponding author: mailto:a.mehazzem@centre-univ-mila.dz

The existence of bright solitons in different cases was then examined using Melnikov's method, assuming a small perturbation, and for the anti-integrability method [1], some localized solutions persist for weak coupling cases. In [6], the variational approach can also be used, but the allowed frequency region cannot be explicitly determined by the variational method. We are looking at the homoclinic orbit approach to the existence of soliton solutions of DNLS equations used in our paper and in [16], it is precisely a generalization of the work in [7]. Homoclinic structures are recognized as sources of sensitivity which, under small perturbations, can bifurcate solutions. The existence of homoclinic orbits in a dynamical system has interesting consequences for its behavior. The problem of the existence of solitons has therefore been replaced by the problem of the existence of homoclinic solutions. However, this approach yields the frequency Ω and the related sequence x_n simultaneously, and therefore the interval of existence of the frequency Ω. Discrete Helmholtz equations are closely related to discrete Schrodinger equations, which appear naturally in the tight-binding model of electrons in crystals [2]. Similar equations also appear in the case of studies involving time harmonic elastic waves in lattice models of crystals [3], see for example, [14], especially in the case d = 2.

We consider spatially localized standing waves for the discrete nonlinear Schrödinger equation (DNLS):

$$\dot{\psi}_n = -H\psi_n - h(\mid \psi_n \mid)\psi_n, n \in \mathbb{Z},$$

,

$$H\psi_n = \frac{1}{w_n}(\psi_{n+1} + \psi_{n-1} + d_n\psi_n),$$

where $w_n > 0, d_n \in \mathbb{R}$, and $(w_n w_{n+1})^{-1}, w_n^{-1} d_n$ are bounded sequences. It gives rise to an operator H, called Helmholtz operator [18], in the weighted Hilbert space $l^2(\mathbb{Z}; w)$ with scalar product:

$$\langle f,\ g\rangle = \sum_{n\in \mathrm{Z}} w_n \overline{f_n} g_n\ ,\ f,\ g \in l^2(\mathbb{Z}; w)\ .$$

There is an interesting link between the Jacobi and Helmholtz operators. in [18] (Theorem 1.14, page 21).

Use the stationary wave ansatz

$$\psi_n = x_n \exp(-i\omega t),$$

where x_n is a sequence with real values and $\omega \in \mathbb{R}$.

We impose the following boundary condition at infinity: $\lim_{n\to\pm\infty} u_n = 0$, and we are looking for non-trivial solutions, i.e the solutions that are not equal to 0.

The objective of this paper is to explore the existence of homoclinic solutions for a given class of periodic difference equations.

We use the symmetry properties of reversible planar maps to improve the homoclinic orbit approach. The results of the existence of the soliton of the discrete Helmholtz-Schrodinger equation will not be obtained by the variational method or the anti-integrability method.

This paper is structured as follows. In the second Section, we outline some basics about reversible planar maps and homoclinic (heteroclinic) points. In addition, we give the fundamental theorem for the existence of a homoclinic (heteroclinic) orbit for a particular class of planar maps so that we can prove the existence results rigorously.

In Section 3, we present the conditions for the existence of bright and dark solitons for local solutions of the discrete Schrödinger equations with the Helmholtz operator.

We also examine the existence of soliton solutions for DNLS equations in certain cases of nonlinearity.

2 Homoclinic Orbits of Planar Reversible Maps

We will give a mathematical description of time-reversal symmetry in the context of dynamical systems. In the most interesting applications, $\Omega = \mathbb{R}^n$. We are interested only in the diffeomorphism of $\mathbb{R}^{2n}$. Let R be a smooth diffeomorphism satisfying the following conditions:

- $R \circ R =$ identity.
- The dimension of the fixed point set of R, $Fix(R)$, is n.

R is known as inverse involution. A diffeomorphism T is called R-reversible if $R \circ T = T^{-1} \circ R$.

Several periodic points are easy to find; they are called symmetrical periodic points and are characterized by the following proposition.

Proposition 2.1 *[5] Let $p \in Fix(R)$ and suppose that $T^k(p) \in Fix(R)$, and therefore, $T^{2k}(p) = p$, then we have*

$$T^k(p) = RT^k(p) = T^{-k}R(p) = T^{-k}(p), \quad therefore: \quad T^{2k}(p) = p.$$

So, symmetrical periodic points can be geometrically identified; we focus on the self-intersections of the set of fixed points of R under the iteration of T. We might also find homoclinic geometrically reversible diffeomorphism of R-geometrically reversible diffeomorphisms.

Proposition 2.2 *[4] Let $p \in Fix(R)$ be a symmetric fixed point of T and let $W^s(p)$ and $W^u(p)$ denote the stable and unstable manifolds of p, respectively. Then $R(W^u(p)) = W^s(p)$ and $R(W^s(p)) = W^u(p)$. In particular, if $q \in W^u(p) \cap Fix(R)$, then q is a homoclinic point.*

Let $x \in W^u(p)$ such that $\lim_{n \longrightarrow \infty} T^{-n}(x) = p$, and so we have

$$p = R \lim_{n \longrightarrow \infty} (T^{-n}(x)) = \lim_{n \longrightarrow \infty} T^n(R(x)).$$

We have $R(x) \in W^s(p)$, where $RW^u(p) \subset W^s(p)$. We also have $RW^s(p) \subset W^u(p)$ such that $RW^u(p) = W^s(p)$. If $q \in W^u(p) \cap Fix(R)$. So, $q = R(q) \in W^s(p) \cap Fix(R)$ also, q is a homoclinic point [4].

Hence, to generate homoclinic points for reversible diffeomorphisms, it is sufficient to find the intersections of $W^u(p)$ with $Fix(R)$. We note that both of these propositions are valid in much more general terms. Homoclinic points which are also in $Fix(R)$ are described as symmetric homoclinic points. Homoclinic points are called regular homoclinic points if the unstable variety (and hence the stable variety) intersects $Fix(R)$ transversely at the homoclinic point.

Proposition 2.3 *[5] Let p be a symmetric fixed point and let q be a symmetric homoclinic point in $W^u(p)$. Let N be any neighborhood of p in $Fix(R)$. Then there exists an infinite number of periodic symmetric points in N.*

Proposition 2.4 *[4] Let p be a non-symmetric periodic point. Suppose $q \in W^u(p) \cap Fix(R)$. Then $q \in W^u(p) \cap W^s(R(p))$. Thus some heteroclinic points can be found geometrically as symmetric homoclinic points. Regular symmetric heteroclinic points are defined as regular homoclinic points.*

Proposition 2.5 *[4] Assume that T is an R-reversible diffeomorphism on the plane and let p be a nonsymmetric saddle point for T. Assume that a branch of $W^u(p)$ and a branch of $W^s(p)$ intersect. Suppose a branch of $W^s(p)$ intersects $Fix(R)$ transversely. Then there exist infinitely many symmetric periodic orbits entering any neighborhood of p and $R(p)$.*

A reversible class of planar maps is derived from symmetrical differential equations of the form [5, 7]

$$x_{n+1} + x_{n-1} = g(x_n). \tag{1}$$

In this paper we treat the most general case. We consider the difference expression

$$H_n x_n = \tfrac{1}{w_n}(x_{n+1} + x_{n-1} + d_n x_n),$$

where $w_n > 0, d_n \in \mathbb{R}$, and $(w_n w_{n+1})^{-1}, w_n^{-1} d_n$ are bounded sequences. It gives rise to an operator H, called the Helmholtz operator [18], in the weighted Hilbert space $l^2(\mathbb{Z}; w)$ with scalar product:

$$\langle f,\ g\rangle = \textstyle\sum_{n\in\mathrm{Z}} w_n \overline{f_n} g_n\ ,\ f,\ g \in l^2(\mathbb{Z}; w),$$

$$x_{n+1} + x_{n-1} = g(x_n, w_n, d_n, h),$$

which regularly appears in analyses of the stationary state of coupled oscillators in one-dimensional lattices [5] . The system can be expressed as a planar map, given by T, of the form

$$\begin{cases} x_{n+1} = z_n, \\ z_{n+1} = -x_n + g(z_n), \end{cases}$$

i.e.,

$$T(x, z) = (z, -x + g(z)) \quad and \quad g_n(x_n) = d_n x_n + \omega_n h(x_n).$$

It is an easy matter to check that T is invertible and

$$\begin{cases} x_{n+1} = -z_n + g(x_n), \\ z_{n+1} = x_n \end{cases}$$

$$T^{-1}(x, z) = (-z + g(x), x).$$

Furthermore, T is a $\mathcal{C}^1$ diffeomorphism if g is $\mathcal{C}^1$. $g_n(x)$ is nonlinear and continuous at x. We have $g_{n+P}(x) = g_n(x)$ for all $n \in \mathbb{Z}$. In this work, we always suppose that g is a $\mathcal{C}^1$ function. We see that T is R_1-reversible with respect to the involution $R_1(x, z) = (z, x)$, and R_2-reversible with respect to the involution $R_2(x, z) = (-z, -x)$ since g is an odd function.

$$R_1 \circ T(x_n, z_n) = R_1(z_n, -x_n + g(z_n)) = (-x_n + g(z_n), z_n),$$
$$T^{-1} \circ R_1(x_n, z_n) = T^{-1}(z_n, x_n) = (-x_n + g(z_n), z_n).$$

Note that the fixed-point sets $Fix(R_1)$ and $Fix(R_2)$ are indicated by the lines $z = x$ and $z = -x$, denoted by S_1 and S_2, respectively. Let $d = \min_{n\in\mathrm{Z}} d_n > 1$, $f(z) = g(z) - dz$ and we fix $w = w_n > 0$.

Theorem 2.1 *Suppose that*

1. *$f(z)$ is a $\mathcal{C}^1$ and odd function, and has three real zeros, $-z_0$, 0 and z_0 ($z_0 > 0$), with $f'(0) > 0$.*
2. *$sup_{z \geq z'}((d-2)z + wf(z) < 0$ for given $z' > z_0$.*
   Then the planar map T has a homoclinic orbit.

Proof. Because f as an odd function has three different real zeros, we can suppose that its real zeros are $-z_0, 0$ and z_0 with $z_0 > 0$. The planar map T has three fixed points $P(-z_0, -z_0), O(0,0)$ and $Q(z_0, z_0)$, all of which are symmetrical with the involution R_1. The origin O is hyperbolic if $f`(0) > 0$. In addition, the unstable manifold $W^{\mathrm{u}}(O)$ and the stable manifold $W^{\mathrm{s}}(O)$ are tangent to the lines $z = \lambda_2 x$ and $z = \lambda_1 x$, respectively, where $\lambda_2 > 1$ and $0 < \lambda_1 < 1$ are eigenvalues of the Jacobian matrix of T at the origin. We first prove that the intersection of $W^{\mathrm{u}}(O)$ with the interior of the segment EQ is non-empty, where $E(0, z_0)$ lies on the z-axis. It is simple to verify that a branch of $W^{\mathrm{u}}(O)$ initially enters the interior of the triangle $\triangle OEQ$, noted by $int(\triangle OEQ)$. For any point $A(x, z) \in int(\triangle OEQ)$, When $0 < x < z < z_0$, the coordinates of the image point $T(A)$ are $(z, -x + dz + wf(z))$. Furthermore, since $f(z)$ is positive and $d \geq 0$ for $z \in (0, z_0)$, the distance between the point $T(A)$ and the line S_1 is $\frac{\sqrt{2}}{2}(wf(z) - x + (d-1)z)$, greater than the distance from A to S_1. Thus, the unstable manifold $W^{\mathrm{u}}(O)$ inside $\triangle OEQ$ never intersects the segments OE and OQ. In the next section, we show by contradiction that $W^{\mathrm{u}}(O)$ intersects the segment EQ.

Suppose that the branch of $W^{\mathrm{u}}(O)$ in the first quadrant always lies inside $\triangle OEQ$. Consider a point $B \in W^{\mathrm{u}}(O) \cap int(\triangle OEQ)$. Then all the image points $T^n(B) \in int(\triangle OEQ)$ for $n = 1, 2, \cdots$. In addition, the sequences of x-coordinates and z-coordinates of $T^n(B)$ are at the same time strictly increasing and bounded above, and therefore converge to x^* and z^*, respectively. Consequently, the sequence of points $T^n(B)$ is convergent to $N(x^*, z^*)$, which is a fixed point of T. Based on the facts that $x^* > 0$ and $z^* > 0$, it thus follows that $N = Q$. On the other part, the sequence of the distance between $T^n(B)$ and S_1 is also strictly increasing, implying that $N \neq Q$, there is a contradiction. Consequently, the unstable manifold $W^{\mathrm{u}}(O)$ pierces the segment EQ. Secondly, we show that $W^{\mathrm{u}}(O)$ in the first quadrant meets the line S_1 at some point. We note $H_0(x_0, z_0)$, the intersection point of $W^{\mathrm{u}}(O)$ with the segment EQ. Let $H_{n+1} = T(H_n), n = 0, 1, \cdots$. The coordinates of H_n are (x_n, z_n). It then follows that $z_1 = -x_0 + dz_0 + wf(z_0) = z_0 + ((d-1)z_0 + x_0) > z_0$. Since $f(z) < 0$ for $z > z_0$, we derive from assumption (ii) that $\sup_{z > z_1}((d-2)z + wf(z) < 0$.
We note

$$\sup_{z \geq z_1}((d-2)z + wf(z)) < 0, \quad so \quad \sup_{z \geq z_1}(d-2)z + wf(z) = -a, \quad (a > 0).$$

Suppose that $W^{\mathrm{u}}(O)$ in the first quadrant does not cross the line S_1. Then $W^{\mathrm{u}}(O)$ is between the z-axis and the line S_1. So, the points H_n are above the line S_1, meaning that $z_{n+1} > x_{n+1} = z_n > x_n = \cdots = z_1 > x_1 = z_0$, and $(d-2)z_n + wf(z_n) \leq -a$ for $n = 1, 2, \cdots$. Consider d_n as the distance between H_n and the line S_1. Then

$$dist_n = \frac{\sqrt{2}}{2}(z_n - x_n) = \frac{\sqrt{2}}{2}(z_n - z_{n-1}), n = 0, 1, (z_{-1} = x_0).$$

Let $z_{n+1} = -x_n + dz_n + wf(z_n)$, so $z_{n+1} - z_n = z_n - z_{n-1} + (d_n - 2)z_n + wf(z_n)$.

Therefore, $\sqrt{2}dis_{n+1} = \sqrt{2}dis_n + (d-2)z_n + wf(z_n), n = 0, 1, \ldots$ It follows that

$$\sqrt{2}dis_1 = \sqrt{2}dis_0 + (d-2)z_0,$$

$$\sqrt{2}dis_2 = \sqrt{2}dis_1 + (d_1-2)z_1 + wf(z_1),$$

$$\sqrt{2}dis_{n+1} = \sqrt{2}dis_n + (d_n-2)z_n + wf(z_n)$$

and hence

$$0 \leq \sqrt{2}dis_{n+1} = \sqrt{2}dis_0 + \sum_{i=1}^{n}[(dis_i - 2)z_i + wf(z_i)] \leq \sqrt{2}dis_0 - na.$$

Let $n \to \infty$, we obtain a contradiction. As a result, the intersection of $W^{\mathrm{u}}(O)$ with the line S_1 is non empty. From Proposition 2.2, it follows that $W^{\mathrm{u}}(O)$ and $W^{\mathrm{s}}(O)$ intersect at a point q on S_1, which means that a homoclinic orbit exists. □

Let (x_0, x_0) be the point of intersection of $W^{\mathrm{u}}(O)$ and S_1. So, the homoclinic orbit $(x_n, z_n) = T^n((x_0, x_0))$ in the first quadrant has the following property: $x_n = z_{-n}$ and $x_{-n} = z_n$ for $n \geq 1$.

From the homoclinic orbit, we derive a sequence $\{x_n\}$ that satisfies (1) and $x_n \to 0$ exponentially as $n \to +\infty$ or $-\infty$.

Theorem 2.2 *Suppose that*
(i) $f(z)$ is a $\mathcal{C}^1$ and odd function, and $f(z) + 2dz$ has only three real zeros, $-z_0, 0$, and $z_0 (z_0 > 0)$ with $f'(0) < -2d$.
(ii) $inf_{z \geq z'}(\{wf(z) + 2dz\}) > 0$, for some $z' > z_0$.
Therefore the planar map T has a homoclinic orbit.

Proof. Note first that we obtain the following symmetry if x_n satisfies the difference equation

$$wf(x_n) = x_{n-1} + x_{n+1} - dx_n, \tag{2}$$

then $\{y_n = (-1)^n x_n\}$ is a solution of the difference equation. We have $g(x_n) = x_{n-1} + x_{n+1}$. So, if n is even, we get,

$$\begin{cases} y_n = (-1)^n x_n, \\ y_{n+1} = (-1)^{n+1} x_{n+1}, \\ y_{n-1} = (-1)^{n-1} x_{n-1}. \end{cases}$$

Therefore

$$\begin{cases} y_n = x_n, \\ y_{n+1} = -x_{n+1}, \\ y_{n-1} = -x_{n-1}. \end{cases}$$

From (2), we can find

$$\begin{aligned} w\widehat{f}(y_n) &= -y_{n+1} - y_{n-1} - dy_n, \\ &= -g(y_n) - dy_n, \\ &= -wf(y_n) - d + y_n - dy_n, \\ &= -wf(y_n) - 2dy_n. \end{aligned}$$

Hence, $w\widehat{f}(z) = -wf(z) - 2dz$ and vice versa. Assumptions (i) and (ii) are satisfied for $\widehat{f}(z)$. It follows that the planar application T induced has a homoclinic orbit,

implying the existence of a homoclinic orbit for the planar application T. □

From Theorem 2.2, we derive a sequence $\{x_n\}$ that satisfies (1), $sign(x_n) = -sign(x_n)$ and $x_n \to 0$ exponentially as $n \to +\infty$ or $-\infty$.

Theorem 2.3 *Suppose that $f(z)$ is a $\mathcal{C}^1$ and odd function, and admits three real zeros,$-z_0, 0$ and $z_0(z_0 > 0)$ with $f'(z_0) > 0$. Therefore, the planar application T has a heteroclinic orbit.*

Proof. The reversible map T has three fixed points, two of which, $P(-z_0, -z_0)$ and $Q(z_0, z_0)$, are hyperbolic if $f'(z_0) > 0$. Similarly to the proof of Theorem 3.1, one can verify that $W_u(Q)$ intersects the $x-$axis at $H(x, 0)$ with $0 < x < z_0$. Simple calculations show that $T(H)$ and H are symmetric with respect to S_2. Then the intersection of $W_u(Q)$ with S_2 is nonempty. Consequently, from Proposition 2.2, it follows that the intersection of $W^u(Q)$ with $W^s(P)$ is nonempty, and hence the planar map T has a heteroclinic orbit.

From Theorem 2.3, we derive a sequence $\{x_n\}$ that satisfies (1) and $x_n \to z_0$ as $n \to +\infty$ and $x_n \to -z_0$ as $n \to -\infty$.

The proof of the present theorem is the same as that of Theorem 2.2.

Theorem 2.4 *Suppose that $f(z)$ is an odd $\mathcal{C}^1$ function, and $f(z)+2dz$ has only three real zeros, $-z_0, 0$ and $z_0(z_0 > 0)$ with $f'(z_0) < -2d$, Therefore, the planar application T has a heteroclinic orbit.*

The conclusion of Theorem 2.4, implies the existence of a solution $\{x_n\}$ that satisfies (1), with the property that $\text{sign}(x_n) = -\text{sign}(x_{n+1})$ as $|x_n| \to z_0$.

3 The DNLS Equations with Helmholtz Operator and General Nonlinearities

In this section, we investigate the DNLS equations with the Helmholtz operator and general nonlinearities

$$i\frac{\partial \psi_n}{\partial t} + h(\mid \psi_n \mid)\psi_n + \frac{1}{w_n}(\psi_{n+1} + \psi_{n-1} - d_n\psi_n) = 0, \tag{3}$$

where h is a C^1 function. Great attention has been paid to localized solutions of the form $\psi_n = x_n e^{-i\Omega t}$, where x_n are time independent. Such solutions are time periodic and spatially localized. The result is a difference equation

$$-\Omega x_n + h(\mid x_n \mid)x_n + \frac{1}{w_n}(x_{n+1} + x_{n-1} - d_n x_n) = 0,$$

$$g_n(x_n) = x_{n+1} + x_{n-1},$$

$$x_{n+1} + x_{n-1} = [\omega_n(\Omega - h(\mid x_n \mid)) + d_n]x_n,$$

$$f(z) = [\omega(\Omega - h(\mid z \mid) + d]z - dz,$$

$$f(z) = \omega(\Omega - h(\mid z \mid))z.$$

Theorem 3.1 *1. Assume that h is strictly increasing in $[0,+\infty[$. Then there exists an unstaggered (staggered) bright solitons of the form $x_n e^{i\Omega t}$ with $h(0) < \Omega < h_\infty$ ($h(0) - 2d/w < \Omega < h_\infty - 2d/w$) for the system (3) with $w > 0$.*

2. Assume that h is strictly decreasing in $[0,+\infty[$. So there are bright solitons of the form $x_n e^{i\Omega t}$ with $h_\infty < \Omega < h(0)$ for the system (3) with $w < 0$.

Proof. Assume that h is strictly increasing and $w > 0$. Then it follows that $f(z)$ has only three zeros if $h(0) < \Omega < h_\infty$ and $f'(0) = (\Omega - h(0))/w < 0$ for $w > 0$. Consequently, the system (3) admits solutions of bright solitons by Theorem (2.1). Similarly, the other cases can be proved by Theorem 2.1.

Theorem 3.2 *Assume that $h'(r) > 0$ (< 0) for $r \in [0,+\infty[$. Then, there exist dark solitons of the form $x_n e^{i\Omega t}$ with $h(0) < \Omega < h_\infty$ ($h_\infty < \Omega < h(0)$) for the system (3) with $w < 0$ (> 0).*

Proof. The proof is obvious by Theorem 2.3.

We are interested in the possibility of finding non-trivial homoclinic solutions for (3). This problem comes up when we look for the discrete solitons of the periodic equation DNLS if

$$h(\mid \psi_n \mid) = \frac{\sigma\chi_n \mid \psi_n \mid^2}{1 + c_n \mid \psi_n \mid^2},$$

where $\sigma = \pm 1$, the given sequences χ_n, c_n are assumed to be T-periodic and positive. The DNLS with saturable nonlinearities can be used to describe the propagation of optical pulses in different doped fibers [9] and have been reviewed in [10]. Being spatially localized and temporally periodic solutions, the solitons decay to zero at infinity. Suppose x_n is a real valued sequence and Ω is the temporal frequency. In this case, (3) becomes

$$-\Omega x_n + \frac{\sigma\chi_n x_n^2}{1 + c_n x_n^2} x_n + \frac{1}{w_n}(x_{n+1} + x_{n-1} - d_n x_n) = 0. \tag{4}$$

The problem on the existence of solitons of (3) has therefore been replaced by the problem on the existence of homoclinic solutions of (4). Pankov [15] in 2005, considered a special case with $h(x_n) = \sigma\chi_n x_n^2$, then posed an open problem on the existence of gap solitons for asymptotically linear nonlinearities as in (4).

The existence of bright soliton solutions of type $x_n e^{-i\Omega t}$ has been studied by the variational method in [8]. The frequency Ω related to the sequence x_n, in which x_n is a minimiser for a variational method. Therefore, one must solve a variational problem first to obtain a minimizer, and then to derive the associated frequency. Thus, one cannot explicitly derive the allowed region of the frequency Ω by the variational method. This approach, however, yields the frequency Ω and the related sequence x_n simultaneously, and therefore one can obtain the interval of existence of the frequency Ω.

$h(x_n) = \sigma\chi_n x_n^2$ is strictly increasing in $[0,+\infty)$ and $h(0) = 0$, $h_\infty = \infty$. It follows that the DNLS equation is studied in one-dimensional lattice:

$$i\frac{\partial \psi_n}{\partial t} + \sigma\chi_n \psi_n^3 + \frac{1}{w_n}(\psi_{n+1} + \psi_{n-1} - d_n\psi_n) = 0. \tag{5}$$

Then, there exists a unstaggered (staggered) bright soliton of the form $x_n e^{i\Omega t}$ with $h(0) < \Omega < h_\infty$ ($h(0) - 2d/w < \Omega < h_\infty - 2d/w$) for the system (3) with $w > 0$.

The DNLS equation with saturable non-linearity is

$$i\frac{\partial \psi_n}{\partial t} + \frac{\sigma \chi_n \psi_n^2}{1 + c_n \psi_n^2} x_n + + \frac{1}{w_n}(\psi_{n+1} + \psi_{n-1} - d_n \psi_n) = 0. \tag{6}$$

Comparing with (3), one has that $h(r) = \frac{\sigma \chi_n r^2}{1+c_n r^2}$ for r positive. Then

$$h'(r) = \frac{\sigma \chi_n 2r}{(1 + c_n r^2)^2}.$$

We can see that h is strictly increasing in $[0, +\infty)$ and $h(0) = 0$, $h_\infty = \infty$.

4 Conclusion

A model of a discrete nonlinear Schrodinger equation has been presented. The existence of bright soliton solutions has been studied for a discrete Schrodinger equation under the Helmholtz operator by the reversible systems approach and not by the variational method or the anti-integrability method. Chaos is often linked to homoclinic orbits in nonlinear determination dynamics. Recently, DNLS equations with periodic coefficients have been addressed in the physics literature. Future work will address the existence of homoclinic solutions for a class of periodic difference equations with saturable nonlinearity. This gives rise to a more general Jacobi operator using the method of reversible systems.

References

[1] S. Aubry. Anti-integrability in dynamical and variational problems. *Physica D: Nonlinear Phenomena* **86** (1-2) (1995) 284–296.

[2] W. A. Harrison. *Electronic Structure and the Properties of Solids: The Physics of the Chemical Bond*. Courier Corporation, 2012.

[3] L. Brillouin. Wave Propagation in Periodic Structures: Electric Filters and Crystal Lattices. In: *Dover Publications*. Mineola, New York, 1953, 80099–6.

[4] R. L. Devaney. Homoclinic bifurcations and the area-conserving Hénon mapping. *Journal of differential equations* **51** (2) (1984) 254–266.

[5] J. S.W. Lamb and J. A.G. Roberts. Time-reversal symmetry in dynamical systems: a survey. *Physica-Section D* **112** (1-2) (1998) 1–39.

[6] A. Pankov and N. Zakharchenko. On some discrete variational problems. *Acta Applicandae Mathematica* **65** (1) (2001) 295–303.

[7] W. X. Qin and X. Xiao. Homoclinic orbits and localized solutions in nonlinear Schrödingerr lattices. *Nonlinearity* **20** (10) (2007) 2305.

[8] M. I. Weinstein. Excitation thresholds for nonlinear localized modes on lattices. *Nonlinearity* **12** (3) (1999) 673.

[9] S. Gatz and J. Herrmann. Soliton propagation in materials with saturable nonlinearity. *JOSA B* **8** (11) (1991) 2296–2302.

[10] A. Pankov and V. Rothos. Periodic and decaying solutions in discrete nonlinear Schrödinger with saturable nonlinearity. *Proceedings of The Royal Society A: Mathematical, Physical and Engineering Sciences* **464** (2100) (2008) 3219–3236.

[11] J. Yang and G. Chen. Periodic discrete nonlinear schrödinger equations with perturbed and sub-linear terms. *Journal of Applied Analysis and Computation* **12** (6) (2022) 2220–2229.

[12] B. X. Zhou and C. Liu. Homoclinic solutions of discrete nonlinear Schrödinger equations with unbounded potentials. *Applied Mathematics Letters* **123** (2022) 107575.

[13] Z. Wang, Y. Hui and L. Pang. Gap solitons in periodic difference equations with sign-changing saturable nonlinearity. *AIMS Mathematics* **7** (10) (2022) 18824–18836.

[14] R. Novikov and B. L. Sharma. Inverse source problem for discrete Helmholtz equation. *arXiv preprint arXiv* **2401** (14103) (2024).

[15] A. Pankov. Gap solitons in periodic discrete nonlinear Schrödinger equations. *Nonlinearity* **19** (1) (2005) 27.

[16] A. Mehazzem, M. S. Abdelouahab and K. Haouam. Homoclinic Orbits and Localized Solutions in Discrete Nonlinear Schrodinger Equation with Long-Range Interaction. *International Journal of Nonlinear Analysis and Applications* **13**(1) (2022) 353–363.

[17] J. Kuang and Z. Guo. Homoclinic solutions of a class of periodic difference equations with asymptotically linear nonlinearities.*Nonlinear Analysis: Theory, Methods and Applications* **89** (2013) 208–218.

[18] T. Gerald. *Jacobi operators and completely integrable nonlinear lattices*. American Mathematical Soc. (72) (2000).

[19] M. U. Uddin, M. A. Nishu and M. W. Ullah. Nonlinear Damped Oscillator with Varying Coefficients and Periodic External Forces. *Nonlinear Dynamics and Systems Theory* **23** (2) (2023) 227–236.

Nonlinear Dynamics and Systems Theory, **25** (4) (2025) 434–444

Existence Results for a Class of Hybrid Fractional Differential Equations Involving Generalized Riemann-Liouville Fractional Derivatives

Ibtissem Merzoug [1*] and Esma Kenef [2]

[1] *Laboratory of Numerical Analysis, Optimisation and Statistics, Badji Mokhtar - Annaba University, 12, P.O.BOX, 23000 Annaba, Algeria.*
[2] *Laboratory of Physical Chemistry and Biology of Materials, Higher Normal School of Technological Education, Skikda, 21000, Algeria.*

Received: July 9, 2024; Revised: July 13, 2025

Abstract: This research paper deals with the uniqueness of solutions for a second-type hybrid fractional differential equation that involves generalized Riemann-Liouville fractional derivatives using the Banach contraction principle. We also discover at least one solution by employing certain assumptions and the Schaefer fixed point theorem. Subsequently, the Ulam–Hyers stability is discussed. Finally, we enhance our study with a relevant example.

Keywords: *hybrid fractional differential equations, generalized Riemann-Liouville fractional derivatives, existence and uniqueness of solution, Ulam-Hyers stability.*

Mathematics Subject Classification (2020): 34A12, 34K37, 93D05, 70k20.

1 Introduction

Fractional differential equations (FDEs) are a fascinating area of mathematics dealing with derivatives of non-integer order and allowing for a more nuanced description of systems with memory effects or long-range interactions. Solving FDEs can be challenging due to the non-integer order of the derivatives, requiring specialized techniques such as fractional calculus. In general, fractional differential equations provide a powerful tool for understanding complex systems with given dynamics [1, 6, 7, 9]. Indeed, though the operations of FDEs are relatively broad, they can not be applied to all systems. The researchers have shown that certain phenomena related to material heterogeneity cannot be adequately modeled using fractional derivatives. In view of this fact, a solution to this

* Corresponding author: mailto:ibtissem.merzoug@univ-annaba.dz

problem was proposed by Caputo in 1967, who introduced a fractional derivative allowing the application of initial conditions with physical meaning. In his researches, new FDEs are defined, called generalized fractional derivatives, for a more extensive collection of fractional calculus.

On the other hand, in the realm of generalized FDEs, the existence and uniqueness of solutions play a vital role in ensuring the validity and reliability of the mathematical problem. The investigation of the existence and uniqueness of solutions for differential equations involving the generalized fractional derivative has been undertaken by numerous researchers (see [3, 10, 13] and the references therein). Furthermore, the stability theory for FDEs has been a significant area of research. In particular, the Ulam-Hyers stability is attracting attention due to its importance in understanding the behavior of dynamic problems. It is essential to predict the long-term evolution and stability of solutions in different applications, making it a key focus in mathematics and science [11, 12]. Many researchers focused on developing the methods of solution of the hybrid fractional differential equations by using different kinds of fixed point theorems, for example, in [2], the researchers studied the existence of solutions for hybrid fractional integral differential equations, involving the generalized Caputo derivative. They used the hybrid fixed point theorem for some of three operators due to Dhage for proving the main results.

This paper is devoted to the study of the existence, uniqueness and stability of solutions for the following second-type hybrid fractional differential equation involving the generalized Riemann-Liouville fractional derivatives:

$$\begin{cases} D_{0^+}^{\alpha,\phi}\left(u(t)-f(t,u(t))\right)+g\left(t,u(t),D_{0^+}^{\alpha,\phi}\left(u(t)-f(t,u(t))\right)\right)=0, \quad t\in J=[0,1],\\ \lim\limits_{t\to 0}(\phi(t)-\phi(0))^{2-\alpha}(u(t)-f(t,u(t)))=0,\\ u(1)=\omega+f(1,u(1)), \qquad \omega\in\mathbb{R}. \end{cases} \tag{P}$$

where $D_{0^+}^{\alpha,\phi}$ is the ϕ -Riemann-Liouville fractional derivative with $1<\alpha<2$.
$f\in C(J\times\mathbb{R},\mathbb{R})$ and $g\in C(J\times\mathbb{R}^2,\mathbb{R})$ are non-linear functions. The function $\phi: J\to\mathbb{R}$ is a strictly increasing function such that $\phi\in C^2(J,\mathbb{R})$ and $\phi'(t)\neq 0$ for all $t\in J$.

The structure of the paper is outlined as follows. Section 2 provides a detailed overview of the foundational concepts and definitions that are pertinent to our investigation. In Section 3, we convert the differential problem into equivalent integral equations via constructing the Green function. Then we establish certain properties for it and we assume some sufficient conditions through which we prove the existence of the solution using Schaefer's fixed point theorem and the uniqueness of the solution using the Banach fixed point theorem. We also study the stability of this solution. Finally, the paper concludes with a practical example to give a clear demonstration of the concepts that are discussed.

2 Notational Preliminaries

Here, we recall some useful definitions, theorems, and lemmas, which play an important role in the results of the paper.

Definition 2.1 [2] Let $f:[a,b]\to\mathbb{R}$ be an integrable function and $\phi:[a,b]\to\mathbb{R}$ be an increasing function such that for all $t\in[a,b]$, $\phi'(t)\neq 0$. The left-sided ϕ-Riemann-Liouville fractional integral of a function f is defined as follows:

$$I_{a+}^{\alpha,\phi} f(t) = \frac{1}{\Gamma(\alpha)} \int_a^t \phi'(s)(\phi(t) - \phi(s))^{\alpha-1} f(s)\, ds.$$

Definition 2.2 [2] Let $n = [\alpha] + 1$. The left-sided ϕ-Riemann-Liouville fractional derivative of order $\alpha > 0$ of a function f corresponding to the ϕ-Riemann-Liouville fractional integral is defined as follows:

$$D_{a^+}^{\alpha,\phi} f(t) = \frac{1}{\Gamma(n-\alpha)} \left(\frac{1}{\phi'(t)} \frac{d}{d(t)}\right)^n \int_a^t \phi'(s)(\phi(t) - \phi(s))^{n-\alpha-1} f(s) ds.$$

Lemma 2.1 *[4, 13] Let $z : J \to \mathbb{R}$ with $1 < \alpha < 2$, then*

- $I_{0^+}^{\alpha,\phi} D_{0^+}^{\alpha,\phi} z(t) = z(t) + C_0(\phi(t) - \phi(0))^{\alpha-1} + C_1(\phi(t) - \phi(0))^{\alpha-2}$, *where* $C_0, C_1 \in \mathbb{R}$.
- $D_{0^+}^{\alpha,\phi} I_{0^+}^{\alpha,\phi} z(t) = z(t)$.

Definition 2.3 *[11].The problem* (P) *is said to be Ulam-Hyers stable (UH stable) if there exists a constant $\Theta > 0$ such that for every function $y \in C(J, \mathbb{R})$ satisfying the inequality*

$$\left|\mathrm{D}_{0^+}^{\alpha,\phi}(\mathrm{y(t)} - \mathrm{f(t, y(t))}) - \mathrm{g}\left(\mathrm{t, y(t), D}_{0^+}^{\alpha,\phi}(\mathrm{y(t)} - \mathrm{f(t, y(t))})\right)\right| \leq \varepsilon, \quad \mathrm{t} \in \mathrm{J}, \tag{1}$$

for each $\varepsilon > 0$, there exists an exact solution $u \in C(J, \mathbb{R})$ of the problem (P) *such that*

$$|y(t) - u(t)| \leq \Theta\varepsilon, \quad t \in J.$$

Remark 2.1 A function $y \in C(J, \mathbb{R})$ is a solution of the inequality (1) if and only if there exists a function $\psi \in C(J, \mathbb{R})$ (which depends on y) such that

1. $|\psi(t)| \leq \varepsilon, \quad t \in J.$

2. $D_{0^+}^{\alpha,\phi}(y(t) - f(t, y(t))) = g\left(t, y(t), D_{0^+}^{\alpha,\phi}(y(t) - f(t, y(t)))\right) + \psi(t), \quad t \in J.$

Theorem 2.1 *(Banach fixed point theorem) [5] Let $\mathbb{E}$ be a non-empty closed subset of a Banach space. Then any contraction mapping A of $\mathbb{E}$ into itself has a unique fixed point, i.e.,*

$$\exists! x \in \mathbb{E} : A(x) = x.$$

Theorem 2.2 *(Schaefer fixed point theorem) [5] Let $\mathbb{E}$ be a non-empty Banach space. Let also $f : \mathbb{E} \to \mathbb{E}$ be a completely continuous mapping. If the set $\chi = \{y \in \mathbb{E} : y = \lambda f(y), 0 < \lambda < 1\}$ is bounded in $\mathbb{E}$, then f admits at least one fixed point in $\mathbb{E}$.*

3 Existence, Uniqueness and Ulam-Hyers Stability Results

The following section is devoted to stating and proving the existence, uniqueness and Ulam stability results for problem (P).

Definition 3.1 The function u from $C(J,\mathbb{R})$ is a solution to the problem (P) if it satisfies the equation

$$D_{0^+}^{\alpha,\phi}\left(u(t)-f(t,u(t))\right)=-g\left(t,u(t),D_{0^+}^{\alpha,\phi}\left(u(t)-f(t,u(t))\right)\right) \tag{2}$$

and the conditions

$$\lim_{t\to 0}\left[\phi(t)-\phi(0)\right)^{2-\alpha}(u(t)-f(t,u(t))\right]=0, \tag{3}$$

$$u\left(1\right)=\omega+f\left(1,u\left(1\right)\right). \tag{4}$$

Lemma 3.1 *Let $h: J\longrightarrow\mathbb{R}$ be a continuous function. Then u is a solution for the second-type hybrid fractional differential equation*

$$D_{0^+}^{\alpha,\phi}\left(u(t)-f(t,u(t))\right)=-h(t),\quad t\in J,$$

and satisfies the conditions (3)-(4) *if and only if u is a solution of the integral equation via the Green function*

$$u(t)=\omega\gamma(t)+f(t,u(t))+\int_0^1 G(t,s)\phi'(s)h(s)ds,\quad t\in J, \tag{5}$$

where

$$G(t,s)=\frac{\gamma(t)}{\Gamma(\alpha)}\begin{cases}(\phi(1)-\phi(s))^{\alpha-1}-\dfrac{1}{\gamma(t)}(\phi(t)-\phi(s))^{\alpha-1}, & 0\le s\le t\le 1,\\ (\phi(1)-\phi(s))^{\alpha-1}, & 0\le t\le s\le 1,\end{cases} \tag{6}$$

with

- $K(t)=\phi(t)-\phi(0)$ *and* $\gamma(t)=\dfrac{(K(t))^{\alpha-1}}{(K(1))^{\alpha-1}}$ *for all* $t\in J$.

Proof. We have u as a solution of the problem (P),

$$I_{0^+}^{\alpha,\phi}\left(D_{0^+}^{\alpha,\phi}\left(u(t)-f(t,u(t))\right)\right)=-I_{0^+}^{\alpha,\phi}(h(t))+C_0(\phi(t)-\phi(0))^{\alpha-1}+C_1(\phi(t)-\phi(0))^{\alpha-2},$$

$$u(t)-f(t,u(t))=-I_{0^+}^{\alpha,\phi}(h(t))+C_0(\phi(t)-\phi(0))^{\alpha-1}+C_1(\phi(t)-\phi(0))^{\alpha-2}.$$

By using the conditions (3)-(4), we obtain $C_1=0$ and

$$C_0=\frac{1}{(\phi(1)-\phi(0))^{\alpha-1}}\left(\omega+\frac{1}{\Gamma(\alpha)}\int_0^1\phi'(s)(\phi(t)-\phi(s))^{\alpha-1}h(s)ds\right).$$

By substitution, we get

$$\begin{aligned}u(t)&=f(t,u(t))+\omega\gamma(t)-\frac{1}{\Gamma(\alpha)}\int_0^t\phi'(s)(\phi(t)-\phi(s))^{\alpha-1}h(s)ds\\&\quad+\frac{\gamma(t)}{\Gamma(\alpha)}\int_0^1\phi'(s)(\phi(1)-\phi(s))^{\alpha-1}h(s)ds\\&=f(t,u(t))+\omega\gamma(t)+\int_0^1 G(t,s)\phi'(s)h(s)ds.\end{aligned}$$

The converse can be easily inferred from Lemma 2.1.

Lemma 3.2 *The following estimates are satisfied by the Green function G defined by equation (6):*
(i) $G(t,s) \leq \dfrac{(\phi(1)-\phi(0))^{\alpha-1}}{\Gamma(\alpha)}$ *for all* $t,s \in J$.
(ii) $G(t,s) \geq 0$ *for all* $t,s \in J$.

Proof.
(i) Since ϕ is a strictly increasing function, we have $\phi(t)-\phi(0) \leq \phi(1)-\phi(0)$ whenever $t \in J$,
which implies that $\gamma(t) \leq 1$. For $0 \leq t \leq s \leq 1$, we can easily conclude that

$$\frac{\gamma(t)}{\Gamma(\alpha)}(\phi(1)-\phi(s))^{\alpha-1} \leq \frac{(\phi(1)-\phi(0))^{\alpha-1}}{\Gamma(\alpha)},$$

and for $0 \leq s \leq t \leq 1$,

$$\begin{aligned}\frac{\gamma(t)}{\Gamma(\alpha)}\left((\phi(1)-\phi(s))^{\alpha-1}-\frac{1}{\gamma(t)}(\phi(t)-\phi(s))^{\alpha-1}\right) &\leq \frac{1}{\Gamma(\alpha)}\Bigg((\phi(1)-\phi(0))^{\alpha-1} \\ &\quad - \frac{(\phi(1)-\phi(0))^{\alpha-1}(\phi(t)-\phi(s))^{\alpha-1}}{(\phi(t)-\phi(0))^{\alpha-1}}\Bigg) \\ &\leq \frac{1}{\Gamma(\alpha)}(\phi(1)-\phi(0))^{\alpha-1} \\ &\quad \left(1-\frac{(\phi(t)-\phi(s))^{\alpha-1}}{(\phi(t)-\phi(0))^{\alpha-1}}\right) \\ &\leq \frac{1}{\Gamma(\alpha)}(\phi(1)-\phi(0))^{\alpha-1}.\end{aligned}$$

Hence, $G(t,s) \leq \dfrac{(\phi(1)-\phi(0))^{\alpha-1}}{\Gamma(\alpha)}$ for $t,s \in J$.
(ii) By a similar calculation, we can prove that $G(t,s) \geq 0$ for all $t,s \in J$. This completes the proof.

Let us define the operator $\mathcal{T} : C(J,\mathbb{R}) \longrightarrow C(J,\mathbb{R})$ by

$$\mathcal{T}(u(t)) = f(t,u(t)) + \omega\gamma(t) + \int_0^1 G(t,s)\phi'(s)\sigma_u(s)ds$$

with $\sigma_u(t) = g\left(t,u(t),D_{0^+}^{\alpha,\phi}(u(t)-f(t,u(t)))\right)$.
Here, $C(J,\mathbb{R})$ is equipped with the norm

$$\|u\|_\infty = \max_{t\in J}|u(t)|.$$

We note that any fixed point of this operator is a solution to the problem (P).

3.1 Existence results

Assume that the functions $f : J\times\mathbb{R} \longrightarrow \mathbb{R}$ and $g : J\times\mathbb{R}^2 \longrightarrow \mathbb{R}$ are continuous and satisfy the following conditions:

(H_1) There exists a constant $\Lambda_g \in \mathbb{R}_+^*$ such that for all $u, v \in \mathbb{R}$ and $t \in J$,

$$|g(t,u,v)| \leq \Lambda_g,$$

(H_2) There exists a constant $\Lambda_f \in \mathbb{R}_+^*$ such that for all $u \in \mathbb{R}$ and $t \in J$,

$$|f(t,u)| \leq \Lambda_f.$$

Theorem 3.1 *We assume that the conditions* $(H_1) - (H_2)$ *are satisfied. Then the problem* (P) *has at least one solution.*

Proof. The proof will be given in four steps.
Step one: $\mathcal{T}$ is continuous. Let (u_n) be a convergent sequence towards $u \in C(J,\mathbb{R})$. Therefore, for all $t \in J$, we have

$$\begin{aligned}
|\mathcal{T}(u_n(t)) - \mathcal{T}(u(t))| &= \Big| f(t,u_n(t)) - f(t,u(t)) + \omega\gamma(t) - \omega\gamma(t) \\
&\quad + \int_0^t G(t,s)\phi'(s)(\sigma_{u_n}(s) - \sigma_u(s))ds \Big| \\
&\leq \Big| f(t,u_n(t)) - f(t,u(t)) \Big| + \int_0^1 G(t,s)\phi'(s) \Big| \sigma_{u_n}(s) - \sigma_u(s) \Big| ds \\
&\leq \Big| f(t,u_n(t)) - f(t,u(t)) \Big| + \frac{(\phi(1)-\phi(0))^{\alpha-1}}{\Gamma(\alpha)} \int_0^1 \phi'(s) \Big| \sigma_{u_n}(s) - \sigma_u(s) \Big| ds \\
&\leq \|f(t,u_n(.)) - f(t,u(.))\|_\infty + \frac{(\phi(1)-\phi(0))^{\alpha}}{\Gamma(\alpha)} \|\sigma_{u_n}(.) - \sigma_u(.)\|_\infty.
\end{aligned}$$

Since the functions f and g are continuous, we get

$$\lim_{n\to\infty} \|\mathcal{T}(u_n(.)) - \mathcal{T}(u(.))\|_\infty = 0.$$

Hence, $\mathcal{T}$ is continuous.
Step two: The image of every bounded set of $C(J,\mathbb{R})$ under $\mathcal{T}$ is uniformly bounded in $C(J,\mathbb{R})$. To establish this, it suffices to demonstrate that for any given $r > 0$, there exists a positive constant $l > 0$. Therefore, for every $u \in B_r$, we have $\|\mathcal{T}u(.)\|_\infty \leq l$ with

$$B_r = \{u \in C(J,\mathbb{R}) : \|u\|_\infty \leq r\}.$$

For every $t \in J$ and by using the conditions (H1) and (H2), we get

$$\begin{aligned}
|\mathcal{T}(u(t))| &\leq |\omega|\gamma(t) + |f(t,u(t))| + \int_0^1 G(t,s)\phi'(s)|\sigma_u(s)|ds \\
&\leq |\omega|\gamma(t) + \Lambda_f + \frac{(\phi(1)-\phi(0))^{\alpha-1}}{\Gamma(\alpha)} \Lambda_g \int_0^1 \phi'(s)ds \\
&\leq |\omega| + \Lambda_f + \frac{(\phi(1)-\phi(0))^{\alpha}}{\Gamma(\alpha)} \Lambda_g = l.
\end{aligned}$$

Hence, $\mathcal{T}(B_r)$ is uniformly bounded.
Step three: The image of every bounded set of $C(J,\mathbb{R})$ under $\mathcal{T}$ is an equicontinuous

set in $C(J,\mathbb{R})$. For each $u \in B_r$ and $t_1, t_2 \in J, t_1 < t_2$, we have

$$\begin{aligned}|\mathcal{T}(u(t_2)) - \mathcal{T}(u(t_1))| &= |f(t_2,u(t_2)) - f(t_1,u(t_1)) + \omega(\gamma(t_2)-\gamma(t_1)) \\ &\quad + \int_0^1 (G(t_2,s)-G(t_1,s))\phi'(s)\sigma_u(s)ds| \\ &\leq |f(t_2,u(t_2)) - f(t_1,u(t_1))| + |\omega||\gamma(t_2)-\gamma(t_1)| \\ &\quad + \int_0^1 |G(t_2,s)-G(t_1,s)|\phi'(s)\sigma_u(s)ds\end{aligned}$$

and

$$|G(t_2,s)-G(t_1,s)| = \left| \frac{(\phi(1)-\phi(s))^{\alpha-1}}{(\phi(1)-\phi(0))^{\alpha-1}\Gamma(\alpha)} \left[(\phi(t_2)-\phi(0))^{\alpha-1} - (\phi(t_1)-\phi(0))^{\alpha-1}\right] \right.$$
$$\left. + \frac{1}{\Gamma(\alpha)} \left[(\phi(t_1)-\phi(s))^{\alpha-1} - (\phi(t_2)-\phi(s))^{\alpha-1}\right] \right|.$$

By applying the mean value theorem [8], we obtain

$$|G(t_2,s)-G(t_1,s)| = |t_2-t_1| \left[\frac{(\phi(1)-\phi(s))^{\alpha-1}}{(\phi(1)-\phi(0))^{\alpha-1}\Gamma(\alpha)} h_1(\xi) + \frac{1}{\Gamma(\alpha)} h_2(\theta) \right]$$

with

$$\begin{aligned}h_1(\xi) &= (\alpha-1)\phi'(\xi)(\phi(\xi)-\phi(0))^{\alpha-2}, \\ h_2(\theta) &= (\alpha-1)\phi'(\theta)(\phi(\theta)-\phi(s))^{\alpha-2},\end{aligned}$$

where $t_1 < \theta, \xi < t_2$. Therefore, as $t_1 \longrightarrow t_2$, $|\mathcal{T}(u(t_2)) - \mathcal{T}(u(t_1))| \longrightarrow 0$.
Hence, by the Arzela-Ascoli theorem, $\mathcal{T}$ is completely continuous.
Step four: We will prove that the set χ is bounded, where

$$\chi = \left\{ u \in C(J,\mathbb{R}) : u(t) = \lambda \mathcal{T}(u(t)), 0 < \lambda < 1 \right\}.$$

Let $u \in \chi$. For all $t \in J$, we have

$$\begin{aligned}u(t) &= \lambda \left[\omega\gamma(t) + f(t,u(t)) + \int_0^1 G(t,s)\phi'(s)\sigma_u(s)ds \right] \\ |u(t)| &< |\omega|\gamma(t) + \Lambda_f + \Lambda_g \int_0^1 G(t,s)\phi'(s)ds \\ &\leq |\omega| + \Lambda_f + \frac{(\phi(1)-\phi(0))^{\alpha}}{\Gamma(\alpha)}\Lambda_g = L.\end{aligned}$$

Hence, χ is bounded. By using Schaefer's fixed point theorem, we found that the problem (P) has at least one solution.

Example 3.1 Consider the problem with the following general fractional differential equations:

$$\begin{cases} D_{0^+}^{\frac{7}{4},\frac{e^t}{7}} (u(t) - f(t,u(t))) + g\left(t, u(t), D_{0^+}^{\frac{7}{4},\frac{e^t}{7}} (u(t) - f(t,u(t)))\right) = 0, t \in J, \\ \lim_{t\to 0} (\phi(t)-\phi(0))^{2-\frac{7}{4}} (u(t) - f(t,u(t))) = 0, \\ u(1) = 1 + f(1,u(1)), \end{cases} \tag{Q}$$

where

$$f(t,u(t)) = (\frac{1}{2}+t)\cos(u(t)),$$

$$g\left(t,u(t),D_{0^+}^{\frac{7}{4},\frac{e^t}{7}}\left(u(t)-f(t,u(t))\right)\right) = (\frac{1}{3}+t)\cos(u(t))+\frac{1}{9}\sin(D_{0^+}^{\frac{7}{4},\frac{e^t}{7}}\left(u(t)-f(t,u(t))\right)).$$

Let us put $f(t,u)=\frac{t}{2}\cos(u)$ and $g(t,u,v)=\frac{1}{3}(1+t)\cos(u)+\frac{1}{9}\sin(v)$. For $u,v\in\mathbb{R}$ and $t\in J$, we have

$$|f(t,u)|\leq\frac{3}{2},\quad |g(t,u,v)|\leq\frac{7}{9}.$$

We can easily verify all conditions of Theorem 3.1 with $\Lambda_f=\frac{3}{2},\Lambda_g=\frac{7}{9}$. Therefore, we conclude that the problem (Q) has at least one solution.

3.2 Uniqueness results

In what follows, we will establish the existence of a unique solution to the problem (P) using the Banach fixed point theorem under certain conditions imposed on the functions f and g. We impose the following conditions:

(H_3) There exist constants $k_1,k_3\in\mathbb{R}_+^*$ and $k_2\in(0,1)$ such that

$$|g(t,u,v)-g(t,\bar{u},\bar{v})|\leq k_1|u-\bar{u}|+k_2|v-\bar{v}|,$$

$$|f(t,u)-f(t,\bar{u})|\leq k_3|u-\bar{u}|$$

for every $u,v,\bar{u},\bar{v}\in\mathbb{R}$ and $t\in J$.

Theorem 3.2 *We assume that the condition (H_3) is satisfied. If*

$$\Upsilon = k_3+\frac{(\phi(1)-\phi(0))^\alpha k_1}{\Gamma(\alpha)(1-k_2)}<1, \tag{7}$$

then the problem (P) *admits a unique solution in $C(J,\mathbb{R})$.*

Proof. We consider the previously defined operator $\mathcal{T}$ for all $x,y\in C(J,\mathbb{R})$ and $t\in J$. By the condition (H_3), we have

$$\begin{aligned}|\mathcal{T}(x(t))-\mathcal{T}(y(t))| &= |f(t,x(t))-f(t,y(t))+\omega\gamma(t)-\omega\gamma(t)\\ &\quad+\int_0^1 G(t,s)\phi'(s)\left(\sigma_x(s)-\sigma_y(s)\right)ds|\\ &\leq |f(t,x(t))-f(t,y(t))|+\int_0^1 G(t,s)\phi'(s)|\left(\sigma_x(s)-\sigma_y(s)\right)|ds.\end{aligned}$$

Then

$$|\mathcal{T}(x(t))-\mathcal{T}(y(t))|\leq k_3|x(t)-y(t)|+\frac{(\phi(1)-\phi(0))^\alpha}{\Gamma(\alpha)}\int_0^1|\sigma_x(s)-\sigma_y(s)|\,ds. \tag{8}$$

On the other hand,

$$\begin{aligned}|\sigma_x(t)-\sigma_y(t)| &= |g\left(t,x(t),D^{\alpha,\phi}\left(x(t)-f(t,x(t))\right)\right)-g\left(t,y(t),D^{\alpha,\phi}\left(y(t)-f(t,y(t))\right)\right)|\\ &\leq k_1|x(t)-y(t)|+k_2|D^{\alpha,\phi}\left(x(t)-f(t,x(t))-D^{\alpha,\phi}\left(y(t)-f(t,y(t))\right)\right)|\\ &\leq k_1|x(t)-y(t)|+k_2\left|\sigma_x(s)-\sigma_y(s)\right|.\end{aligned}$$

Then

$$|\sigma_x(s) - \sigma_y(s)| \leq \frac{k_1}{(1-k_2)}|x(t) - y(t)|. \tag{9}$$

By substituting (9) in (8), we get

$$\begin{aligned}|\mathcal{T}(x(t)) - \mathcal{T}(y(t))| &\leq k_3|x(t) - y(t)| + \frac{(\phi(1) - \phi(0))^\alpha k_1}{\Gamma(\alpha)(1-k_2)}|x(t) - y(t)| \\ &\leq \left[k_3 + \frac{(\phi(1) - \phi(0))^\alpha k_1}{\Gamma(\alpha)(1-k_2)}\right]|x(t) - y(t)|.\end{aligned}$$

Thus,

$$\|\mathcal{T}x(.) - \mathcal{T}y(.)\|_\infty \leq \Upsilon\|x - y\|_\infty.$$

According to (7), the operator $\mathcal{T}$ is a contraction. Then, by Banach's fixed point theorem, it admits a unique fixed point, and it is the unique solution of the problem (P).

Example 3.2 Consider the problem (Q). According to the condition (H_3), we have for $u, v, \bar{u}, \bar{v} \in \mathbb{R}$ and $t \in J$,

$$|f(t,u) - f(t,\bar{u})| \leq \frac{1}{2}|u - \bar{u}|,$$

$$|g(t,u,v) - g(t,\bar{u},\bar{v})| \leq \frac{2}{3}|u - \bar{u}| + \frac{1}{9}|v - \bar{v}|.$$

Hence, the satisfaction of the conditions of Theorem (3.2) can be easily checked, and $\Upsilon = 0.5698569 < 1$ with $k_1 = \frac{2}{3}, k_2 = \frac{1}{9}, k_3 = \frac{1}{2}$. Therefore, there exists a unique solution of the problem (Q).

3.3 Ulam-Hyers stability results

Lemma 3.3 *If y is a solution for the following fractional differential inequality:*

$$D^{\alpha,\phi}\left(y(t) - f(t,y(t))\right) + g\left(t, y(t), D^{\alpha,\phi}\left(y(t) - f(t,y(t))\right)\right) < \varepsilon \tag{10}$$

for $\varepsilon > 0$, then y is a solution of the following inequality:

$$|y(t) - \mathcal{T}(y(t))| \leq \frac{(\phi(1) - \phi(0))^\alpha}{\Gamma(\alpha)}\varepsilon. \tag{11}$$

Proof. Let y be a solution of the inequality (11). For $\varepsilon > 0$ and by using Lemma 3.1 and Remark 2.1, $|\psi(t)| < \varepsilon$, $t \in J$, and according to (10), we have

$$y(t) = \omega\gamma(t) + f(t,y(t)) + \int_0^1 G(t,s)\phi'(s)\left[\sigma_y(s) + \psi(s)\right]ds.$$

Then

$$\begin{aligned}|y(t)-\mathcal{T}y(t)| =&\Big|\omega\gamma(t)+f(t,y(t))+\int_0^1 G(t,s)\phi'(s)\left[\sigma_y(s)+\psi(s)\right]ds\\&-\omega\gamma(t)-f(t,y(t))-\int_0^1 G(t,s)\phi'(s)\sigma_y(s)ds\Big|\\=&\left|\int_0^1 G(t,s)\phi'(s)\psi(s)ds\right|\\\leq&\int_0^1 G(t,s)\phi'(s)|\psi(s)|ds\\\leq&\frac{(\phi(1)-\phi(0))^\alpha}{\Gamma(\alpha)}\varepsilon.\end{aligned}$$

Theorem 3.3 *We assume that the conditions* (H_3) *and the inequality* (7) *are satisfied. Then the problem* (P) *is Ulam-Hyers stable.*

Proof. Under the condition (H_3) and the inequality (7), there exists a unique solution for the problem (P) in $C(J,\mathbb{R})$. Let $y\in C(J,\mathbb{R})$ be a solution to the inequality (11). Therefore, for $t\in J$, we have

$$\begin{aligned}|y(t)-u(t)| =&|y(t)-\omega\gamma(t)-f(t,u(t))-\int_0^1 G(t,s)\phi'(s)\sigma_u(s)ds|\\\leq&|y(t)-\mathcal{T}(y(t))+\mathcal{T}(y(t))-\mathcal{T}(u(t))|\\\leq&|y(t)-\mathcal{T}(y(t))|+|\mathcal{T}(y(t))-\mathcal{T}(u(t))|\\\leq&\frac{(\phi(1)-\phi(0))^\alpha}{\Gamma(\alpha)}\varepsilon+\Upsilon|y(t)-u(t)|.\end{aligned}$$

Thus,

$$|y(t)-u(t)|\leq\frac{(\phi(1)-\phi(0))^\alpha}{\Gamma(\alpha)(1-\Upsilon)}\varepsilon.$$

We put $\Theta=\dfrac{(\phi(1)-\phi(0))^\alpha}{\Gamma(\alpha)(1-\Upsilon)}$, then we get

$$|y(t)-u(t)|\leq\Theta\varepsilon.$$

Therefore, the problem (P) is stable according to Ulam-Hyers.

Example 3.3 *Consider the problem* (Q). *All conditions of Theorem 3.3 hold with* $\Theta=0.2165387$. *Then the unique solution of the problem* (Q) *is Ulam-Hyers stable.*

4 Concluding Remarks

In this paper, the authors provided some sufficient conditions guaranteeing the existence of solutions for a class of second-type hybrid fractional differential equations involving generalized Riemann-Liouville fractional derivatives of order $1<\alpha<2$. We have developed some adequate conditions for the uniqueness of solution. Also, this paper constitutes a successful application of the Ulam-Hyers stability concept to investigate the stability of solutions to this class of problems. The respective results have been verified by providing a suitable example.

References

[1] S. Abbas, M. Benchohra and J. R. Graef. Upper and Lower Solutions for Fractional q-Difference Inclusions. *Nonlinear Dynamics and Systems Theory* **21** (1) (2021) 1–12.

[2] N. Adjimi, M. Benbachir and K. Guerbati. Existence results for (ψ)-Caputo hybrid fractional integro-differential equations. *Malaya Journal of Matematics* **9** (2) (2021) 46–54.

[3] H. Afshari and E. A. Karapinar. Discussion on the existence of positive solutions of the boundary value problems via ψ-Hilfer fractional derivative on b-metric spaces. *Adv. Differ. Equ* **2020** 616 (2020). https://doi.org/10.1186/s13662-020-03076-z.

[4] R. Almeida and A. Caputo. Fractional derivative of a function with respect to an other function. *Communications in Nonlinear Science and Numerical Simulation* **44** (2017) 460–481.

[5] G. Andrzej and D. James. *Fixed Point Theory*. Springer Monographs in Mathematics. New York, Springer-Verlag, 2003.

[6] Z. Bai. On positive solutions of a non-local fractional boundary value problem. *Nonlinear Analysis, Theory, Methods and Applications* **72** (2) (2010) 916–924.

[7] R. Barkat and T. Menacer. Dynamical Analysis, Stabilization and Discretization of a Chaotic Financial Model with Fractional Order. *Nonlinear Dynamics and Systems Theory* **20** (3) (2020) 253–266.

[8] T. M. Flett. "2742. a mean value theorem". *Mathematical Gazette* **42** (339) (1958) 38–39.

[9] R (ed). Hilfer. *Applications of Fractional Calculus in Physics*. World Scientific Publishing Co., Inc., River Edge, NJ. 2000.

[10] R. W. Ibrahim. Generalized Ulam-Hyers stability for fractional differential equations. *Int. J. Math.* **23** (2012) 1250056.

[11] E. Kenef, I. Merzoug and A. Guezane-Lakoud. Existence, uniqueness and Ulam stability results for a mixed-type fractional differential equations with p-Laplacian operator. *Arabian Journal of Mathematics* **12** (3) (2023) 633–645.

[12] A. Samadi, S. K. Ntouyas and J. Tariboon. Nonlocal fractional hybrid boundary value problems involving mixed fractional derivatives and integrals via a generalization of Darboís theorem. Journal of Mathematics **2021** (1) (2021) 6690049.

[13] A. Seemab, M. Ur Rehman, J. Alzabut and A. Hamdi. On the existence of positive solutions for generalized fractional boundary value problems. *Boundary Value Problems* **2019** (2019) 1–20.

Nonlinear Dynamics and Systems Theory, **25** (4) (2025) 445–456

Fractional Nonlinear Reaction-Diffusion System with Gradient Source Terms

Houria Selatnia and Nabila Barrouk *

Faculty of Science and Technology, Department of Mathematics, University of Souk Ahras, B.P. 1553 Souk Ahras 41000, Algeria

Received: October 14, 2024; Revised: July 21, 2025

Abstract: Over the years, partial reaction-diffusion systems have attracted the attention of numerous researchers due to their application in various fields such as, for example, population dynamics, the dynamics of gas, dynamic systems, fusion process, certain biological models, etc. The aim of this work is to prove the global existence of a solution for an arbitrary-order fractional reaction-diffusion system. The inspiration for this study arises from the research conducted recently by Barrouk and Mesbahi [2].

Keywords: *semigroups; fractional reaction-diffusion systems; local solution; global solution.*

Mathematics Subject Classification (2020): 35R11, 35K57, 35K55, 37L05, 70K99, 93A30.

1 Introduction

In recent years, fractional differential equations have garnered significant attention from researchers because of their extensive applications across various scientific, technological, and medical fields, we can find important applications, for example, in finance [15], mechanics [14], biomedicine [9], pattern formation [8], we find numerous real applications in biology, medicine and ecology, see the works of Djemai and Mesbahi [6], Khayar, Brouri and Ouzahra *[12]* and corresponding references therein, etc.

* Corresponding author: mailto:n.barrouk@univ-soukahras.dz

Our particular objective in this type of anomalous diffusion problems is to study the following fractional reaction-diffusion system:

$$\begin{cases} \dfrac{\partial \vartheta_1}{\partial t} - d_1 \left(-\Delta\right)^{\alpha_1} \vartheta_1 = f_1 \left(t, x, \vartheta, \nabla\vartheta\right) & \text{in } \mathbb{R}^+ \times \Omega, \\ \vdots & \vdots \\ \dfrac{\partial \vartheta_m}{\partial t} - d_m \left(-\Delta\right)^{\alpha_m} \vartheta_m = f_m \left(t, x, \vartheta, \nabla\vartheta\right) & \text{in } \mathbb{R}^+ \times \Omega, \\ \frac{\partial \vartheta_i}{\partial \eta} = 0 \quad \text{or} \quad \vartheta_i = 0 \ , \ \text{for all} \ \ 1 \leq i \leq m & \text{on } \mathbb{R}^+ \times \partial\Omega, \\ \vartheta_i \left(0, .\right) = \vartheta_{i_0} \left(.\right) \ \text{for all} \ \ 1 \leq i \leq m & \text{in } \Omega, \end{cases} \tag{1}$$

where $\vartheta = \left(\vartheta_1, \ldots, \vartheta_m\right)$, $\nabla\vartheta = \left(\nabla\vartheta_1, \ldots, \nabla\vartheta_m\right)$, $m \geq 2$, Ω is a bounded and regular domain of $\mathbb{R}^N$ with boundary $\partial\Omega$, $N \geq 2$, $\vartheta_i = \vartheta_i \left(t, x\right)$, $1 \leq i \leq m$ for $(t, x) \in Q_T = (0, T) \times \Omega$ and f_i are real functions, the presence of the non local operator $\left(-\Delta\right)^{\alpha_i}$, $0 < \alpha_i < 1$ for all $1 \leq i \leq m$, which accounts for the anomalous diffusion [11, 16], means that the sub-populations face some obstacles that slow their movement, and the constants of diffusion d_i are assumed to be nonnegative, $f_i : (0, T) \times \Omega \times \mathbb{R}^m \times \mathbb{R}^{mN} \to \mathbb{R}^m$ are enough regular, ϑ_{i_0} are nonnegative functions in $L^1 \left(\Omega\right)$, for all $1 \leq i \leq m$.

The local existence in time of the solution ϑ_i is classical. The positivity of the solution stems from the positivity of ϑ_{i_0}, which are assumed to be continuous, for all $1 \leq i \leq m$.

Several mathematical researchers have investigated the system derived from (1) by substituting the abnormal diffusion operator with the standard Laplacian operator $(-\Delta)$, employing various methods and techniques. Notable studies include those by Barrouk and Mesbahi [2], Barrouk and Abdelmalek [1], Moumeni and Dehimi [17], and Moumeni and Mebarki [18].

Note that over the past years, very important works have appeared in fractional reaction-diffusion equations. We mention the following.

The work of Hnaien et *al.* [10], is devoted to the study of the fractional systems: an abnormal diffusion system describing the propagation of an epidemic in a confined population of the SIR type, the fractional temporal Brusselator system and a reaction-diffusion system, temporal fractional with an equilibrium law. This study is based on Banach's fixed point theorem, semigroup estimates and Sobolev's integration theorem.

In [3], Besteiro and Rial studied the initial value problem for finite dimensional fractional non-autonomous reaction-diffusion equations. They proved the global existence and the asymptotic behavior of solutions by applying the general time splitting method and the technique of invariant regions.

We emphasize that there are many other references that approach this subject in various analytical and numerical ways.

This paper is organized as follows. In the next section, we provide some results necessary to understand the content of this work. In the next three sections, we give some results concerning the approximate problem. In Section 6, we state our main result and also present its proof in detail. The penultimate section is devoted to an application of the obtained result. Finally, we close with a conclusion.

2 Important Results

2.1 Hypotheses

To study problem (1), we assume that the functions $f_i : (0,T) \times \Omega \times \mathbb{R}^m \times \mathbb{R}^{mN} \to \mathbb{R}$, $1 \leq i \leq m$, satisfy the following simple assumptions, which allow them to be chosen from a wide range.

(A1) We preserve for all time the nonnegativity of the solutions, so we assume that f_i are quasipositive for all $1 \leq i \leq m$.

(A2) There exists $C \geq 0$ independent of $\vartheta_1, \ldots, \vartheta_m$ such that

$$f_i(t,x,\vartheta,\nabla\vartheta) \leq C \sum_{i=1}^{m} \vartheta_i \ , \ \forall \vartheta_i \geq 0, \ 1 \leq i \leq m. \tag{2}$$

(A3) The functions $f_i : (0,T)\times\Omega\times\mathbb{R}^m\times\mathbb{R}^{mN} \to \mathbb{R}$ are measurable and $f_i : \mathbb{R}^m\times\mathbb{R}^{mN} \to \mathbb{R}$ are locally Lipschitz continuous for all $1 \leq i \leq m$.

2.2 Preliminaries

To prove the main result, we need the following results.

Theorem 2.1 *Let Ω be an open bounded domain in $\mathbb{R}^N$. The following system*

$$\begin{cases} (-\Delta)^{\alpha} \varphi_k = \lambda_k^{\alpha} \varphi_k & \text{in } \Omega, \\ \dfrac{\partial \varphi_k}{\partial \eta} = 0 & \text{on } \partial\Omega, \end{cases}$$

where

$$D\left((-\Delta)^{\alpha}\right) = \left\{ \vartheta \in L^2(\Omega), \ \frac{\partial \vartheta}{\partial \eta} = 0, \ \left\|(-\Delta)^{\alpha} \vartheta\right\|_{L^2(\Omega)} < +\infty \right\},$$

$$\left\|(-\Delta)^{\alpha} \vartheta\right\|_{L^2(\Omega)}^2 = \sum_{k=1}^{+\infty} \left|\lambda_k^{\alpha} \langle \vartheta, \varphi_k \rangle\right|^2,$$

has a countable sequence of eigenvalues $\lambda_1 < \lambda_2 < \ldots < \lambda_k < \ldots$ and $\lambda_k \to \infty$ as $k \to \infty$, and φ_k are the corresponding eigenvectors for all $k \geq 1$.

So, for $\vartheta \in D\left((-\Delta)^{\alpha}\right)$, we have

$$(-\Delta)^{\alpha} \vartheta = \sum_{k=1}^{+\infty} \lambda_k^{\alpha} \langle \vartheta, \varphi_k \rangle \varphi_k.$$

Also, we have the formula of integration by parts as follows:

$$\int_{\Omega} \vartheta(x) (-\Delta)^{\alpha} \bar{\vartheta}(x) \, dx = \int_{\Omega} \bar{\vartheta}(x) (-\Delta)^{\alpha} \vartheta(x) \, dx, \ \text{for } \vartheta, \bar{\vartheta} \in D\left((-\Delta)^{\alpha}\right). \tag{3}$$

Proof. See Hnaien et *al.* [10] and corresponding references therein.

Lemma 2.1 ([13]) *Let $\theta \in C_0^\infty(Q_T)$, $\theta \geq 0$, then there exists a nonnegative function $\Phi \in C^{1,2}(Q_T)$ being the solution of the system*

$$\begin{cases} -\Phi_t - d\Delta\Phi = \theta & \text{in } Q_T, \\ \Phi(t,x) = 0 & \text{on } \Sigma_T, \\ \Phi(T,x) = 0 & \text{in } \Omega, \end{cases}$$

where $\Sigma_T = (0,T) \times \partial\Omega$, for all $q \in (1,\infty)$, there exists $C \geq 0$, not dependent on θ, such that

$$\|\Phi\|_{L^{q'}(Q_T)} \leq C \|\theta\|_{L^q(Q_T)}.$$

And for all $\vartheta_0 \in L^1(\Omega)$ and $h \in L^1(Q_T)$, we obtain the equalities

$$\int_{Q_T} (S(t)\vartheta_0(x))\,\theta dxdt = \int_\Omega \vartheta_0(x)\,\Phi(0,x)\,dx \tag{4}$$

and

$$\int_{Q_T} \left(\int_0^t S(t-s)\,h(s,x,\vartheta(s),\nabla\vartheta(s))\,ds \right) \theta dxdt = \int_{Q_T} h(s,x,\vartheta(s),\nabla\vartheta(s))\,\Phi(s,x)\,dxds. \tag{5}$$

Proof. *To prove this Lemma, see Bonafede and Schmitt [4].*

3 Local Existence of the Solution

We will transform the system (1) to an abstract system of first order in the Banach space $X = \left(L^1(\Omega)\right)^m$. For this, we define the functions $\vartheta_{i_0}^n$, for all $n > 0$ and $1 \leq i \leq m$, by

$$\vartheta_{i_0}^n = \min\{\vartheta_{i_0}, n\}.$$

Obviously, $\vartheta_{i_0}^n$ satisfies

$$\vartheta_{i_0}^n \in L^1(\Omega) \text{ and } \vartheta_{i_0}^n \geq 0 \text{ for all } 1 \leq i \leq m.$$

Now, consider the problem

$$\begin{cases} \dfrac{\partial\vartheta_{1_n}}{\partial t} - d_1(-\Delta)^{\alpha_1}\vartheta_{1_n} = f_1(t,x,\vartheta_n,\nabla\vartheta_n) & \text{in } Q_T, \\ \vdots \\ \dfrac{\partial\vartheta_{m_n}}{\partial t} - d_m(-\Delta)^{\alpha_m}\vartheta_{m_n} = f_m(t,x,\vartheta_n,\nabla\vartheta_n) & \text{in } Q_T, \\ \dfrac{\partial\vartheta_{i_n}}{\partial\eta} = 0 \text{ or } \vartheta_{i_n} = 0\ ,\ 1 \leq i \leq m & \text{in } \Sigma_T, \\ \vartheta_{i_n}(0,x) = \vartheta_{i_0}^n(x) \geq 0\ ,\ 1 \leq i \leq m & \text{in } \Omega. \end{cases} \tag{6}$$

Hence, if $(\vartheta_{1_n}, \ldots, \vartheta_{m_n})$ is a solution of (6), then it satisfies the following integral equation:

$$\vartheta_{i_n}(t) = S_i(t)\,\vartheta_{i_0}^n + \int_0^t S_i(t-s)\,f_i(s,.,\vartheta_n(s),\nabla\vartheta_n(s))\,ds, \tag{7}$$

where $S_i(t)$ is the semigroup which is generated by the operator $d_i(-\Delta)^{\alpha_i}$, $1 \leq i \leq m$. (See Pazy [19]).

Theorem 3.1 *There exists $T_M > 0$ and $(\vartheta_{1_n}, \ldots, \vartheta_{m_n})$ being a local solution of (6) for all $t \in [0, T_M]$.*

Proof. Note that $S_i(t)$ are contraction semigroups and F is locally Lipschitz, $0 \leq \vartheta_{i_0}^n \leq n$, which ensures the existence of $T_M > 0$ such that $(\vartheta_{1_n}, \ldots, \vartheta_{m_n})$ becomes a local solution of (6) on $[0, T_M]$.

Theorem 3.2 *Let $\vartheta_{i_0}^n \in L^1(\Omega)$, then there exist a maximal time $T_{\max} > 0$ and a unique solution $(\vartheta_{1_n}, \ldots, \vartheta_{m_n}) \in \left(C\left([0, T_{\max}), L^1(\Omega)\right)\right)^m$ of the system (6), with the alternative:*

- either $T_{\max} = +\infty$,

- or $T_{\max} < +\infty$ and $\lim\limits_{t \to T_{\max}} \left(\sum_{i=1}^m \|\vartheta_{i_n}(t)\|_\infty\right) = +\infty$.

Proof. For $T > 0$, we define the following Banach space:

$$E_T := \{(\vartheta_{1_n}, \ldots, \vartheta_{m_n}) \in \left(C\left([0, T_{\max}), L^1(\Omega)\right)\right)^m, \\ \|(\vartheta_{1_n}, \ldots, \vartheta_{m_n})\| \leq 2\left\|\left(\vartheta_{1_0}^n, \ldots, \vartheta_{m_0}^n\right)\right\| = R\},$$

where $\|.\|_\infty := \|.\|_{L^\infty(\Omega)}$ and $\|.\|$ is the norm of E_T defined by

$$\|(\vartheta_{1_n}, \ldots, \vartheta_{m_n})\| := \sum_{i=1}^m \|\vartheta_{i_n}\|_{L^\infty([0,T], L^\infty(\Omega))}.$$

Next, for every $(\vartheta_{1_n}, \ldots, \vartheta_{m_n}) \in E_T$, we define

$$\Psi(\vartheta_{1_n}, \ldots, \vartheta_{m_n}) := (\Psi_1(\vartheta_{1_n}, \ldots, \vartheta_{m_n}), \ldots, \Psi_m(\vartheta_{1_n}, \ldots, \vartheta_{m_n})),$$

where for $t \in [0, T]$ and $1 \leq i \leq m$,

$$\Psi_i(\vartheta_{1_n}, \ldots, \vartheta_{m_n}) = S_i(t)\,\vartheta_{i_0}^n + \int_0^t S_i(t-s)\, f_i(s, ., \vartheta_n, \nabla\vartheta_n)\, ds.$$

Using the Banach fixed point theorem, we will demonstrate the local existence.

• $\Psi : E_T \to E_T$. Let $(\vartheta_{1_n}, \ldots, \vartheta_{m_n}) \in E_T$, we obtain, by the maximum principle,

$$\|\Psi_i(\vartheta_{1_n}, \ldots, \vartheta_{m_n})\|_\infty \leq \left\|\vartheta_{i_0}^n\right\|_\infty + C\sum_{i=1}^m \|\vartheta_{i_n}\|_\infty T.$$

So, we have

$$\begin{aligned} \|\Psi(\vartheta_{1_n}, \ldots, \vartheta_{m_n})\| &\leq \sum_{i=1}^m \left\|\vartheta_{i_0}^n\right\|_\infty + mC\sum_{i=1}^m \|\vartheta_{i_n}\|_\infty T, \\ &\leq 2\sum_{i=1}^m \left\|\vartheta_{i_0}^n\right\|_\infty, \text{ by choosing } T \text{ such that } T \leq \frac{1}{2mC}. \end{aligned}$$

Then $\Psi(\vartheta_{1_n}, \ldots, \vartheta_{m_n}) \in E_T$ for $T \leq \frac{1}{2mC}$.

Ψ is a contraction mapping for $(\vartheta_{1_n},\ldots,\vartheta_{m_n})$, $\left(\tilde{\vartheta}_{1_n},\ldots,\tilde{\vartheta}_{m_n}\right)\in E_T$, we have

$$\begin{aligned}
&\left\|\Psi_1\left(\vartheta_{1_n},\ldots,\vartheta_{m_n}\right)-\Psi_1\left(\tilde{\vartheta}_{1_n},\ldots,\tilde{\vartheta}_{m_n}\right)\right\|_\infty\\
\leq\ & L\int_0^t\left\|\left(\vartheta_{1_n},\ldots,\vartheta_{m_n}\right)-\left(\tilde{\vartheta}_{1_n},\ldots,\tilde{\vartheta}_{m_n}\right)\right\|_\infty d\tau,\\
\leq\ & LT\left(\sum_{i=1}^m\left\|\vartheta_{i_n}-\tilde{\vartheta}_{i_n}\right\|_\infty\right).
\end{aligned}$$

Similarly, we obtain, for $2\leq k\leq m$,

$$\left\|\Psi_k\left(\vartheta_{1_n},\ldots,\vartheta_{m_n}\right)-\Psi_k\left(\tilde{\vartheta}_{1_n},\ldots,\tilde{\vartheta}_{m_n}\right)\right\|_\infty\leq LT\left(\sum_{i=1}^m\left\|\vartheta_{i_n}-\tilde{\vartheta}_{i_n}\right\|_\infty\right).$$

These estimates imply that

$$\begin{aligned}
&\left\|\Psi\left(\vartheta_{1_n},\ldots,\vartheta_{m_n}\right)-\Psi\left(\tilde{\vartheta}_{1_n},\ldots,\tilde{\vartheta}_{m_n}\right)\right\|_\infty\\
\leq\ & mLT\left(\sum_{i=1}^m\left\|\vartheta_{i_n}-\tilde{\vartheta}_{i_n}\right\|_\infty\right),\\
\leq\ & \frac{1}{2}\left\|\left(\vartheta_{1_n},\ldots,\vartheta_{m_n}\right)-\left(\tilde{\vartheta}_{1_n},\ldots,\tilde{\vartheta}_{m_n}\right)\right\|
\end{aligned}$$

for $T\leq\max\left(\frac{1}{2mC},\frac{1}{2mL}\right)$.

Consequently, according to the Banach fixed point theorem, the problem (6) has a unique mild solution $(\vartheta_{1_n},\ldots,\vartheta_{m_n})\in E_T$.

We can extend the solution on a maximal interval $[0,T_{\max})$, where

$$T_{\max}:=\sup\left\{T>0,\ \ \left(\vartheta_{1_n},\ldots,\vartheta_{m_n}\right)\ \text{is a solution to (6) in } E_T\right\}.$$

For the global existence, we need the fact that the solutions are positive.

4 Positivity of the Solution

Lemma 4.1 *Let $(\vartheta_{1_n},\ldots,\vartheta_{m_n})$ be a solution of the system (6) satisfying*

$$\vartheta_{i_0}^n(x)\geq 0,\quad\forall x\in\Omega.$$

Then

$$\vartheta_{i_n}(t,x)\geq 0,\quad\forall(t,x)\in[0,T)\times\Omega,\quad 1\leq i\leq m.$$

Proof. Let $\bar{\vartheta}_{1_n}(t,x)=0$ in $]0,T[\times\Omega$, then $\dfrac{\partial\bar{\vartheta}_{1_n}}{\partial t}=0$, $\nabla\bar{\vartheta}_{1_n}=0$ and $(-\Delta)^{\alpha_1}\bar{\vartheta}_{1_n}=0$, then according to the hypothesis (A1), we obtain

$$\begin{aligned}
0\ &=\ \frac{\partial\vartheta_{1_n}}{\partial t}-d_1(-\Delta)^{\alpha_1}\vartheta_{1_n}-f_1\left(t,x,\vartheta_n,\nabla\vartheta_n\right)\\
&\geq\ \frac{\partial\bar{\vartheta}_{1_n}}{\partial t}-d_1(-\Delta)^{\alpha_1}\bar{\vartheta}_{1_n}-f_1\left(t,x,\bar{\vartheta}_{1_n},\ldots,\vartheta_{m_n},\nabla\bar{\vartheta}_{1_n},\ldots,\nabla\vartheta_{m_n}\right)
\end{aligned}$$

and

$$\vartheta_{1_n}(0,x) = \vartheta_{1_0}^n(x) \geq 0 = \bar{\vartheta}_{1_n}(0,x).$$

Therefore, by the comparison theorem ([5] or [7]), we get $\vartheta_{1_n}(t,x) \geq \bar{\vartheta}_{1_n}(t,x)$, where $\vartheta_{1_n}(t,x) \geq 0$.

In the same way, we find

$$\vartheta_{k_n}(t,x) \geq 0 \quad , \quad 2 \leq k \leq m.$$

Then $\vartheta_{i_n}(t,x) \geq 0$ for all $1 \leq i \leq m$.

5 Global Existence of the Solution

To show the global existence of the solution of the problem (6) for all $t \geq 0$, it suffices to find an estimate of the solution for all $t \geq 0$, from the alternative. The following Lemma shows the existence of an estimate of the solution of (6) in $L^1(\Omega)$.

Lemma 5.1 *Consider $(\vartheta_{1_n}, \ldots, \vartheta_{m_n})$ as the solution of the system (6), then there exists $M(t)$, depending only on t, such that for all $0 \leq t \leq T_M$, we have*

$$\left\| \sum_{i=1}^{m} \vartheta_{i_n} \right\|_{L^1(\Omega)} \leq M(t).$$

From this estimate, we conclude that the solution $(\vartheta_{1_n}, \ldots, \vartheta_{m_n})$ given by Theorem 3.1 is a global solution.

Proof. Adding the equations of system (6), we obtain

$$\frac{\partial}{\partial t} \sum_{i=1}^{m} \vartheta_{i_n} - \sum_{i=1}^{m} d_i (-\Delta)^{\alpha_i} \vartheta_{i_n} = \sum_{i=1}^{m} f_i(t, x, \vartheta_n, \nabla \vartheta_n).$$

Taking into account (2), we get

$$\frac{\partial}{\partial t} \sum_{i=1}^{m} \vartheta_{i_n} - \sum_{i=1}^{m} d_i (-\Delta)^{\alpha_i} \vartheta_{i_n} \leq Cm \sum_{i=1}^{m} \vartheta_{i_n}.$$

Let us integrate on Ω, so by using the formula (3) of integration by parts

$$\int_\Omega (-\Delta)^{\alpha_i} \vartheta_{i_n}(x)\, dx = 0,$$

we obtain

$$\frac{\partial}{\partial t} \int_\Omega \sum_{i=1}^{m} \vartheta_{i_n} dx \leq Cm \int_\Omega \sum_{i=1}^{m} \vartheta_{i_n} dx,$$

so

$$\int_\Omega \sum_{i=1}^{m} \vartheta_{i_n} dx \leq \exp\{Cmt\} \int_\Omega \sum_{i=1}^{m} \vartheta_{i_0}^n dx,$$

and for $\vartheta_{i_0}^n \leq \vartheta_{i_0}$, we have

$$\int_\Omega \sum_{i=1}^{m} \vartheta_{i_n} dx \leq \exp\{Cmt\} \int_\Omega \sum_{i=1}^{m} \vartheta_{i_0} dx.$$

If we put

$$M(t) = \exp\{Cmt\} \left\| \sum_{i=1}^{m} \vartheta_{i_0} \right\|_{L^1(\Omega)},$$

then

$$\left\| \sum_{i=1}^{m} \vartheta_{i_n} \right\|_{L^1(\Omega)} \leq M(t) \quad , \quad 0 \leq t \leq T_M.$$

The following Lemma ensures the existence of estimate of the solution $(\vartheta_{1_n}, \ldots, \vartheta_{m_n})$ of the system (6) in $\left(L^1(Q_T)\right)^m$.

Lemma 5.2 *For any solution $(\vartheta_{1_n}, \ldots, \vartheta_{m_n})$ of (6), there exists a constant $K(t)$ depending only on t and such that*

$$\left\| \sum_{i=1}^{m} \vartheta_{i_n} \right\|_{L^1(Q)} \leq K(t) \left\| \sum_{i=1}^{m} \vartheta_{i_0} \right\|_{L^1(\Omega)}.$$

Proof. We multiply the first equation of (7) by θ in $C_0^{\infty}(Q)$ with $\theta \geq 0$ and we integrate on Q_T, by using (4) and (5), we obtain, for all $1 \leq i \leq m$,

$$\begin{aligned} \int_{Q_T} \vartheta_{i_n} \theta dx dt &= \int_{\Omega} \vartheta_{i_0}^n(x) \Phi(0,x) dx \\ &\quad + \int_{Q_T} f_i(t,x,\vartheta_n, \nabla\vartheta_n) \Phi(s,x) dx ds, \end{aligned}$$

therefore

$$\begin{aligned} \int_{Q_T} \sum_{i=1}^{m} \vartheta_{i_n} \theta dx dt &= \int_{\Omega} \sum_{i=1}^{m} \vartheta_{i_0}^n(x) \Phi(0,x) dx + \\ &\quad \int_{Q_T} \sum_{i=1}^{m} f_i(t,x,\vartheta_n, \nabla\vartheta_n) \Phi(s,x) dx ds. \end{aligned}$$

According to (3) and as $\vartheta_{i_0}^n \leq \vartheta_{i_0}$, we have

$$\int_{Q_T} \sum_{i=1}^{m} \vartheta_{i_n} \theta dx dt \leq \int_{\Omega} \sum_{i=1}^{m} \vartheta_{i_0}(x) \Phi(0,x) dx + Cm \int_{Q_T} \sum_{i=1}^{m} \vartheta_{i_n} \Phi(s,x) dx ds.$$

Using the Hölder inequality, we deduce

$$\begin{aligned} \int_{Q_T} \sum_{i=1}^{m} \vartheta_{i_n} \theta dx dt &\leq \left\| \sum_{i=1}^{m} \vartheta_{i_0} \right\|_{L^1(\Omega)} \|\Phi(0,.)\|_{L^{\infty}(Q)} \\ &\quad + Cm \left\| \sum_{i=1}^{m} \vartheta_{i_n} \right\|_{L^1(Q)} \|\Phi\|_{L^{\infty}(Q)}, \end{aligned}$$

$$\leq \left(\left\| \sum_{i=1}^{m} \vartheta_{i_0} \right\|_{L^1(\Omega)} + Cm \left\| \sum_{i=1}^{m} \vartheta_{i_n} \right\|_{L^1(Q)} \right) . \|\Phi\|_{L^{\infty}(Q)}.$$

$$\leq \max\{1, Cm\} \left(\left\| \sum_{i=1}^{m} \vartheta_{i_0} \right\|_{L^1(\Omega)} + \left\| \sum_{i=1}^{m} \vartheta_{i_n} \right\|_{L^1(Q)} \right) . \|\Phi\|_{L^\infty(Q)},$$

$$\leq k_1(t) \left(\left\| \sum_{i=1}^{m} \vartheta_{i_0} \right\|_{L^1(\Omega)} + \left\| \sum_{i=1}^{m} \vartheta_{i_n} \right\|_{L^1(Q)} \right) . \|\theta\|_{L^\infty(Q)},$$

where $k_1(t) \geq \max\{c, cCm\}$.

Since θ is arbitrary in $C_0^\infty(Q_T)$, we get

$$\left\| \sum_{i=1}^{m} \vartheta_{i_n} \right\|_{L^1(Q)} \leq k_1(t) \left(\left\| \sum_{i=1}^{m} \vartheta_{i_0} \right\|_{L^1(\Omega)} + \left\| \sum_{i=1}^{m} \vartheta_{i_n} \right\|_{L^1(Q)} \right).$$

Taking $k(t) = \frac{k_1(t)}{1-k_1(t)}$, we find

$$\left\| \sum_{i=1}^{m} \vartheta_{i_n} \right\|_{L^1(Q)} \leq k(t) \left\| \sum_{i=1}^{m} \vartheta_{i_0} \right\|_{L^1(\Omega)}.$$

6 Main Result

Now, we present the main result of this work, which states that the existence of global solutions for the system (1) is equivalent to the existence of ϑ_i for all $1 \leq i \leq m$, it is formulated in the following theorem.

Theorem 6.1 *Under the hypotheses (A1)-(A3), there exists $(\vartheta_1, \ldots, \vartheta_m)$ being a solution of the following system:*

$$\begin{cases} \vartheta_i \in C\left([0, +\infty[, L^1(\Omega)\right), \\ f_i(t, x, \vartheta, \nabla\vartheta) \in L^1(Q_T), \\ \vartheta_i(t) = S_i(t)\vartheta_{i_0} + \int_0^t S_i(t-s) f_i(s, ., \vartheta(s), \nabla\vartheta(s))\, ds, \ \forall t \geq 0, \end{cases} \tag{8}$$

where $S_i(t)$ are the semigroups of contractions in $L^1(\Omega)$ generated by $d_i(-\Delta)^{\alpha_i}$, $1 \leq i \leq m$.

Proof. We define the map L by

$$L : (\vartheta_0, h) \to S_d(t)\vartheta_0 + \int_0^t S_d(t-s) h(s, ., \vartheta(s), \nabla\vartheta(s))\, ds,$$

where $S_d(t)$ is the contraction semigroup generated by the operator $-d(-\Delta)^\delta$. According to the compactness of the application L of $\left(L^1(Q_T)\right)^m$ in $L^1(Q_T)$ (see [1, 2]), there is a subsequence $\left(\vartheta_{1_n}^j, \ldots, \vartheta_{m_n}^j\right)$ of $(\vartheta_{1_n}, \ldots, \vartheta_{m_n})$ and ϑ_i of $\left(L^1(Q_T)\right)^m$ such that $\left(\vartheta_{1_n}^j, \ldots, \vartheta_{m_n}^j\right)$ converges towards $(\vartheta_1, \ldots, \vartheta_m)$.

Let us now show that $\left(\vartheta_{1_n}^j, \ldots, \vartheta_{m_n}^j\right)$ is a solution of (7), we have, for all $1 \leq i \leq m$,

$$\vartheta_{i_n}^j(t, x) = S_i(t)\vartheta_{i_0}^j + \int_0^t S_i(t-s) f_i\left(s, ., \vartheta_n^j, \nabla\vartheta_n^j\right) ds. \tag{9}$$

It suffices to show that $(\vartheta_1, \ldots, \vartheta_m)$ verifies (8). Obviously, if $j \to +\infty$, we obtain, for all $1 \leq i \leq m$, the limit as follows:

$$\vartheta_{i_0}^j \to \vartheta_{i_0},$$

and

$$f_i\left(s, ., \vartheta_n^j, \nabla\vartheta_n^j\right) \to f_i\left(s, ., \vartheta, \nabla\vartheta\right). \tag{10}$$

Thus, to show that $(\vartheta_1, \ldots, \vartheta_m)$ verifies (8), it remains to show that, for all $1 \leq i \leq m$,

$$f_i\left(s, x, \vartheta_n^j, \nabla\vartheta_n^j\right) \to f_i\left(s, x, \vartheta, \nabla\vartheta\right)$$

in $L^1(Q)$ when $j \to +\infty$.

Make the integration by part of (6) on Q_T by taking (3) into consideration, we obtain

$$-d_i \int_{Q_T} (-\Delta)^{\alpha_i} \vartheta_{i_n}^j dxdt = 0.$$

We have

$$\int_\Omega \vartheta_{i_n}^j dx - \int_\Omega \vartheta_{i_0}^j dx = \int_{Q_T} f_i\left(s, ., \vartheta_n^j, \nabla\vartheta_n^j\right) dxdt,$$

from where

$$-\int_{Q_T} f_i\left(s, ., \vartheta_n^j, \nabla\vartheta_n^j\right) dxdt \leq \int_\Omega \vartheta_{i_0} dx \quad , \quad 1 \leq i \leq m. \tag{11}$$

We denote

$$N_{i_n} = C\left(\sum_{i=1}^m \vartheta_{i_n}^j\right) - f_i\left(s, ., \vartheta_n^j, \nabla\vartheta_n^j\right) \quad , \quad 1 \leq i \leq m.$$

It is clear that N_{i_n} are positive according to (2), we obtain

$$\int_{Q_T} N_{i_n} dxdt \leq C \int_{Q_T} \left(\sum_{i=1}^m \vartheta_{i_n}^j\right) dxdt + \int_\Omega \vartheta_{i_0} dx.$$

Lemma 5.2 gives $\int_{Q_T} N_{i_n} dxdt < +\infty$, which implies

$$\int_{Q_T} \left|f_i\left(s, ., \vartheta_n^j, \nabla\vartheta_n^j\right)\right| dxdt \leq C \int_{Q_T} \left(\sum_{i=1}^m \vartheta_{i_n}^j\right) dxdt + \int_{Q_T} N_{i_n} dxdt < +\infty.$$

Let

$$h_{i_n} = N_{i_n} + C\left(\sum_{i=1}^m \vartheta_{i_n}^j\right) \quad , \quad 1 \leq i \leq m,$$

h_{i_n} are in $L^1(Q)$ and positive. Furthermore,

$$\left|f_i\left(s, ., \vartheta_n^j, \nabla\vartheta_n^j\right)\right| \leq h_{i_n} \quad \text{a.e.} \quad 1 \leq i \leq m.$$

Combining this result with (10) and by applying Lebesgue's dominated convergence theorem, we obtain

$$f_i\left(s, ., \vartheta_n^j, \nabla\vartheta_n^j\right) \to f_i\left(s, ., \vartheta, \nabla\vartheta\right) \text{ in } L^1(Q).$$

By passage to the limit when $j \to +\infty$ of (9) in $L^1(Q_T)$, we find, for all $1 \leq i \leq m$,

$$\vartheta_i(t) = S_i(t)\,\vartheta_{i_0} + \int_0^t S_i(t-s)\, f_i\left(s, ., \vartheta_1(s), \ldots, \vartheta_m(s), \nabla\vartheta_1(s), \ldots, \nabla\vartheta_m(s)\right) ds.$$

Then $(\vartheta_1, \ldots, \vartheta_m)$ verifies (8), consequently, $(\vartheta_1, \ldots, \vartheta_m)$ is the solution of the system (1).

7 Application

The concept of fractional calculus is also found in the study of diffusion phenomena. Numerous studies have shown the presence of abnormal diffusion processes such as the Lévy processes, for instance, in physical models where diffusive phenomena are more accurately represented by the Lévy processes rather than by other processes, reaction-diffusion equations featuring the fractional Laplacian instead of the standard Laplacian are used (see, for example, [16]).

The fractional reaction diffusion systems are systems involving constituents locally transformed into each other by chemical reactions and transported in space by diffusion. They arise in many applications, in chemistry, chemical engineering, physics, and various biological processes including population dynamics and biology. They have been the subject of countless studies in the past few decades. One of the most important aspects of this broad field is proving the global existence of solutions under certain assumptions and restrictions

8 Conclusion

This paper has explained the important factors needed to study the global existence of a solution for fractional nonlinear reaction-diffusion system. We have carried out this study by using the compact semigroup methods coupled with certain mathematical estimates and techniques. By building upon previous works, we have confirmed a global existence of a solution to the fractional system. For attaining our purpose, we have introduced and derived several theoretical results related to the existence theory.

There will be future research and applications on fractional reaction-diffusion system.

Acknowledgment

We thank the referees for the insightful review of our manuscript.

References

[1] N. Barrouk and K. Abdelmalek. Generalized result on the global existence of positive solutions for a parabolic reaction-diffusion model with an $m \times m$ diffusion matrix. *Demonstratio Mathematica* **57** (1) (2024) 20230122.

[2] N. Barrouk and S. Mesbahi. Existence of global solutions of a reaction-diffusion system with a cross-diffusion matrix and fractional derivatives. *Palest. J. Math.* **13** (3) (2024) 340–353.

[3] A. Besteiro and D. Rial. Global existence for vector valued fractional reaction-diffusion equations, arXiv:1805.09985 [math.AP], (2018).

[4] S. Bonafede and D. Schmitt. Triangular reaction-diffusion systems with integrable initial data. *Nonlinear Anal.* **33** (1998) 785–841.

[5] X. Cabre and J. Roquejoffre. The influence of fractional diffusion in Fisher-KPP equation. Preprint, arXiv:1202.6072v1, (2012).

[6] S. Djemai and S. Mesbahi. Singular Reaction-Diffusion System Arising From Quenching. *Nonlinear Dyn. Syst. Theory* **23** (5) (2023) 499–506.

[7] H. Engler. On the speed of spread for fractional reaction-diffusion equations. *Int. J. Differ. Equ.* **2010** (2010) 16 pages.

[8] V.V. Gafiychuka and B.Yo. Datsko. Pattern formation in a fractional reaction-diffusion system.*Physica A* **365** (2006) 300–306.

[9] G. Gonzàlez-Parra, A.J. Arenas and B. M. Chen-Charpentier. A fractional order epidemic model for the simulation of outbreaks of influenza A (H1N1). *Math. Methods Appl. Sci.* **37** (15) (2014) 2218–2226.

[10] D. Hnaien, F. Kellil and R. Lassoued. Asymptotic behavior of global solutions of an anomalous diffusion system. *Publié dans Journal of Mathematical Analysis and Applications* **421** (2015) 1519–1530.

[11] M. Ilic, F. Liu, I. Turner, and V. Anh. Numerical approximation of a fractional-in-space diffusion equation (ii)- with nonhomogeneous boundary conditions. *Fract. Calc. Appl. Anal.* **9** (2006) 333–349.

[12] M.J. Khayar, A. Brouri, and M. Ouzahra. Exact Controllability of the Reaction-Diffusion Equation under Bilinear Control. *Nonlinear Dyn. Syst. Theory* **22** (5) (2022) 538–549.

[13] O.A. Ladyzenskaya, V.A. Solonnikov and N.N. Uralceva. *Linear and Quasilinear Equations of Parabolic Type*, Translations of mathematical monographs, vol. 23, AMS; Providence, R. I, (1968).

[14] F. Mainardi. Fractional calculus and waves in linear viscoelasticity. Imperial College Press, London, 2010.

[15] F. Mainardi, M. Roberto, R. Gorenflo and E. Scalas. Fractional calculus and continuous-time finance ii: The waiting time distribution. *Physica A* **287** (2000) 468–481.

[16] R. Mancinelli, D. Vergni and A. Vulpiani. Front propagation in reactive systems with anomalous diffusion. *Phys. D* **185** (2003) 175–195.

[17] A. Moumeni and M. Dehimi. Global existence's solution of a system of reaction-diffusion. *IJMA* **4** (1) (2013) 122–129.

[18] A. Moumeni and M. Mebarki. Global existence of solution for reaction-diffusion system with full matrix via the compactness. *GJPAM* **12** (6) (2016) 4913–4928.

[19] A. Pazy. Semigroups of linear operators and applications to partial differential equations. Springer-Verlag, New York, 1983.

Nonlinear Dynamics and Systems Theory, **25** (4) (2025) 457–470

Exploring Boundary Layer Flow Dynamics on a Semi-Infinite Plate: A Numerical Study of Transpiration Effects and Dual Solutions

Mahmmoud M. Syam [1], Rahmah Al-Qatbi [2], Mays Haddadi [2], Alreem Alameri [2] and Muhammed I. Syam [2*]

[1] *Mechanical and Industrial Engineering Department, Abu Dhabi University, P.O.Box 59911, Abu Dhabi, UAE.*
[2] *Department of Mathematical Sciences, UAE University, Al-Ain, United Arab Emirates.*

Received: September 24, 2024; Revised: Jully 22, 2025

Abstract: This paper explores the flow of a uniform stream with no pressure gradient on a parallel semi-infinite plate. This study unveils a novel perspective on the significant influence of the mass transfer parameter and the velocity parameter on the behavior of self-similar boundary layer flows over moving surfaces, governed by the Prandtl boundary layer equations. The analysis reveals that these parameters are pivotal in determining the existence and multiplicity of solutions, which may include no solution, a unique solution, or dual solutions, depending on their specific values. The modified operational matrix method was employed to reduce the complex nonlinear system to a manageable linear third-order boundary value problem, facilitating a more thorough investigation. The numerical validations conducted, including the calculation of L_2-truncation errors, comparison with exact boundary conditions, and consistency checks against established results in the literature, not only affirm the robustness and accuracy of the proposed method but also instill confidence in its reliability. This work contributes to understanding boundary layer flows over moving surfaces by elucidating the critical roles of mass transfer and velocity parameters. It offers a reliable numerical method for solving these complex fluid dynamics problems and provides valuable insights into the physical phenomena governing such flows.

Keywords: *Prandtl boundary layer equations; heat and mass transfer, boundary layer; dual solutions; semi-infinite plate.*

Mathematics Subject Classification (2020): 93C20, 93A30, 93C95.

* Corresponding author: mailto:m.syam@uaeu.ac.ae

1 Introduction

Different studies over the past few decades have demonstrated the presence of multiple solutions in boundary layer flows driven by moving surfaces, both with and without external pressure gradients. This paper presents a novel examination of the uniform flow over a belt moving towards or away from the origin at a constant speed. This topic is closely related to the seminal works by Klemp and Acrivos [1] and Syam [2], who explored the flow induced by finite and semi-infinite flat plates moving at a constant velocity beneath a uniform mainstream. In the scenario where a similarity reduction to an ordinary differential equation is applicable, dual solutions were identified when the plate moved toward the oncoming stream. Mourad et al. [4] and others [5, 6] investigate the multiple solutions to the Falkner–Skan equation in the flow over a stretching boundary. The authors explore the conditions under which dual solutions emerge, specifically focusing on how variations in boundary stretching influence the flow characteristics. They provide a detailed mathematical analysis, demonstrating that the Falkner–Skan equation admits more than one solution under specific parameter regimes. This work contributes to understanding boundary layer behavior in fluid dynamics, particularly in cases where stretching boundaries are present. Hussaini et al. [3] and others [7, 8] later confirmed the non-uniqueness of the similarity solutions for a boundary layer problem involving an upstream-moving wall. The study analyzes the impact of the wall's motion on the boundary layer flow, identifying conditions that lead to multiple solutions. Through a rigorous mathematical approach, the authors demonstrate the existence of non-unique similarity solutions and give a deep understanding of the behavior of the boundary layer under these conditions. Their findings highlight the complexities of upstream-moving walls in fluid dynamics and contribute to a deeper understanding of boundary layer theory. As part of a broader investigation of the Falkner–Skan flows with stretching boundaries, these novel findings open up new avenues for research in the field of fluid dynamics and boundary layer flows. A mathematically analogous problem on the uniform viscous flow over a moving plate arises in the mixed convection boundary layer flow within a fluid-saturated porous medium adjacent to a heated vertical semi-infinite rigid plate. The governing similarity equations include a nondimensional parameter that quantifies the balance between natural and forced convection with two primary scenarios. In the first scenario, where buoyancy and the uniform external flow are aligned, the solutions are singular, as discussed by Cheng [5]. In the second scenario, where buoyancy opposes the uniform external flow, in [9–12], the authors identified the exact dual solutions mentioned in [1–8], where the investigation of the mixed convection boundary layer flow along a vertical surface within saturated porous medium yields significant findings. The study examines the combined effects of natural and forced convection on the boundary layer, offering a detailed analysis of the governing equations. Merkin identifies the critical parameters that influence the flow behavior and provides solutions that describe the boundary layer's response to varying conditions. This work enhances the understanding of convection processes in porous media, particularly in vertical configurations, and underscores the complex interactions between buoyancy-driven and externally imposed flows. Of particular relevance to this study are Merkin and some subsequent works [13–15], which explore the phenomenon of dual solutions in mixed convection within a porous medium. The studies delve into the conditions under which multiple solutions arise, mainly focusing on the interplay between natural and forced convection. The authors present a comprehensive analysis, showing that dual solutions can occur depending on the relative strength of

buoyancy forces compared to the imposed flow. Finally, Weidman et al. [20] and other authors [17–19] present a unified formulation for stagnation-point flow overstretching surfaces, introducing new findings in this area of fluid dynamics. The authors develop a comprehensive and exhaustive mathematical model that encapsulates various cases of stagnation-point flow, incorporating both classical and stretching boundary conditions. Through their analysis, they uncover novel results that extend the understanding of how stretching surfaces influence flow behavior near stagnation points. This work contributes significantly to the field, offering insights and generalizations that enhance the theoretical framework for studying stagnation-point flows. This work, with its thorough and comprehensive nature, provides significant insights into the complexities of mixed convection in porous media and contributes to a broader understanding of fluid behavior in such environments. These implications are crucial for further research and applications in the field of fluid dynamics and boundary layer flows.

2 Mathematical Model

When a uniform stream with velocity U flows parallel to a semi-infinite plate positioned at $y = 0$ for $x \geq 0$, the flow exhibits no pressure gradient. The velocity components in the directions along and perpendicular to the plate are denoted as u and v, respectively. The dimensional unsteady Prandtl boundary layer equations governing this scenario are

$$\frac{\partial u}{\partial x} = -\frac{\partial v}{\partial y}, \tag{1}$$

$$\frac{\partial u}{\partial t} + u\frac{\partial u}{\partial x} = \eta\frac{\partial^2 u}{\partial y^2} - v\frac{\partial u}{\partial y} \tag{2}$$

with boundary conditions specified as

$$u(x,0) = \alpha_2 U, \quad v(x,0) = -\alpha_1\sqrt{\frac{\eta U}{2x}}, \quad x > 0, \tag{3}$$

$$u = U, \quad x \in \mathbb{R}, \quad y \to \infty. \tag{4}$$

Figure 1 illustrates the physical setup of the model.

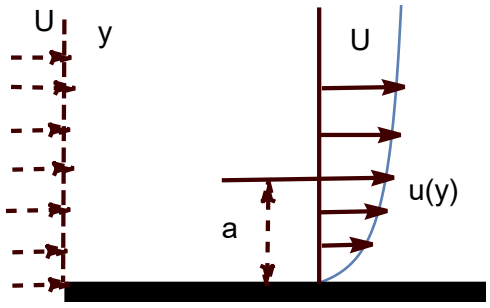

Figure 1: Schematic representation of the physical model.

By introducing the similarity variables

$$u = Uf'(\zeta), \quad v = \sqrt{\frac{\eta U}{2x}}(\zeta f'(\zeta) - f(\zeta)), \quad \zeta = y\sqrt{\frac{U}{2\eta x}}, \tag{5}$$

the chain rule yields

$$\frac{\partial u}{\partial x} = \frac{\partial u}{\partial \zeta}\frac{\partial \zeta}{\partial x} = -\frac{yUf''(\zeta)}{2x}\sqrt{\frac{U}{2\eta x}}, \tag{6}$$

$$\frac{\partial v}{\partial y} = \frac{\partial v}{\partial \zeta}\frac{\partial \zeta}{\partial y} = \frac{yUf''(\zeta)}{2x}\sqrt{\frac{U}{2\eta x}}, \tag{7}$$

$$\frac{\partial u}{\partial y} = \frac{\partial u}{\partial \zeta}\frac{\partial \zeta}{\partial y} = Uf''(\zeta)\sqrt{\frac{U}{2\eta x}}, \tag{8}$$

$$\frac{\partial^2 u}{\partial y^2} = \frac{\partial}{\partial \zeta}\left(\frac{\partial u}{\partial y}\right)\frac{\partial \zeta}{\partial y} = \frac{U^2}{2\eta x}f'''(\zeta). \tag{9}$$

Substituting these into equations (1) and (2) simplifies the latter to

$$f'''(\zeta) + f(\zeta)f''(\zeta) = 0 \tag{10}$$

with the boundary conditions

$$f(0) = \alpha_1, \quad f'(0) = \alpha_2, \quad f'(\infty) = 1. \tag{11}$$

It is crucial to note that the mass transfer parameter α_1 and the velocity parameter α_2 are key factors in determining the nature of the solution. Depending on their values, the system may have no solution, a unique solution, or multiple solutions (specifically, two). This paper will examine these scenarios and identify the critical values of α_1 and α_2. Additionally, when $\alpha_1 > 0$, suction is present, and when $\alpha_2 > 0$, the plate moves downstream from the origin. Furthermore, the wall shear stress is expressed as

$$S = \sqrt{\frac{\rho^3 U^3 \eta}{2x}}f''(0). \tag{12}$$

3 Numerical Methodology

Given the nonlinear nature of the system described by equations (10) and (11), obtaining an exact closed-form solution is challenging and impractical. Therefore, we employ an innovative numerical approach developed by Syam et al. [7, 19], which utilizes the operational matrix method. The following substitutions are made:

$$\lambda_1 = f, \quad \lambda_2 = \lambda_1', \quad \lambda_3 = \lambda_2'. \tag{13}$$

This transforms the original system (10) and (11) into the following set of equations:

$$\lambda_1' = \lambda_2, \quad \lambda_2' = \lambda_3, \quad \lambda_3' = -\lambda_1\lambda_3, \tag{14}$$

$$\lambda_1(0) = \alpha_1, \quad \lambda_2(0) = \alpha_2, \quad \lambda_3(0) = \xi. \tag{15}$$

The parameter ξ is determined by solving the system of equations (14) and (15), followed by the application of the shooting method to meet the boundary condition $\lambda_2(\infty) = 1$.

Given the nonlinear nature of system (14)-(15), obtaining an exact closed-form solution is challenging. Thus, we employ a novel numerical approach based on the operational

matrix technique, as proposed by Syam et al. [7,19]. We represent the system in matrix form as

$$\Lambda' = \Omega(\Lambda(\zeta)), \quad \Lambda(0) = \Lambda_0, \tag{16}$$

where

$$\Lambda = \begin{bmatrix} \lambda_1 \\ \lambda_2 \\ \lambda_3 \end{bmatrix}, \quad \Lambda_0 = \begin{bmatrix} \alpha_1 \\ \alpha_2 \\ \xi \end{bmatrix}, \quad \Omega(\Lambda) = \begin{bmatrix} \lambda_2 \\ \lambda_3 \\ -\lambda_1\lambda_3 \end{bmatrix}. \tag{17}$$

Following the methodology outlined in [7,19], the solution is expressed as

$$\Lambda(\zeta) = \sum_{k=0}^{M} \Lambda_k \varphi_k(\zeta), \tag{18}$$

where $\{\varphi_0(\zeta), \varphi_1(\zeta), \ldots, \varphi_M(\zeta)\}$ represent block pulse functions defined by

$$\varphi_k(\zeta) = \begin{cases} 1, & \text{if } \zeta_k \le \zeta < \zeta_{k+1}, \\ 0, & \text{otherwise,} \end{cases} \tag{19}$$

and $\{\zeta_0, \zeta_1, \ldots, \zeta_{M+1}\}$ denotes a uniform partition of the interval $[0, \zeta_\infty]$ with step size Δ, while $\{\Lambda_0, \Lambda_1, \ldots, \Lambda_M\}$ are constant vectors. Integrating both sides of equation (16) yields

$$\Lambda(\zeta) = \Lambda_0 + \int_0^{\zeta} \Omega(\Lambda(s))\, ds. \tag{20}$$

At $\zeta = \zeta_j$, for $j = 1, 2, \ldots, M+1$, we have

$$\varphi_k(\zeta_j) = \begin{cases} 1, & \text{if } j = k, \\ 0, & \text{otherwise,} \end{cases} \tag{21}$$

which leads to

$$\Lambda(\zeta_j) = \sum_{k=0}^{M} \Lambda_k \varphi_k(\zeta_j) = \Lambda_j. \tag{22}$$

Thus, we can write

$$\begin{aligned} \Lambda(\zeta_j) &= \Lambda_j \\ &= \Lambda_0 + \int_0^{\zeta_j} \Omega(\Lambda(s))\, ds \\ &= \Lambda_0 + \sum_{k=0}^{j-1} \int_{\zeta_k}^{\zeta_{k+1}} \Omega(\Lambda(s))\, ds \\ &= \Lambda_0 + \sum_{k=0}^{j-1} \int_{\zeta_k}^{\zeta_{k+1}} \Omega\left(\sum_{i=0}^{M} \Lambda_i \varphi_i(s)\right) ds. \end{aligned} \tag{23}$$

Since

$$\varphi_k(s) = \begin{cases} 1, & \text{if } i = k, \\ 0, & \text{otherwise,} \end{cases} \qquad s \in [\zeta_k, \zeta_{k+1}), \tag{24}$$

we obtain

$$\Lambda_j = \Lambda_0 + \sum_{k=0}^{j-1} \int_{\zeta_k}^{\zeta_{k+1}} \Omega\left(\Lambda_k\right)\, ds = \Lambda_0 + \Delta \sum_{k=0}^{j-1} \Omega(\Lambda_k).$$

For further details on this approach, including its convergence and error analysis, refer to [7,19]. As indicated in equation (25), this method is direct, iterative, and highly precise for solving nonlinear systems, offering computational efficiency and reduced processing times compared to other methods for similar problems.

4 Validation

To validate the solution, we define the L_2-truncation error as follows:

$$\epsilon(\alpha_1, \alpha_2) = \sqrt{\int_0^1 \parallel \Lambda'(\zeta) - \Omega(\Lambda(\zeta)) \parallel_E^2 \, d\zeta}, \tag{25}$$

where $\parallel \, . \, \parallel_E$ denotes the Euclidean norm. Table 1 presents the computed truncation errors for various values of α_1 and α_2.

α_1	α_2	$\epsilon(\alpha_1, \alpha_2)$
-0.5	0	1.91×10^{-14}
-0.25	0.25	1.94×10^{-14}
0	0.5	11.881×10^{-14}
0.25	0.75	1.80×10^{-14}
0.5	-0.25	1.77×10^{-14}
0.75	-0.5	1.71×10^{-14}

Table 1: The L_2-truncation error for different values of α_1 and α_2.

In Table 2, we evaluate the boundary condition values to compare them with the expected boundary condition $f'(\infty)$ for various values of α_1 and α_2. These values should ideally be 1, indicating that the shooting method used is accurate.

α_1	α_2	$f'(\infty)$
-0.5	0	1.000000000001
-0.25	0.25	1.000000000001
0	0.5	1
0.25	0.75	0.9999999999999
0.5	-0.25	1.000000000001
0.75	-0.5	0.9999999999999

Table 2: The value of $f'(\infty)$.

To compare our results with those in [20], we determine the critical value of the velocity parameter α_{2c}, which dictates whether the system (10)-(11) has a solution for different values of the mass transfer parameter α_1. Our findings align with those reported in Table 3.

α_1	α_{2c}
-0.5	-0.103499999998
-0.25	-0.212499999999
0	-0.354100000001
0.25	-0.52240000001
0.5	-0.720000000000

Table 3: The critical value of the velocity parameter α_{2c}.

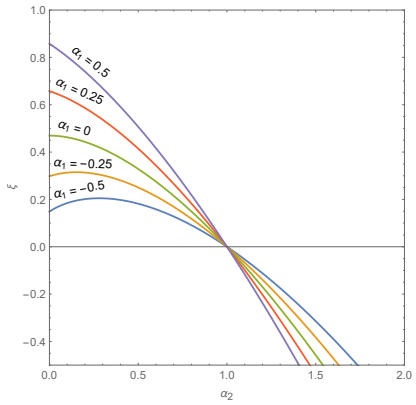

Figure 2: The parametric relationship between the velocity parameter and ξ.

These results suggest that for $\alpha_2 < \alpha_{2c}$, no solution exists. When $\alpha_2 \in [\alpha_{2c}, 0]$, there are two solutions. Finally, for $\alpha_2 > \alpha_{2c}$, a unique solution is obtained. The parametric relationship between α_2 and ξ is shown in Figure 2.

In Figure 3, we investigate the impact of suction and blowing at positive values of the velocity parameter. For $\alpha_2 = 0.5$, the plate moves away from the origin at half the speed of the free stream, whereas for $\alpha_2 = 1.5$, the plate moves approximately 50% faster than the free stream. In both cases, suction increases skin friction, indicated by $f''(0)$, and decreases the boundary layer thickness. Conversely, blowing results in the opposite effect. This phenomenon is depicted in Figure 3.

The results shown in Figure 3 are consistent with the findings of [20]. Additionally, in Figure 4, we explore the effect of the mass transfer parameter α_1 on ξ for different values of the velocity parameter. The outcomes are illustrated in Figure 4.

5 Results and Discussion

The influence of transpiration on self-similar boundary layer flow over moving surfaces was analyzed using the modified operational matrix method. When a uniform stream with velocity U flows parallel to a semi-infinite plate located at $y = 0$ for $x \geq 0$, the flow exhibits no pressure gradient. The velocity components along and perpendicular to the plate are denoted as u and v, respectively. By employing similarity variables, the dimensional unsteady Prandtl boundary layer equations are reduced to a linear boundary value problem of third order. Our numerical method was validated through four approaches: computing the L_2-truncation error, comparing the boundary condition values between

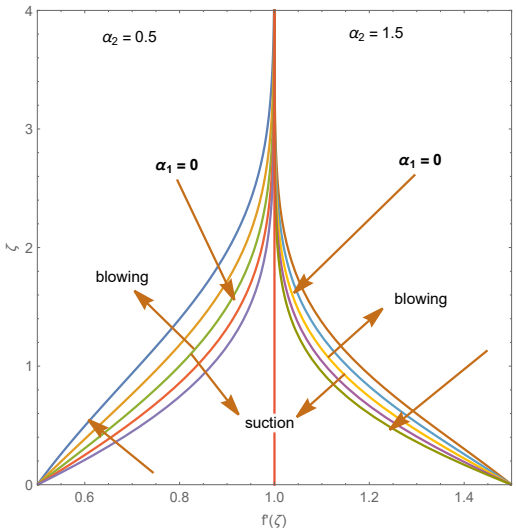

Figure 3: Influence of suction and blowing at positive values of the velocity parameter.

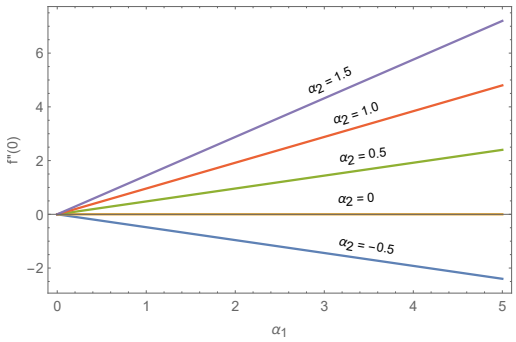

Figure 4: The effect of the mass transfer parameter α_1 on ξ.

the exact condition and those produced by the OMM at ∞, comparing our critical velocity parameter value with that obtained in [20], and graphically comparing our results with those in [20]. These validations are detailed in Tables 1-3 and Figures 2-4.

To gain physical insight into the flow problem and numerical calculations, we graphically discuss the influence of the main parameters in system (10)-(11) in Figures 2 through 16. Figure 2 shows the influence of the velocity parameter on the wall shear stress via $f''(0)$ for different values of the mass transfer parameter α_1. Figure 3 illustrates the effect of suction and blowing at positive values of the velocity parameter. Figure 4 depicts the impact of the mass transfer parameter α_1 on $f''(0)$. Figures 5-8 display the influence of the mass transfer parameter α_1 on the velocity profile when the velocity parameter $\alpha_2 = 0.5, 1.5, 0$ and -0.1. Figures 9-11 examine the effect of the velocity parameter α_2 on the velocity profile for several values of the mass transfer parameter $\alpha_1 = -0.5, 0$ and 0.5. Figures 12-14 analyze the impact of the velocity parameter α_2 on the stream profile for various values of the mass transfer parameter $\alpha_1 = 0, 0.5$, and 1.5. Finally, Figures 15-16 investigate the influence of the mass transfer parameter α_1 on the stream profile when the velocity parameter $\alpha_2 = 0.25$ and 1.25.

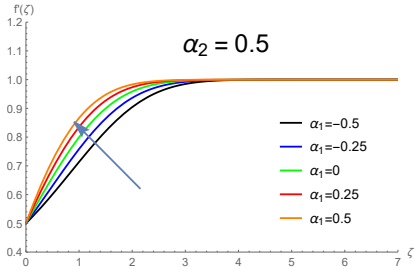

Figure 5: Influence of the mass transfer parameter α_1 on the velocity profile for the velocity parameter $\alpha_2 = 0.5$.

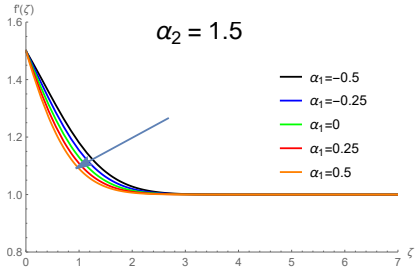

Figure 6: Influence of the mass transfer parameter α_1 on the velocity profile for the velocity parameter $\alpha_2 = 1.5$.

From Figures 2 through 16, we can draw the following conclusions:

1. Table 3 presents the critical values of the velocity parameter. These findings indicate that for $\alpha_2 < \alpha_{2c}$, no solution exists. When $\alpha_2 \in [\alpha_{2c}, 0]$, there are two solutions, and for $\alpha_2 > \alpha_{2c}$, a unique solution is obtained. For instance, when $\alpha_1 = -0.5$, no solution exists for $\alpha_2 < -0.103499999998$, and there are two solutions for $\alpha_2 \in [-0.103499999998, 0]$. For $\alpha_2 > 0$, a unique solution is present.

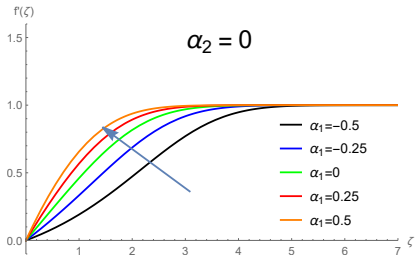

Figure 7: Influence of the mass transfer parameter α_1 on the velocity profile for the velocity parameter $\alpha_2 = 0$.

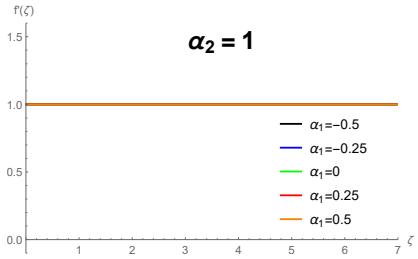

Figure 8: Influence of the mass transfer parameter α_1 on the velocity profile for the velocity parameter $\alpha_2 = 1$.

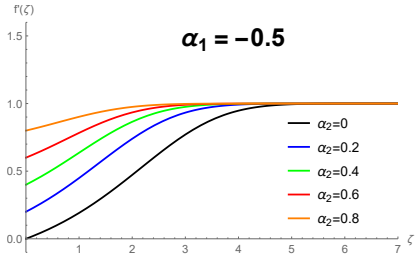

Figure 9: Influence of the velocity parameter α_2 on the velocity profile for the mass transfer parameter $\alpha_1 = -0.5$.

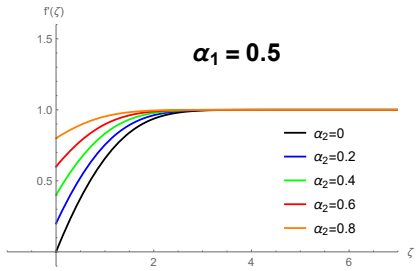

Figure 10: Influence of the velocity parameter α_2 on the velocity profile for the mass transfer parameter $\alpha_1 = 0.5$.

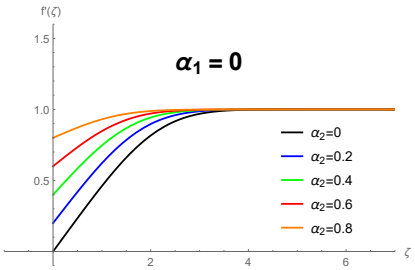

Figure 11: Influence of the velocity parameter α_2 on the velocity profile for the mass transfer parameter $\alpha_1 = 0$.

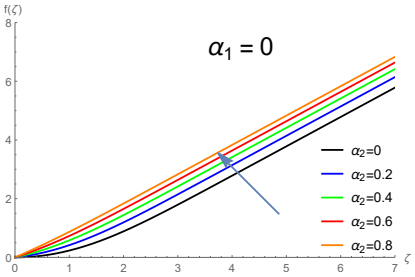

Figure 12: Influence of the velocity parameter α_2 on the stream profile for the mass transfer parameter $\alpha_1 = 0$.

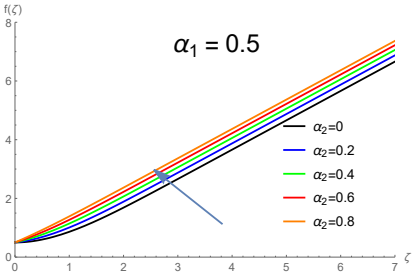

Figure 13: Influence of the velocity parameter α_2 on the stream profile for the mass transfer parameter $\alpha_1 = 0.5$.

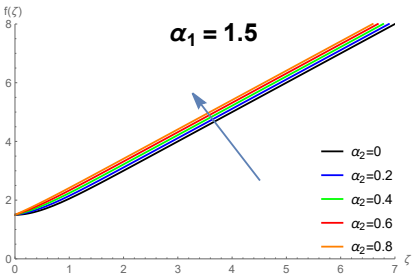

Figure 14: Influence of the velocity parameter α_2 on the stream profile for the mass transfer parameter $\alpha_1 = 1.5$.

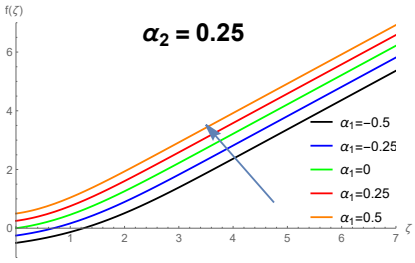

Figure 15: Influence of the mass transfer parameter α_1 on the stream profile for the velocity parameter $\alpha_2 = 0.25$.

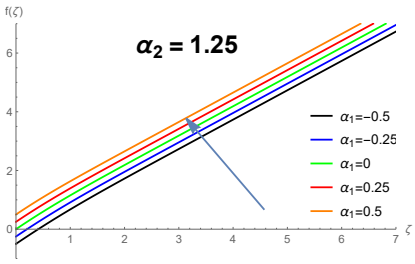

Figure 16: Influence of the mass transfer parameter α_1 on the stream profile for the velocity parameter $\alpha_2 = 1.2$.

The parametric relationship between $\alpha_2 > 0$ and ξ is illustrated in Figure 2. From this figure, it is evident that as the velocity parameter increases for a fixed mass transfer parameter, the wall shear stress decreases.

2. Figure 3 illustrates the impact of suction and blowing at positive values of the velocity parameter. For $\alpha_2 = 0.5$, the plate moves away from the origin at half the speed of the free stream, while for $\alpha_2 = 1.5$, the plate moves approximately 50% faster than the free stream. In both scenarios, suction increases skin friction, as indicated by $f''(0)$, and reduces the boundary layer thickness. Conversely, blowing produces the opposite effect. This phenomenon is depicted in Figure 3. It is also noteworthy that the results shown in Figure 3 are consistent with the findings of [20].

3. Figure 4 explores the effect of the mass transfer parameter $\alpha_1 > 0$ on $\xi = f''(0)$ for different values of the velocity parameter. Additionally, it is observed that as the mass transfer parameter increases for a fixed velocity parameter, the wall shear stress decreases. Furthermore, it is noted that when the velocity parameter is negative, the wall shear stress is in the negative direction, while it is positive when the velocity parameter is positive. It is zero when the velocity parameter is zero.

4. Figures 5-8 demonstrate the effect of the mass transfer parameter α_1 on the velocity profile for different values of the velocity parameter α_2. It is observed that the velocity profiles increase as the mass transfer parameter increases when the velocity parameter is -0.1, 0, and 0.5. The behavior changes when the velocity parameter is

1. From our investigation, we notice that when the velocity parameter is less than one, the velocity profile increases as the mass transfer parameter increases, while the velocity profile decreases as the mass transfer parameter increases when the velocity parameter is greater than one. Notably, when the velocity parameter is one, all velocity profiles coincide for different values of the mass transfer parameter.

5. Figures 9-11 demonstrate the substantial effect of the velocity parameter α_2 on the velocity profile for fixed values of α_1. It is observed that as the velocity parameter increases, the velocity profile also increases. This behavior was examined for various values of the mass transfer parameter such as -0.5, 0, and 0.5. It is noted that the velocity profile stabilizes and approaches one as ξ approaches infinity.

6. Figures 12-14 illustrate the considerable influence of the velocity parameter α_2 on the stream profile for fixed values of α_1. It is observed that as the velocity parameter increases, the stream profile also increases. This behavior was tested for different values of the mass transfer parameter such as 0, 0.5, and 1.5.

7. Figures 15-16 depict the significant impact of the mass transfer parameter α_1 on the stream profile for fixed values of α_2. It is noted that as the mass transfer parameter increases, the stream profile also increases. This behavior was examined for various values of the velocity parameter such as 0.25 and 1.25.

8. Table 1 shows that the L_2-truncation error is of the order 10^{-14}, indicating the rapid convergence of the approximate solution to the exact solution of system (10)-(11).

9. Table 2 reveals that the boundary condition is satisfied, confirming that the shooting method is operating correctly.

Acknowledgment

All authors would like to express their gratitude to the United Arab Emirates University, Al Ain, UAE, for providing financial support with Grant No. 12S116.

References

[1] J.B. Klemp and A.A. Acrivos. A method for integrating the boundary-layer equations through a region of reverse flow. *J. Fluid Mech.* **53** (1972) 177–199.

[2] M.M. Syam and M.I. Syam. Impacts of energy transmission properties on non-Newtonian fluid flow in stratified and non-stratified conditions. *Int. J. Thermofluids* **23** (2024) 100824. https://doi.org/10.1016/j.ijft.2024.100824.

[3] M.Y. Hussaini, W.D. Lakin and N. Nachman. On similarity solutions of a boundary layer problem with an upstream moving wall. *SIAM J. Appl. Math.* **47** (1987) 699–709.

[4] A.-H.I. Mourad, et al. Utilization of additive manufacturing in evaluating the performance of internally defected materials. *IOP Conf. Ser.: Mater. Sci. Eng.* **362** (1) (2018) 012026. https://doi.org/10.1088/1757-899X/362/1/012026.

[5] M.I. Syam, et al. An accurate method for solving the undamped Duffing equation with cubic nonlinearity. *Int. J. Appl. Comput. Math.* **4** (2018) 1–10.

[6] N. Teyar. Properties of MDTM and RDTM for nonlinear two-dimensional Lane-Emden equations. *Nonlinear Dynamics and Systems Theory* **24** (3) (2024) 309–320.

[7] S.M. Syam, Z. Siri, S.H. Altoum, M.A. Aigo and R.M. Kasmani. A new method for solving physical problems with nonlinear phoneme within fractional derivatives with singular kernel. *ASME J. Comput. Nonlinear Dynam.* **19** (2024) 041001. https://doi.org/10.1115/1.4064719.

[8] M.M. Syam, F. Morsi, A. Abu Eida and M.I. Syam. Investigating convective Darcy–Forchheimer flow in Maxwell Nanofluids through a computational study. *Partial Differential Equations in Appl. Math.* **11** (2024) 100863. https://doi.org/10.1016/j.padiff.2024.100863.

[9] M.I. Syam, et al. An accurate method for solving the undamped Duffing equation with cubic nonlinearity. *Int. J. Appl. Comput. Math.* **4** (2) (2018). https://doi.org/10.1007/s40819-018-0502-1.

[10] A. Oultou, O. Baiz and H. Benaissa. Thermo-electroelastic contact problem with temperature dependent friction law. *Nonlinear Dynamics and Systems Theory* **24** (1) (2024) 80–98.

[11] H.M. Jaradat, M. Alquran and M.I. Syam. A reliable study of new nonlinear equation: Two-mode Kuramoto–Sivashinsky. *Int. J. Appl. Comput. Math.* **4** (2018) 64. https://doi.org/10.1007/s40819-018-0497-7.

[12] Salah Al Omari, et al., An investigation on the thermal degradation performance of crude glycerol and date seeds blends using thermogravimetric analysis (TGA), 5th Int. Conf. on Renewable Energy: Generation and Application, ICREGA 2018, 2018-January, pp. 102–106. https://doi.org/10.1109/ICREGA.2018.8337642.

[13] B. Fadlia, A. Zarour, R. Faizi and M. Dalah. Stability analysis of a coupled system of two nonlinear differential equations with boundary conditions. *Nonlinear Dynamics and Systems Theory* **24** (3) (2024) 246–258.

[14] M.I. Syam, M. Sharadga and I. Hashim. A numerical method for solving fractional delay differential equations based on the operational matrix method. *Chaos, Solitons & Fractals* **147** (2021) 110977. https://doi.org/10.1016/j.chaos.2021.110977.

[15] P.D. Weidman, D.G. Kubitschek and A.M.J. Davis. The effect of transpiration on self-similar boundary layer flow over moving surfaces. *Int. J. Eng. Sci.* **44** (2006) 730–737.

[16] L. Abdelhaq, S.M. Syam and M.I. Syam. An efficient numerical method for two-dimensional fractional integro-differential equations with modified Atangana–Baleanu fractional derivative using operational matrix approach. *Partial Differential Equations in Appl. Math.* **11** (2024) 100824. https://doi.org/10.1016/j.padiff.2024.100824.

[17] M.M. Syam, et al. Mini Containers to Improve the Cold Chain Energy Efficiency and Carbon Footprint. *Climate* **10** 76. https://doi.org/10.3390/cli10050076.

[18] T. Syam, et al. *Statistical Analysis of Car Data Using Analysis of Covariance (ANCOVA)*. Springer Proceedings in Mathematics & Statistics, 2023.

[19] S.M. Syam, Z. Siri and R.M. Kasmani. Operational matrix method for solving fractional system of Riccati equations. 2023 International Conference on Fractional Differentiation and Its Applications (ICFDA), Ajman, United Arab Emirates, 2023, pp. 1–6. https://doi.org/10.1109/ICFDA58234.2023.10153350.

[20] P.D. Weidman, D.G. Kubitschek and A.M.J. Davis. The effect of transpiration on self-similar boundary layer flow over moving surfaces. *Int. J. Eng. Sci.* **44** (2006) 730–737. https://doi.org/10.1016/j.ijengsci.2006.04.005.